

## ABSTRACT

Title of Document: EXOPOLYSACCHARIDE ANALYSIS AND EPS  
DEPOLYMERASES AS POSSIBLE BIOFILM  
CONTROL STRATEGIES

Patrick Bales, Master of Science, 2014

Directed By: Associate Professor Daniel C. Nelson,  
Department of Veterinary Medicine

Bacteria form biofilms by adhering to surfaces and secreting high molecular weight macromolecules. When in the biofilm mode of growth, bacteria possess increased resistance to the action of antimicrobials and the immune system. By gaining an increased understanding of the structure of the biofilm extrapolymeric substance (EPS) and investigating ways to break up the EPS matrix, more effective treatment of biofilm-related infections can be achieved. In this thesis, the isolation and characterization of the polysaccharide portion of the EPS of several bacterial species is reported. The identification of 14 possible biofilm-degrading enzymes is described. One of these enzymes, HexNW, is shown to be highly thermostable and effective as a biofilm treatment.

EXOPOLYSACCHARIDE ANALYSIS AND EPS DEPOLYMERASES  
AS POSSIBLE BIOFILM CONTROL STRATEGIES

By

Patrick Bales

Thesis submitted to the Faculty of the Graduate School of the  
University of Maryland, College Park in partial fulfillment  
of the requirements for the degree of  
Master of Science  
2014

Advisory Committee:  
Associate Professor Daniel C. Nelson, Chair  
Associate Professor Richard Stewart  
Professor Steven Hutcheson

© Copyright by  
Patrick Bales  
2014

## ACKNOWLEDGEMENTS

I would like to thank Steve Swift for his work on the alginate lyases that were synthesized, Emilija Miljkovic Renke for her assistance with exopolysaccharide purification, Ryan Heselpoth for his help with the CD and DSC experiments, Sarah May for her assistance in assaying depolymerases for anti-biofilm activity, and Yang Shen for his invaluable advice and expertise in pretty much everything and also for his help with the confocal microscope.

Thanks also to my family for their unending support and encouragement to follow my dreams.

Finally, the author wishes to thank Daniel Nelson for his never-relenting support (professionally and personally) and for having more faith in me than I did, at times.

## TABLE OF CONTENTS

<b>ACKNOWLEDGEMENTS</b> .....	II
<b>TABLE OF CONTENTS</b> .....	III
<b>LIST OF TABLES</b> .....	V
<b>LIST OF FIGURES</b> .....	VI
<b>LIST OF ABBREVIATIONS</b> .....	VII
<b>CHAPTER 1: BACKGROUND AND LITERATURE REVIEW</b> .....	1
OVERVIEW .....	1
BIOFILM STRUCTURE .....	2
BIOFILM FORMATION .....	8
PROBLEMS ASSOCIATED WITH BIOFILMS .....	10
WAYS TO ELIMINATE BIOFILMS .....	13
ESKAPE PATHOGENS .....	20
<i>Enterococcus faecium</i> .....	21
<i>Staphylococcal species</i> .....	21
<i>Klebsiella pneumoniae</i> .....	23
<i>Acinetobacter baumannii</i> .....	23
<i>Pseudomonas aeruginosa</i> .....	23
<i>Enterobacteriaceae species</i> .....	24
<b>CHAPTER 2: PURIFICATION AND CHARACTERIZATION OF BIOFILM-ASSOCIATED EPS EXOPOLYSACCHARIDES FROM ESKAPE ORGANISMS AND OTHER PATHOGENS</b> .....	27
ABSTRACT .....	28
INTRODUCTION .....	29
MATERIALS AND METHODS .....	32
<i>Bacterial strains and growth conditions</i> .....	32
<i>EPS Extraction</i> .....	33
<i>Purification of exopolysaccharides</i> .....	33
<i>Composition and linkage analysis</i> .....	34
<i>Biofilm microscopy</i> .....	35
RESULTS AND DISCUSSION .....	35
<i>EPS purification</i> .....	36
<i>Composition and linkage analysis</i> .....	38
<i>Strain variability within a species</i> .....	44
<i>Species-specific findings</i> .....	45

<i>Mannose contribution to EPS</i> .....	48
<i>EPS staining of E. coli strain 43894 biofilms</i> .....	50
ACKNOWLEDGMENTS.....	53
<b>CHAPTER 3: HEXNW IS A HIGHLY THERMOSTABILE GLUCOSAMINIDASE THAT DISPERSES S. EPIDERMIDIS BIOFILMS</b> .....	54
ABSTRACT .....	55
BACKGROUND.....	56
MATERIALS AND METHODS .....	58
<i>Bacterial strains, growth conditions, and biofilm formation</i> .....	58
<i>Gene synthesis, expression, and purification</i> .....	59
<i>Enzyme activity assays</i> .....	60
<i>Chitinase experiments</i> .....	61
<i>pH profile assays</i> .....	62
<i>Thermostability assays</i> .....	62
<i>Amino sugar assays</i> .....	64
<i>CFU release</i> .....	64
<i>MIC and MBEC assays</i> .....	65
RESULTS .....	66
<i>Identification, expression, and purification</i> .....	66
<i>Enzyme kinetics</i> .....	69
<i>Substrate specificity</i> .....	73
<i>pH activity profile</i> .....	75
<i>Thermostability</i> .....	78
<i>Antibiofilm properties</i> .....	84
DISCUSSION .....	92
ACKNOWLEDGMENTS.....	94
<b>CHAPTER 4: OTHER PUTATIVE EPS DEPOLYMERASES</b> .....	95
SELECTION OF DEPOLYMERASES .....	95
PRELIMINARY ANTI-BIOFILM EXPERIMENTS .....	102
<b>CHAPTER 5: DISCUSSION AND FUTURE DIRECTIONS</b> .....	106
FUTURE DIRECTIONS .....	107
<b>CONCLUDING REMARKS</b> .....	108
<b>APPENDIX A</b> .....	109
<b>APPENDIX B</b> .....	111
<b>APPENDIX C</b> .....	113
<b>BIBLIOGRAPHY</b> .....	115

## LIST OF TABLES

### Chapter 2

Table 2-1: Glycosyl composition analysis.....	40
Table 2-2: Glycosyl linkage analysis.....	42

### Chapter 3

Table 3-1: DspB and HexNW enzyme kinetics.....	72
Table 3-2: DSC thermostability data.....	83
Table 3-3: Melting point summary.....	83
Table 3-4: MBEC and MIC values.....	91

### Chapter 4

Table 4-1: Summary of synthesized depolymerases.....	97
--	----

# LIST OF FIGURES

## Chapter 1

Figure 1-1: EPS stabilizing forces.....	4
Figure 1-2: Biofilm formation.....	9
Figure 1-3: Dispersin B and <i>S. epidermidis</i> biofilms.....	18
Figure 1-4: <i>P. aeruginosa</i> and <i>E. coli</i> -produced exopolysaccharides.....	26

## Chapter 2

Figure 2-1: Diagram of exopolysaccharide purification.....	37
Figure 2-2: EPS staining of <i>E. coli</i> strain 43894 biofilms.....	51

## Chapter 3

Figure 3-1: HexNW alignment with dispersin B.....	68
Figure 3-2: Reaction of HexNW with pNP-GlcNAc.....	71
Figure 3-3: Chitinase activity.....	74
Figure 3-4: pH activity profile.....	76
Figure 3-5: Temperature stability.....	80
Figure 3-6: CD and DSC melting point analysis.....	81
Figure 3-7: Biofilm treatment schematic.....	85
Figure 3-8: Morgan-Elson assay.....	87
Figure 3-9: CFU release.....	90
Figure 3-10: Depolymerase-mediated reduction in MBEC.....	91

## Chapter 4

Figure 4-1: Depolymerase-mediated prevention of biofilm formation.....	104
--	-----

## LIST OF ABBREVIATIONS

In alphabetical order

ATCC	American Type Culture Collection
AU	Absorbance Units
BP buffer	40 mM boric acid 40 mM phosphoric acid buffer
CD	Circular dichroism
CNS	Coagulase-negative staphylococci
CFTR	Cystic fibrosis transmembrane conductance regulator
DSC	Differential scanning calorimetry
DspB	Dispersin B
eDNA	Extracellular DNA
ESS	Extracellular slime substance
EPS	Extrapolymeric substance
FGE	Fresh garlic extract
GC/MS	Gas chromatography/mass spectrometry
GlcA	Glucuronic acid
HHA	Hippeastrum hybrid lectin
LPS	Lipopolysaccharides
MSD	Mass selective detector
MRE	Mean residue ellipticity
MSCRAMMs	Microbial surface components recognizing adhesive matrix molecules
MBEC	Minimum biofilm elimination concentration
MWCO	Molecular weight cut-off
MDR	Multidrug resistant
GalNAc	<i>N</i> -acetyl-galactosamine
GlcNAc	<i>N</i> -acetylglucosamine
NARSA	Network on Antimicrobial Resistance in <i>S. aureus</i>
NMR	Nuclear magnetic resonance
pNP-GlcNAc	<i>Para</i> -nitrophenylated <i>N</i> -acetylglucosamine
PSMs	Phenol-soluble modulins
PBS	Phosphate-buffered saline
PNAG	Poly- <i>N</i> -acetylglucosamine
PGA	Poly- $\gamma$ -glutamic acid
PIA	Polysaccharide intercellular adhesin
SDS	Sodium dodecyl sulfate
SAA	Slime associated antigen
TCA	Trichloroacetic acid
UPEC	Uropathogenic <i>E. coli</i>

# CHAPTER 1

## Background and Literature Review

### Overview

While bacterial pathogenesis mechanisms, virulence factors, and antimicrobial resistance vary greatly between species, the ability and preference to grow as biofilms represents the vast majority of human bacterial infections. Biofilms are formed when planktonic bacteria (i.e., free, individual cells) adsorb onto a wound surface and form colonies (Hall-Stoodley et al. 2004; Stewart et al. 2008; Stoodley, et al. 2002). Once the colonies become established, phenotypic changes cause them to secrete high molecular weight carbohydrates (i.e., polysaccharides) that serve as the structural backbone for the biofilm. Non-cellular components and debris, including additional carbohydrates, proteins, lipids, and nucleic acids, become entangled in the polysaccharide backbone and constitute the “slime” layer of a biofilm which is technically known as the extrapolymeric substance, or EPS (Flemming and Wingender 2010). The EPS is thought to protect the bacteria from antimicrobials, antibodies, and circulating immune cells.

The natural resilience of biofilms along with the rise of antibiotic-resistant pathogens illustrates the urgent need for new and innovative ways to treat biofilm-related infections. Biofilms are responsible for complications such as secondary wound infections, chronic *P. aeruginosa* infection in the lungs of cystic fibrosis patients, and the colonization of medical implant devices. As an example,

coagulase-negative staphylococci, which are typically viewed as less virulent than their coagulase-positive counterparts, including *S. aureus*, are responsible for about 250,000 cases of intravascular catheter infections per year with a cost of about \$25,000 per case and hospital stays exceeding 7 days (Otto 2012).

Research focused on ways of treating bacterial infections specific to biofilm-formers is lacking. Methods include the use of metal chelators, phages, or modifications to surfaces with silver nanoparticles. In addition, proteins that digest components of the EPS (EPS depolymerases) can be effective. As the matrix that encapsulates bacterial cells is degraded, they revert to a planktonic lifestyle and are resensitized to the action of immune cells and antibiotics. In order to understand how to degrade the EPS, it is important to know its composition. In this thesis, the discovery of many EPS polysaccharide depolymerases is described that have good prospects as antibiofilm agents. In addition, the analysis of the structural components of the polysaccharide portion of the EPS of many clinically relevant human pathogens is reported in an effort to aid in the identification of enzymes targeted to specific species.

### **Biofilm structure**

Biofilms allow prokaryotes to live in varied and often harsh environments and reflects a level of adaptation that is not possible by multicellular eukaryotes (Hall-Stoodley et al. 2004). Genetic regulation and selection for certain structures or matrix components combined with an increased resistance to environmental stressors allows for this increased level of adaptation. The structures of mature

biofilms can be incredibly varied and depend on the environment in which the biofilm bacteria live. For example, biofilms growing in fast-moving water often form filamentous “streamers” whereas biofilms growing in calm water tend to form mushroom- or mound-like structures. In addition, there is a great deal of heterogeneity within individual biofilms and they often consist of multiple bacterial species. The EPS is used to create numerous microdomains within the overall biofilm structure that vary both in terms of structure and of biochemical composition, as demonstrated by lectin staining (Lawrence et al. 2007; Flemming and Wingender 2010).

The EPS matrix allows biofilms to be mechanically stable while also dynamic in their responses to shear stress and other mechanical forces. The entanglement of matrix components and interactions between them such as hydrogen bonds, Van der Waals interactions, and electrostatic interactions confers stability, as illustrated in **Figure 1-1**. Charged groups in the EPS are often capable of chelating multivalent ions (shown with  $\text{Ca}^{2+}$  in *P. aeruginosa* biofilms, K rstgens et al. 2001). Biofilms’ elasticity allows it to resist breakage (demonstrated in *S. aureus*, Lawrence et al. 2007). In addition, biofilms are capable of phenotypic adaptation in response to changes in mechanical stresses (for example, increasing EPS production in response to stress, Stoodley et al. 2003). Increased fluid shear has been shown to result in the growth of denser and stronger biofilms (Shaw et al. 2004).

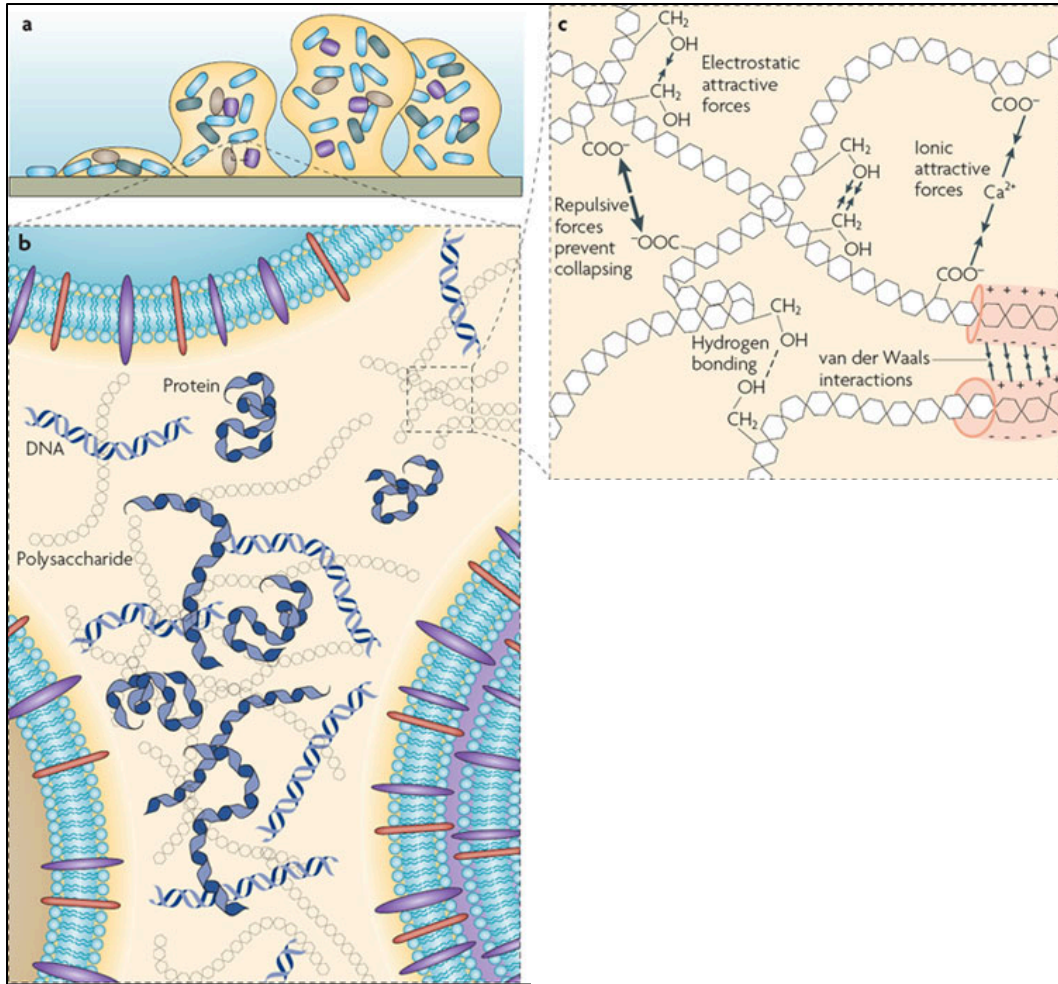


**Figure 1-1: EPS stabilizing forces.** The extracellular polymeric substances that make up a typical bacterial biofilm are visualized at several dimensions. (A) Biofilm development begins with attachment, then microcolony formation and further development with increased cell division and EPS production. (B) Components of the EPS visualized, including DNA, proteins, and polysaccharides. (C) Various cohesive forces within the EPS are depicted. Figure taken from Flemming and Wingender 2010. Used with permission.

The EPS can account for over 90% of the biofilm's dry mass (Wingender et al. 1999) and allows for a lifestyle that is vastly different from that of planktonic (free-living) cells. Common components of the EPS include polysaccharides, proteins, DNA, and humic substances (compounds formed by the degradation of organic matter). The EPS mediates adherence of the biofilm to surfaces and allows the cells within the biofilm to aggregate together. It permits retention of water, nutrients, and digestive enzymes due to hydrogen bonding, charged interactions, and other intermolecular forces facilitated by the macromolecules present in the matrix. The EPS also serves as a physical barrier between bacterial cells and the host immune system (in the case of pathogens). It can shield bacterial cells from antimicrobial compounds, protozoan grazers, and ultraviolet radiation. The presence of extracellular DNA in the EPS (which is due to both cell lysis and active export of DNA segments) also facilitates the exchange of genetic information between members of bacterial populations. The EPS can even serve as a food source in and of itself during starvation conditions (Flemming and Wingender 2010).

Exopolysaccharides (secreted polysaccharides) are a major constituent of the EPS matrix and are ubiquitous in environmental and disease-associated biofilms. In many cases, they are essential for biofilm formation because of their role in surface attachment and maintaining the physical stability of the biofilm. They are typically long and high molecular weight ( $0.5 \times 10^6$  Da to  $2 \times 10^6$  Da) (Flemming and Wingender 2010). While some exopolysaccharides, such as cellulose, are homopolysaccharides, most are heterogenous and consist of a

mixture of charged and neutral sugar residues (Zogaj et al. 2001). Many exopolysaccharides, such as alginate, are polyanionic (Ryder et al. 2007), whereas others, such as intercellular adhesin (partially deacetylated  $\beta$ -1,6-*N*-acetylglucosamine, which is present in *Staphylococcus aureus* and *Staphylococcus epidermidis*), are polycationic (Götz 2002). In some cases, a single bacterial species utilizes multiple types of exopolysaccharides. *Pseudomonas aeruginosa*, for example, uses at least 3 different exopolysaccharides during biofilm development, including alginate, Pel, and Psl (Ryder et al. 2007).

Proteins that exist in the EPS serve a variety of functions, including enzymes that degrade EPS components and other biopolymers that serve as a food source (Flemming and Wingender 2010). They are also often implicated in the detachment of individual cells or larger sections of biofilm for the purpose of colonizing other areas. They can serve as virulence factors in the case of pathogens. The effect of extracellular enzymes is enhanced by the fact that the interactions between enzymes and other matrix components keep them from diffusing away from the biofilm. These interactions also serve the purpose of enhancing the *in situ* thermostability and resistance to proteolysis of these enzymes. Proteins such as lectins and lectin-like proteins can serve a structural role in biofilms by cross-linking exopolysaccharides and linking exopolysaccharides to bacterial cells themselves. Amyloids are common matrix proteins that serve as adhesins and also cytotoxins (Otzen and Nielsen 2008). Structural proteins that serve other functions for bacterial cells, such as flagella,

fimbriae, and pili, can also play a role in the stabilization of the EPS matrix. *P. aeruginosa* type IV pili, for example, bind DNA and are likely involved in the cross-linking of cells to extracellular DNA (Zogaj et al. 2001).

Extracellular DNA (eDNA) is present in different amounts in different biofilms. While *S. aureus* and *S. epidermidis* are closely related species, eDNA plays a much larger role in *S. aureus* than *S. epidermidis* (Izano et al. 2008). eDNA is also important in cell-cell adhesion in *P. aeruginosa* biofilms (Whitchurch et al. 2002). While some eDNA is present in the EPS as a byproduct of “accidental” cell lysis, it is apparent that, in some cases, subpopulations of cells are specifically lysed for the sake of utilizing their DNA as a component of the EPS matrix. This is the case for *S. epidermidis*, which mediates cell lysis through the AtlE autolysin (Molin and Tolker-Nielsen 2003). In addition, the eDNA sequence of bacterial cells is not always identical to that of genomic DNA, suggesting that DNA may be exported from cells specifically for the purpose of building the EPS matrix (Böckelmann et al. 2006).

While the polysaccharides, proteins, and DNA that are present in the EPS are highly hydrophilic, bacteria can also use hydrophobic molecules to allow for attachment to otherwise uncolonizable surfaces such as pyrite, oil droplets, Teflon, and waxy leaves. These molecules include lipopolysaccharides (LPS), other lipids, surfactin, emulsan, and various biosurfactants (Flemming and Wingender 2010). The EPS matrix allows biofilms to retain water during periods of desiccation while at the same time acting like a molecular sieve, retaining ions and even toxic compounds such as heavy metals. By allowing bacteria to

colonize hydrophobic surfaces such as oil slicks and also providing an effective way of retaining toxic metals, biofilms provide numerous environmental benefits in addition to allowing bacteria to colonize diverse environments.

### **Biofilm formation**

Biofilms develop in a regulated sequence (illustrated in **Figure 1-2**), beginning with loose association with a surface followed by strong adhesion as EPS is produced and facilitates increased binding (Stoodley et al. 2002). Irreversible attachment in *S. epidermidis* is caused by the production of polysaccharide intercellular adhesion (PIA), which holds adherent cells closely together (Gerke et. al 1998). In *P. putida*, the transition from reversible to irreversible attachment is correlated with a switch from flagellar to twitching motility (Sauer et al. 2001). Twitching motility is thought to contribute to microcolony formation (O'Toole and Kolter 1998). Motility contributes to these initial steps of biofilm formation by allowing for attached cells to redistribute themselves on a surface, whereas cell division is the driving force of the lateral and vertical growth of the biofilm structures. In addition, planktonic cells in the medium can be recruited to the developing biofilm. Quorum sensing has been shown to play a role in bacterial biofilm formation, causing an upregulation of EPS producing genes as the number of adherent cells increases. In *P. aeruginosa*, a strain lacking the autoinducer gene *lasI* produced biofilms that were only 20% as thick as wild-type biofilms (Davies 1998). Quorum sensing is also thought to

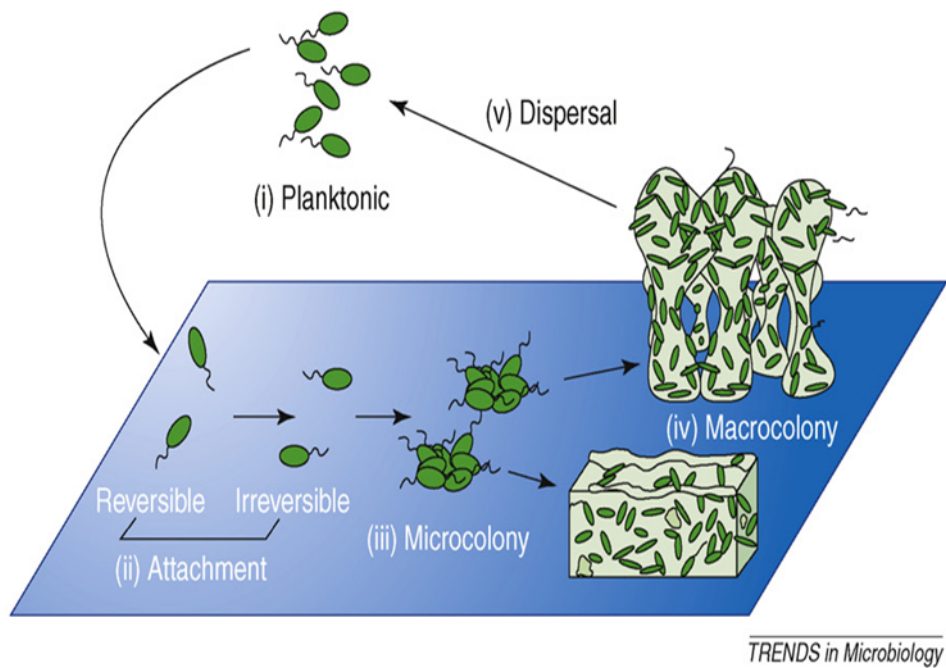


**Figure 1-2: Biofilm formation.** The development of a biofilm as a five stage process: Stage 1: initial attachment of planktonic cells to the surface. Stage 2: production of EPS resulting in more firmly adhered “irreversible” attachment. Stage 3: early development of biofilm architecture. Stage 4: maturation of biofilm architecture. Stage 5: dispersion of single cells from the biofilm that can then seed new biofilms in other locations. Taken from Monds and O’Toole 2009. Used with permission.

be involved in the conversion of biofilm cells to stationary phase and the expression of stress-response genes.

As adherent cells divide, they manifest as microcolonies. Confocal laser microscopy has shown biofilms as matrix-enclosed microcolonies with water channels between them to allow for efficient nutrient uptake and waste removal (Hall-Stoodley et al. 2004; Lawrence et al. 1991). They then develop into mature biofilm structures with the increased production of EPS. Biofilm structure varies based on the environment that the biofilm-forming cells are in. Mature biofilms can have the appearance of mushroom-like mounds, flat mounds, or filaments if they are growing in an area of flowing water. The nature of the EPS being produced also has a large impact on the nature of the mature biofilm architecture.

If conditions permit, mature biofilms can disperse its cells with the goal of colonizing new niches. Dispersal can occur through swarming/seeding dispersal, in which individual cells are released, dumping dispersal, in which clumps of cells are shed all at once, or surface dispersal, in which whole biofilm structures move across surfaces. Dispersal is caused by enzymatic degradation of the EPS molecules that anchor cells to a surface, by external forces such as increased fluid shear, or the release of the EPS or surface-binding proteins that connect cells to the surface they are adhered to (Hall-Stoodley et al. 2004).

### **Problems associated with biofilms**

As already mentioned, biofilms serve to protect bacterial cells from environmental stresses such as UV radiation, metal toxicity, dehydration,

phagocytosis, and the action of antimicrobial agents. The EPS matrix functions as a protective physical barrier and even if antimicrobials are able to penetrate, biofilm cells are usually in stationary phase and phenotypically well adapted to withstand stress (Hall-Stoodley et al. 2004). As an example,  $\beta$ -lactam antibiotics (which act by inhibiting cell wall biosynthesis and are regularly used to treat infections caused by Gram-positive bacteria) are often either ineffective or require a higher killing dose because of the slow-growing nature of biofilm cells (Walters et al. 2003). Antimicrobial degrading enzymes, such as  $\beta$ -lactamases, can also accumulate in biofilms and increase the likelihood of resisting antibiotic treatment even further (Dibdin et al. 1996). The EPS also decreases the rate of diffusion of antibiotics through the biofilm, decreasing the effective antibiotic concentration and increasing the likelihood of bacterial survival. Finally, in many biofilms, pockets of cells known as persisters exist that exhibit resistant phenotypes.

The adaptations listed above create significant problems for humans being treated with a biofilm-forming bacterial species because while an initial treatment course of antibiotics may effectively kill planktonic bacteria and eliminate symptoms of infection, bacteria in a biofilm often resist such treatment and are then free to disperse and cause secondary infections. Free-floating bacteria can also adhere to and colonize medical implant devices such as heart valves, catheters, and prosthetic joints. It is even possible for the body's defense mechanisms to actually encourage biofilm formation. It has been shown that certain host inflammatory molecules facilitate bacterial adhesion to surfaces. Many biofilm-forming bacteria possess receptors for host cell proteins that

facilitate adhesion. For example, several bacterial species, including *S. aureus*, possess adhesins for fibronectin, a common eukaryotic structural protein (Vaudaux et al. 1994).

Bacterial endocarditis is an example of how bacterial biofilms can incorporate host components as a part of the biofilm extracellular matrix (Hall-Stoodley et al. 2004). When heart valves are damaged, platelets and fibrin build up on the surface of heart valve tissue and allow for colonization by staphylococci and streptococci. Colonization encourages further damage and inflammation of the heart tissue and the deposition of additional layers of fibrin. Over time, a calcified lesion is formed in which bacterial cells exist as a hardy biofilm and are protected from leukocytes by the layers of fibrin, secreted bacterial EPS components, and fibroblasts. In addition, it is thought that the turbulent environment near heart valves encourages the deposition of additional EPS on the part of the bacteria due to increased mechanical stress that encourages phenotypic adaptation.

The lung colonization of patients with cystic fibrosis is another example of an environment in which bacteria frequently cause persistent infections as biofilms (Hall-Stoodley et al. 2004). In this disease, recessive mutations in the cystic fibrosis transmembrane conductance regulator (CFTR) gene causes dysfunctional electrolyte secretion and absorption. The respiratory system's mucous becomes thick as a result as clearance by ciliated epithelial cells in the lungs is impaired, facilitating chronic infection. *P. aeruginosa* is the most common cause of persistent infection in CF lungs and may adhere to lung

epithelial cells with the help of the thick mucus, which it may use as an EPS scaffold (Worlitzsch et al. 2002). Another hypothesis is that inflammation of lung epithelial cells may allow adherence. *P. aeruginosa* biofilm formation also coincides with the development of antibiotic resistance (John et al. 1999). Considering that the majority of clinically relevant human pathogens form biofilms, that biofilm formation significantly reduces the treatability of bacterial infections, and that antibiotic resistance is already developing at an alarming rate, the necessity to invest in this area of research is clear.

### **Ways to eliminate biofilms**

Infections caused by bacteria in the biofilm mode of growth are notoriously difficult to eradicate and the most common control strategies are often insufficient. Antibiotics are the most-often turned to method of treating bacterial infections, but are less than ideal because of broad damage to host microbiota. To further compound this problem, many notable biofilm formers that are common human pathogens are resistant to the most commonly used antibiotics. Biofilms can also create microenvironments of low pH and high metal ion concentrations, which can inactivate antibiotics. Antibiotic treatment is usually completely ineffective as a means of combating medical implant device infection. In these cases, it is often necessary to surgically excise the device in order to control the bacterial load within the body. It is clear that additional ways of treating biofilm infections are necessary.

Since adherence to a surface is an essential first step in biofilm formation, many studies have focused on ways to prevent adherence of bacterial cells to host cells or to abiotic surfaces (Kostakioti 2014). Efforts to prevent adherence of uropathogenic *E. coli* (UPEC) to the urinary tract have included the development of compounds that interfere with the adherence or assembly of type 1 pili, which are the primary mediator of UPEC adherence. Crystal structures of the FimH adhesin (utilized in type 1 pili for adhesion) bound to mannose have been used to design mannosides which fit the FimH binding pocket and competitively inhibit FimH binding to its receptor, thus preventing UPEC biofilm formation. Optimized mannosides have also been shown to be effective in reducing pre-formed biofilms *in vitro* and *in vivo* (Cusumano et al. 2011). Mannosides also have no effect on cell growth and are purely anti-adherence. This type of treatment may be useful because of the reduced likelihood of the development of resistance. Another example of this type of potential therapeutic involves using exopolysaccharides of one bacterial species to prevent the formation of biofilms of another species (Qin et al. 2009). In addition, genetic studies have identified possible means of interfering with biofilm formation signal transduction cascades (Njoroge and Sperandio 2009).

Bacteriophage are promising as antibiofilm agents because they are abundant and easy to grow, typically have narrow host ranges (the normal flora in humans would likely be unaffected), and low dosages would likely be sufficient for treatment because of their self-replicating nature (Kostakioti et al. 2014; Donlan 2009). Phages are often adapted to infect stationary phase bacterial cells

and many encode proteins that are specifically used to degrade the EPS matrix to allow access to their bacterial hosts. Transfer of virulence genes is minimized by using exclusively lytic phage and resistance to phage infection is often mitigated by phages' high mutation rate and ability to co-evolve with its host. Bacteriophage products such as tail spike proteins and lysins can also be used separately as anti-biofilm agents.

Silver and gold nanoparticles coated onto medical devices have also been proposed as effective antimicrobial agents. Silver has been used as an antimicrobial for hundreds of years and is toxic to bacteria due to thiol-group reactivity with enzymes, causing inhibition of DNA replication, protein expression, and metabolism (Chen and Schluesener 2008). The positively charged ions interact with negatively charged bacterial membranes and are imported into the cell. While the use of silver and gold as antimicrobials was discouraged for many years due to toxicity of the metals to humans, nanotechnology has allowed the creation of very small particles that allow for intimate interactions with bacterial membranes without being toxic to humans. Silver nanoparticles have been shown to inhibit biofilms of *P. aeruginosa*, *Staphylococcus aureus*, and *Staphylococcus epidermidis* (Kalishwaralal et al. 2010; Secinti et al. 2011).

Antimicrobial peptides are produced by the innate immune system and are possible antibiofilm agents as well as alternatives to antibiotics due to activity against many strains of multidrug resistant (MDR) bacteria (Yang et al. 2002). Some cathelicidins (the most well-studied group of antimicrobial peptides) are

very effective at inhibiting biofilm formation and also dispelling existing biofilms formed by *P. aeruginosa* cells isolated from cystic fibrosis patients (Pompilio et al. 2011). Some peptides are lytic and are promising antibiofilm agents. The lytic peptide PTP-7 remains active in acidic and metal-rich environments (which is often the environment of *S. aureus* biofilms), is capable of deeply penetrating into biofilm structures, and was capable of killing 99.9% of biofilm bacteria (Kharidia and Liang 2011).

Some molecules are produced by biofilm-forming bacteria specifically to mediate dispersal and allow for the colonization of new environments. These products can be utilized as anti-biofilm agents by applying them exogenously. D-amino acids, which disperse *S. aureus*, *P. aeruginosa*, and possibly other biofilms, work by disrupting the localization of adherence proteins to the bacterial cell surface (Kolodkin-Gal et al. 2010). Nonspermidine is another biofilm-disassembly molecule in *B. subtilis* that targets the EPS and is effective in treating *B. subtilis*, *S. aureus*, and *E. coli* pellicle biofilms (biofilms at the air-liquid interface) (Kolodkin-Gal et al. 2012). Bacteria also produce proteins for the purpose of cell dispersal which can be used to the same end.

Many enzymes are capable of degrading the various components of biofilm EPS. Enzymes that cleave the glycosidic bonds within biofilm exopolysaccharides (“EPS depolymerases”) have been shown to be efficacious in dispersing biofilms (Kaplan et al. 2003; Bartell et al. 1969; Ghalambor et al. 1971; Hughes et al. 1998; Kassa and Chhibber 2012). As the polysaccharide “glue” that holds the biofilm together is broken up, individual cells are separated

from the bulk biofilm and diffuse into the surrounding medium, where they are much more accessible to antibiotics and the immune system. Dispersin B (DspB) is a glycoside hydrolase produced by *Actinobacillus actinomycetemcomitans* that is produced to mediate biofilm dispersal (Kaplan et al. 2003). As a  $\beta$ -1-6-*N*-acetylglucosaminidase, it is effective against biofilms that contain polymers of *N*-acetylglucosamine, or PNAG. This includes *S. aureus*, *S. epidermidis*, and *E. coli*. The effectiveness of DspB in treating *S. epidermidis* biofilms is illustrated in **Figure 1-3**. Enzymes that target other parts of the biofilm matrix can also be effective in breaking up biofilms. DNase I can prevent *Staphylococcus* and *Enterococcus* biofilm formation by digesting the extracellular DNA (eDNA) present in the biofilms of these pathogens (Guiton et al. 2009).

As already mentioned, biofilms often contain metal cations that play a role in maintaining EPS integrity. Metal chelators, therefore, are an attractive possibility as antibiofilm agents, especially in species in which metal ions play an especially prominent role in biofilm integrity. EDTA has been used to treat as well as prevent biofilm formation in *P. aeruginosa* and staphylococcal species (Bookstaver et al. 2009).

It is possible to engineer materials used for medical devices so as to discourage bacterial adherence and colonization (Desrousseaux et al. 2013). In general, bacteria adhere more effectively to hydrophobic surfaces than hydrophilic surfaces. As a result, hydrophilic materials such as hydrogels (notably polyethyleneglycol) are not colonized as readily as more hydrophobic

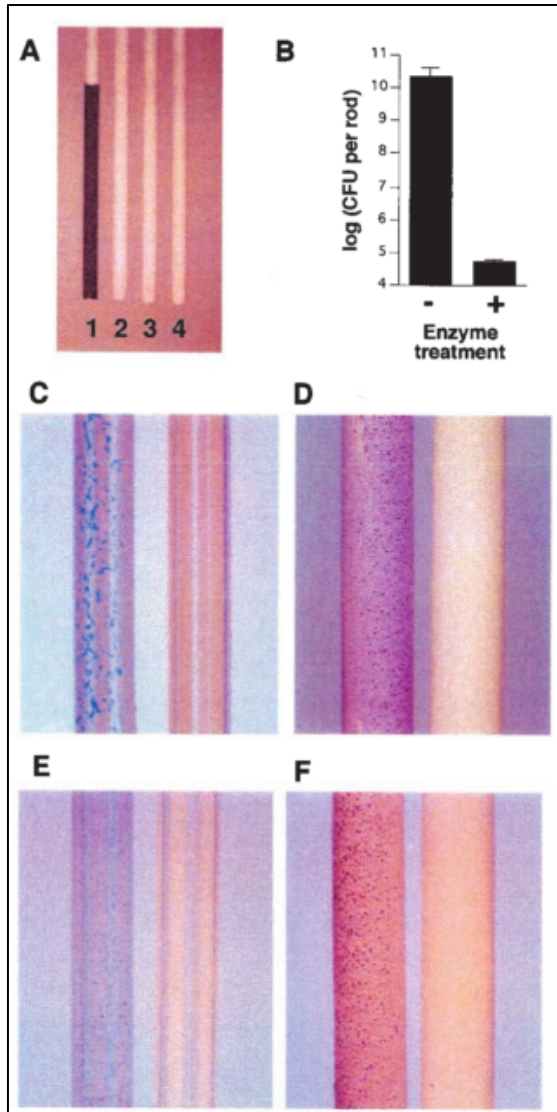


**Figure 1-3: Dispersin B and *S.***

***epidermidis* biofilms** (A) Polystyrene rods

stained with crystal violet. Rods were

incubated in broth containing *S. epidermidis*

strain NJ9709 (rods 1 to 3) or in

uninoculated broth (rod 4). Prior to staining,

rod 1 was mock treated, rod 2 was treated

with DspB, and rod 3 was sonicated. (B)

The bacteria remaining attached to the

polystyrene rods after mock treatment and

treatment with DspB were removed by

sonication and enumerated by plating of

serial dilutions on agar. Values indicate

mean numbers of bacteria per rod for

triplicate rods. (C) Polyurethane catheters

were incubated in broth containing *S.*

*epidermidis* strain NJ9709 and then mock

treated (left catheter) or treated with DspB

(right catheter). Catheters were then rinsed

and stained with methylene blue. (D) Teflon catheters were treated as described for panel (C),

except that bacteria were stained with crystal violet. (E) Polyurethane catheters were precoated

with PBS (left catheter) or PBS plus DspB (right catheter), rinsed with water, and then incubated

in broth containing *S. epidermidis* strain NJ9709 for an additional 6 h. Catheters were then rinsed

and stained with methylene blue. (F) Teflon catheters were treated as described for panel (E),

except that bacteria were stained with crystal violet. Taken with permission from Kaplan et al.

2004.

materials (Banerjee et al 2011). Materials can be modified by the addition of polar molecules such as heparin and hyaluronic acid in order to make them more hydrophilic (Carlson et al. 2004). Another way of designing adhesion-resistant biomaterials involves minimizing the number of surface contacts that bacteria can make. This has been done by grafting long-chain polymers onto the surface of materials to make brush-like structures that use steric hindrance to minimize covalent interactions between the material and the bacterial cells (Banerjee et al. 2011). Nanotechnology has also been employed to create porous or “spiky” materials that similarly limit the number of contacts between bacteria and the material surface (Puckett et al. 2010). In addition, anti-biofilm molecules in some cases have been attached to a material in order to prevent biofilm formation. An example is the coating of polyurethane (a material commonly used in medical catheters) with DspB to prevent *S. epidermidis* biofilm formation (Donelli et al. 2007). The use of natural products as biofilm antagonists has been explored due to the increased incidence of antibiotic resistance and a general trend in the American public towards more natural remedies (Taraszkievics et al. 2013). In addition, they are often easy and inexpensive to produce. Many plant extracts have been tested against a variety of bacterial biofilms, the results being reviewed in (Taraszkievics et al. 2013). One noteworthy example is that of *Allium sativum* extract (fresh garlic extract or FGE). Preventative use of 35 mg/ml FGE for 14 days in a mouse model resulted in 1,000-fold fewer bacterial cells than control mice when exposed to *P. aeruginosa* (Harjai et al. 2010).

Biofilms can be disrupted by chemical or physical methods. In fact, surgical debridement of a wound is not only a way to remove dead or diseased tissue, but it is the best way to mechanically disrupt biofilms. However, the frequency of debridement is limiting and many other harsh methods to disrupt biofilms (i.e., extreme heat, pH conditions, abrasion, etc.) are often not compatible with biological systems such as wounds.

The complex structure of bacterial biofilms includes many macromolecules. As has been described, the specific composition of the EPS of biofilms of one species is usually quite different from other species, even if they are closely related. In addition, the EPS of biofilms of just one species often contains many different components. In order to design treatments for biofilm-related infections, understanding the composition of a biofilm's EPS can be very useful. This is the subject of Chapter 2 (Purification and Characterization of Biofilm-associated EPS Exopolysaccharides from ESKAPE Organisms and other Pathogens).

## **ESKAPE**

The ESKAPE pathogens (*Enterococcus faecium*, *Staphylococcus aureus*, *Klebsiella pneumoniae*, *Acinetobacter baumannii*, *Pseudomonas aeruginosa*, and Enterobacteriaceae species) are common sources of nosocomial (hospital-acquired) and war-wound infections and represent a significant threat to public health due to their propensity for innate antibiotic resistance (Boucher et al. 2009; Calhoun et al. 2008). In addition, they readily form biofilms on indwelling

medical devices, such as catheters and prosthetic heart valves. *S. epidermidis*, while not technically an ESKAPE pathogen, is closely related to *S. aureus* and is also a formidable pathogen.

### *Enterococcus faecium*

*E. faecium* is a commensal in human digestive tracts that is also an important cause of opportunistic infections, such as bacteremia, endocarditis, and urinary tract infections (Guiton et al 2009). Its ability to form biofilms is a significant contributor to its virulence and it possesses several virulence factors related to biofilm formation (e.g. Fsr, GelE, SprE, and the autolysin AtlA). These proteins all contribute to cell lysis and reflect the large role that eDNA plays in *E. faecium* biofilms. AtlA and sortase A (SrtA) are also used to mediate surface attachment.

### Staphylococcal species

*Staphylococcus aureus* is one of the most prevalent causes of hospital-acquired infections, whereas its close relative, *Staphylococcus epidermidis*, is the most prevalent colonizer of medical implant devices (Campoccia et al. 2013) and is a major colonizer of the skin of almost every human (Otto 2012). While it lacks the many toxins that *S. aureus* utilizes to cause serious illness and is non-invasive, it is more than capable of acting as a potent opportunistic pathogen in its own right. Most diseases caused by *S. epidermidis* are chronic, medical device-

related infections that begin by the introduction of a contaminated medical device (such as a catheter or artificial joint) to the host's body (Otto 2012).

Many *S. epidermidis* virulence factors are related to biofilm formation. As a biofilm growing on the surface of medical devices, its resistance to clearance by the immune system and antimicrobials contributes to the chronic nature of its infections and the need for prolonged antibiotic therapy. In many cases, it is necessary to completely remove the device. The widespread presence of antibiotic resistance genes in *S. epidermidis* increases the number of untreatable cases that require device removal. Antibiotic resistance is usually due to the presence of the *mecA* gene which encodes for a protein that confers methicillin resistance. Polysaccharide intercellular adhesin (PIA) is the main constituent of *S. epidermidis* biofilm EPS and consists of long chains of  $\beta$ -1,6-linked *N*-acetylglucosamine with partially *N*-deacetylated amine groups. It is also known as poly-*N*-acetylglucosamine (PNAG) and is usually greater than or equal to 130 residues.

*S. epidermidis* has several microbial surface components recognizing adhesive matrix molecules (MSCRAMMs), which are proteins used for attachment to tissues and other protein-covered surfaces. These surfaces can include fibrinogen, collagen, and fibronectin. Embp is an example of a *S. epidermidis* MSCRAMM. It is necessary and sufficient for protein-dependent adherence to fibronectin. Teichoic acid is another biofilm-related virulence factor that is present in all Gram-positive bacteria and assists in *S. epidermidis* pathogenesis, adhesion, physiology, colonization, and inflammation induction.

Poly- $\gamma$ -glutamic acid (PGA) is a virulence factor that is important for immune evasion, whereas another group of molecules used in pathogenesis called phenol-soluble modulins (PSMs) are often cytolytic and pro-inflammatory.

### *Klebsiella pneumoniae*

*K. pneumoniae* frequently causes urinary tract, respiratory tract, and blood infections (Lery et al 2014). The *K. pneumoniae* capsule exists in over 75 variations/serotypes and is an important factor in immune evasion. In addition, biofilm formation is aided by genes encoding for the synthesis and transport of the PGA polysaccharide (polyglutamic acid) and for YidA, which is thought to contribute to adherence. Autoinducer-2 and type III fimbria are also important in biofilm formation.

### *Acinetobacter baumannii*

*A. baumannii* is an increasingly important pathogen that causes pneumonia, bacteremia, meningitis, and urinary tract infections (Choi et al 2009). *A. baumannii* virulence factors include a pilus and PNAG producing proteins, all of which are involved in biofilm formation. *A. baumannii* also utilizes Omp38, an autoinducer synthase, and a siderophore-mediated iron acquisition system to enhance its ability to cause disease.

### *Pseudomonas aeruginosa*

*P. aeruginosa* is a common human opportunistic pathogen that is capable of thriving in a wide range of environments. Its resilience often results in chronic infection and it is the most commonly recognized pathogen associated with chronic pneumonia in the lungs of cystic fibrosis patients (Ryder et al 2007, Mann and Woziak 2011). *P. aeruginosa* is also capable of producing several biofilm-associated polysaccharides, including alginate, Pel, and Psl (see **Figure 1-4A**).

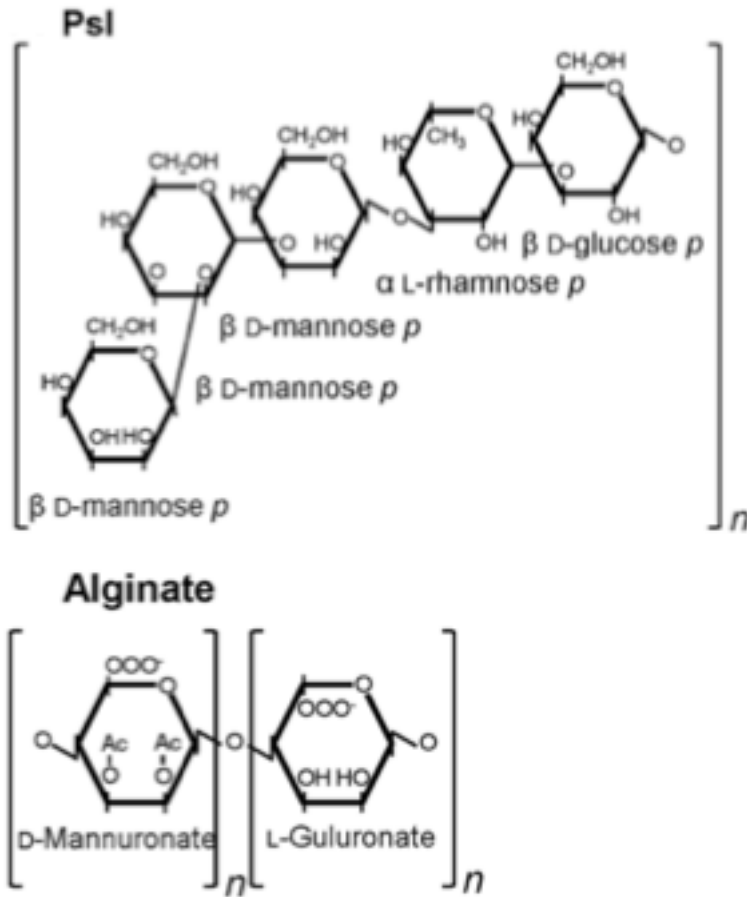
Alginate, while not essential for biofilm formation, confers considerable resistance properties and confers the “mucoid” phenotype associated with pseudomonal infections in cystic fibrosis patients (Mann and Wozniak 2011). Psl is mannose- and galactose-rich and is thought to serve as a major scaffold that crosslinks *P. aeruginosa* biofilm components. The structure of Pel, while not fully known, is rich in glucose. Pel is essential for the formation of pellicles in *P. aeruginosa*, which are biofilms at the air-liquid interface.

#### Enterobacteriaceae species

The Enterobacteriaceae is a large family of Gram-negative bacteria that includes pathogens such as *Salmonella*, *E. coli*, *Y. pestis*, *Shigella*, *Enterobacter*, and others. *E. coli* is probably the most studied member of this family and can cause food-borne and other infections (Whitfield 2006). While much is known about its capsular polysaccharides, little is known about other polysaccharides that may play a role in biofilm formation. Capsular polysaccharides include O antigens, K antigens, enterobacterial common antigen, and colonic acid, also known as M antigen (see **Figure 1-4B**). In addition to other toxins that are

present in other serotypes, *E. coli* serotype O157:H7 produces Shiga toxin, which causes severe, bloody diarrhea (Biscola et al 2011). This strain is of particular clinical relevance because of its ability to cause severe diseases such as hemorrhagic colitis and hemolytic-uremic syndrome.

A



B

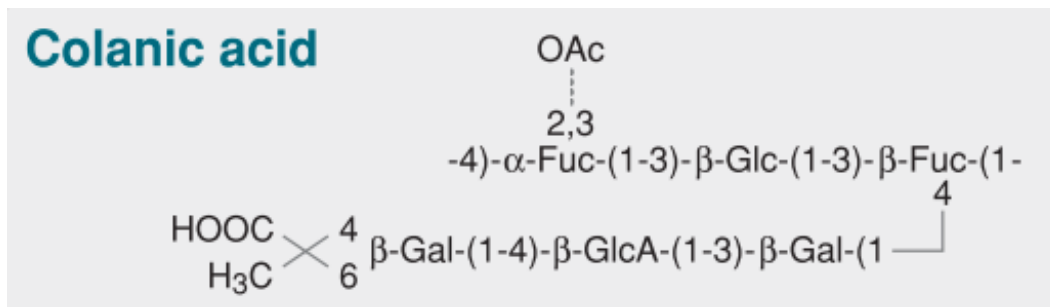


**Figure 1-4: *P. aeruginosa* and *E. coli*-produced exopolysaccharides.** (A) Pseudomonal exopolysaccharides include Psl, alginate, and Pel. The structure of Pel is not shown because it is not known (Mann and Wozniak 2012). (B) Colanic acid is a commonly-produced extracellular polysaccharide of *E. coli* (Whitfield 2006).

## CHAPTER 2

### **Purification and Characterization of Biofilm-Associated EPS Exopolysaccharides from ESKAPE Organisms and Other Pathogens**

**Patrick M. Bales**<sup>1</sup>, Emilija Miljkovic Renke<sup>1</sup>, Sarah L. May<sup>1</sup>, Yang Shen<sup>1</sup>, &  
Daniel C. Nelson<sup>1,2</sup>

<sup>1</sup>Institute for Bioscience and Biotechnology Research, University of Maryland, Rockville, Maryland, United States of America, <sup>2</sup>Department of Veterinary Medicine, University of Maryland, College Park, Maryland, United States of America

This chapter has been published as follows:

Purification and Characterization of Biofilm-Associated EPS Exopolysaccharides from ESKAPE Organisms and Other Pathogens.

Bales PM, Renke EM, May SL, Shen Y, Nelson DC.

PLoS One. 2013 Jun 21; 8(6):e67950.

## Abstract

In bacterial biofilms, high molecular weight, secreted exopolysaccharides can serve as a scaffold to which additional carbohydrates, proteins, lipids, and nucleic acids adhere, forming the matrix of the developing biofilm. Here we report methods to extract and purify high molecular weight (>15 kDa) exopolysaccharides from biofilms of eight human pathogens, including species of *Staphylococcus*, *Klebsiella*, *Acinetobacter*, *Pseudomonas*, and a toxigenic strain of *Escherichia coli* O157:H7. Glycosyl composition analysis indicated a high total mannose content across all strains with *P. aeruginosa* and *A. baumannii* exopolysaccharides comprised of 80-90% mannose, *K. pneumoniae* and *S. epidermidis* strains containing 40-50% mannose, and *E. coli* with ~10% mannose. Galactose and glucose were also present in all eight strains, usually as the second and third most abundant carbohydrates. N-acetylglucosamine and galacturonic acid were found in 6 of 8 strains, while arabinose, fucose, rhamnose, and xylose were found in 5 of 8 strains.

For linkage analysis, 33 distinct residue-linkage combinations were detected with the most abundant being mannose-linked moieties, in line with the composition analysis. The exopolysaccharides of two *P. aeruginosa* strains analyzed were consistent with the Psl carbohydrate, but not Pel or alginate. The *S. epidermidis* strain had a composition rich in mannose and glucose, which is consistent with the previously described slime associated antigen (SAA) and the extracellular slime substance (ESS), respectively, but no polysaccharide intracellular adhesion (PIA) was detected. The high molecular weight

exopolysaccharides from *E. coli*, *K. pneumoniae*, and *A. baumannii* appear to be novel, based on composition and/or ratio analysis of carbohydrates.

## **Introduction**

Microorganisms that infect humans differ in mechanisms of pathogenesis, virulence factors, and antimicrobial resistance profiles. However, one common trait shared by most is the ability and propensity to form biofilms (National Institutes of Health 2002). Along with upregulation of adhesins, phenotypic changes cause bacteria to secrete high molecular weight exopolysaccharides during conversion from planktonic to biofilm modes of growth (Crawford et al. 2008; Danese et al 2000; Kaplan et al 2004, Shemesh et al 2007). These exopolysaccharides can make up a crucial part of the extracellular polymeric substance (EPS) associated with biofilm development that serves to cement whole bacterial populations to a surface rather than enclosing individual cells (Sutherland 2001). Also included in the EPS are proteins, secreted nucleic acids, humic substances, and metal ions. Together, the EPS protects biofilm bacteria from environmental stress (Hall-Stoodley et al 2004; Kives et al 2006).

The role of the EPS in pathogenesis has been studied in many organisms where the biofilm mode of growth has been shown to allow for increased resistance to antibiotic treatment, the immune response, and nutrient-limiting conditions within the host, promoting long-term persistence (Sandal et al. 2011). Biofilm formation on medical implant devices such as catheters and mechanical heart valves is also a major problem that is closely tied to the adhesion- and

resistance-related abilities granted them by the ability to synthesize and secrete exopolysaccharides (Flemming and Wingender 2010; Lewis 2001; Tsuneda et al. 2003) Human pathogens associated with biofilm development include species of *Enterococcus faecalis*, *Staphylococcus aureus*, *Klebsiella pneumoniae*, *Acinetobacter baumannii*, *Pseudomonas aeruginosa*, and *Enterobacter spp.* These “ESKAPE” pathogens are the leading causes of nosocomial infections (Boucher et al. 2009; Revdiwala et al 2012) and are so-named to emphasize their ability to “escape” the effects of antimicrobial treatment due to acquisition of resistance genes as well as formation of biofilms.

While surface-associated exopolysaccharides and capsules play a role in both extracellular and intracellular adherence during the conversion from planktonic to biofilm growth, our interests focus on the secreted exopolysaccharides, particularly the high molecular weight exopolysaccharides that are believed to form the “backbone” of the EPS to which proteins, nucleic acids, and capsular polysaccharides adhere (Sutherland 2001; Matsukawa 2004) While there are many protocols in the literature for isolation of capsular polysaccharides or for the extraction of total bacterial EPS, only a few have attempted to fractionate exopolysaccharides by size (Sea et al. 2011) and none have been specifically tailored for the isolation of high molecular weight backbone exopolysaccharides from biofilms. Bulk EPS extraction requires methods that physically break up the biofilm matrix such as ultrasonication or EDTA, which promotes EPS separation by chelating cations that are thought to crosslink polysaccharide chains within the EPS. The use of glutaraldehyde or

formaldehyde is also common to fix bacterial cells to prevent contamination via cell lysis during the extraction steps (Azeredo et al. 1999; Liu and Fang 2002). Once the bulk EPS is extracted, the polysaccharide fraction must be separated from DNA, proteins, and lipids. Oliveira and colleagues successfully utilized 20% trichloroacetic acid (TCA) for the precipitation of proteins from the EPS (Oliveira et al. 1999), whereas Sutherland used ethanol to precipitate the polysaccharide fraction (Sutherland and Wilkinson 1965). Similar protocols have also included the use of NaOH to promote dissociation of acid groups within the EPS for increased solubility, cation exchange chromatography, differential centrifugation, and selective dialysis (Sandal et al. 2011; Anderson 2009; Comte et al. 2007; Pan et al. 2010).

Our laboratory has combined portions of the above protocols and added a size exclusion chromatography step to produce an effective method of purifying high molecular weight EPS exopolysaccharides. We then apply this methodology to biofilms of eight medically important pathogens, including several representative ESKAPE organisms, as well as a methicillin-resistant *Staphylococcus epidermidis* strain and a toxigenic strain of *Escherichia coli* O157:H7, both of which are known biofilm producers. Finally, we characterized the resulting EPS exopolysaccharides by composition and linkage analysis.

Exopolysaccharide purification was done by Emilija Miljkovic Renke and Patrick Bales. Composition and linkage analysis was done by the Center for

Complex Carbohydrate Research (Athens, GA). Lectin staining and confocal laser scanning microscopy was done by Patrick Bales and Yang Shen.

## **Materials and Methods**

### Bacterial strains and growth conditions

Unless otherwise indicated, all reagents were purchased from Thermo-Fisher Scientific and were of the highest purity available. *S. epidermidis* strain NRS-101 was obtained from the Network on Antimicrobial Resistance in *S. aureus* (NARSA). All other strains were purchased from the American Type Culture Collection (ATCC). These include two *P. aeruginosa* strains, 700829 and 700888, both known biofilm production strains; two *K. pneumoniae* strains, 700603, a multi-drug resistant strain and 700831, a biofilm strain; two *A. baumannii* strains, BAA-1878 and BAA-1605, a multi-drug resistant strain; and one *E. coli* strain, 43894, a toxigenic O157:H7 serotype. *S. epidermidis* strain NRS101 was grown in brain-heart infusion media, *K. pneumoniae* strain 700603 was grown in Luria broth, and all other strains were grown in tryptic soy broth. Glycerol stocks of all strains were stored at  $-80^{\circ}\text{C}$ . Biofilms grown for EPS purification were prepared by inoculating 20 ml of overnight culture into 400 ml of fresh media in a 1.5 L Fernbach flask to provide a large surface area for biofilm adherence. Biofilms were grown at  $37^{\circ}\text{C}$  without shaking for 4–5 days until a thick biofilm “sludge” was observed.

### EPS Extraction

After development of a mature biofilm, 60  $\mu$ l of formaldehyde (36.5% solution) was added to each 10 ml of sludge to fix the cells and prevent cell lysis during subsequent steps. The formaldehyde-sludge mixture was incubated at room temperature in a chemical hood with gentle shaking (100 rpm) for 1 hour. Four ml of 1 M NaOH was added for each 10 ml of sludge and incubated at room temperature, with shaking, for 3 hours to extract EPS. Cell suspensions were then centrifuged (16,800 $\times$ g) for 1 hour at 4°C. The supernatant containing soluble EPS was filtered through a 0.2  $\mu$ m filter (Corning) and dialyzed against distilled water using a 12–14 kDa molecular weight cut-off (MWCO) membrane for 24 hours at 25°C.

### Purification of exopolysaccharides

TCA was added (20% w/v) to extracted EPS solutions on ice to precipitate proteins and nucleic acids. After 30 minutes, the solution was centrifuged (16,800 $\times$ g) for 1 hour at 4°C, the supernatant was collected, and 1.5 volumes of 95% ethanol was added and the mixture was placed at –20°C for 24 hours to precipitate exopolysaccharides away from lipids. The solution was then centrifuged (16,800 $\times$ g) for 1 hour at 4°C and the exopolysaccharide pellet was resuspended in Milli-Q water and dialyzed against the same for 24 hours at 4°C using a 12–14 kDa MWCO membrane to remove low molecular weight impurities and the remaining retentate was lyophilized overnight. The lyophilized powder was then resuspended in 5–10 ml of phosphate buffered-saline (pH 7.4)

and purified on a 26/60 S-200 gel filtration column (GE Healthcare) using an AKTA FPLC system (GE Healthcare) that had been calibrated with gel filtration standards (Bio-Rad) to generate a standard curve of apparent molecular mass vs. retention volume. Fractions were tested for the presence of carbohydrates by the phenol-sulfuric acid method of DuBois as previously described (1956) and only high molecular weight fractions, defined as >15 kDa, containing carbohydrates were pooled, dialyzed against Milli-Q water to remove PBS, and lyophilized a final time for subsequent composition and linkage analysis.

#### Composition and linkage analysis

Carbohydrate composition and linkage analysis was performed at the Complex Carbohydrate Research Center (Athens, GA) as previously described (Merkle and Poppe 1994; York et al. 1986). Briefly, for glycosyl composition analysis, an aliquot (~500 µg) was taken from the purified EPS exopolysaccharide sample and added to a separate tube with 20 µg of inositol as an internal standard. Methyl glycosides were then prepared from the dry sample by methanolysis in 1 M HCl in methanol, followed by re-*N*-acetylation with pyridine and acetic anhydride in methanol for detection of amino sugars. The sample was then per-*O*-trimethylsilylated (TMS) by treatment with Tri-Sil (Pierce). Combined gas chromatography/mass spectrometry (GC/MS) analysis of the TMS methyl glycosides was performed on an Agilent 6890N GC interfaced to a 5975B MSD (mass selective detector), using a Supelco EC-1 fused silica capillary column (30 m×0.25 mm ID). For glycosyl linkage analysis, an aliquot

(~500  $\mu\text{g}$ ) was taken from the purified EPS exopolysaccharide sample and suspended in ~300  $\mu\text{l}$  of dimethyl sulfoxide and placed on a magnetic stirrer for 2 days. The sample was then permethylated by the method of Ciukanu and Kerek (1984), hydrolyzed for 2 hours with 2 M trifluoroacetic acid in a sealed tube at 121°C, reduced with  $\text{NaBD}_4$ , and acetylated using acetic anhydride/pyridine. The resulting partially methylated alditol acetates were analyzed by GC/MS as described above. No replicates were done for exopolysaccharide composition or linkage analyses.

#### Biofilm microscopy

Biofilms were grown in two-well chamber slides (Lab-Tek) with 1 ml of tryptic soy broth for 1 or 3 days. Biofilm wells were washed 2X with PBS and then stained with 5  $\mu\text{g}$  of the FITC-labeled *Hippeastrum* hybrid lectin (HHA) from Amaryllis (EY Labs) and Hoechst 33342, a nucleic acid stain (Invitrogen), in PBS for 1 hour at room temperature. After incubation, the wells were again washed 2X with PBS, chambers were removed from the glass slide, and biofilms attached to the slides were imaged by an Eclipse 80i fluorescent microscope workstation (Nikon) or an LSM710 laser scanning confocal microscope workstation (Zeiss) as previously described (Strathmann et al. 2002). NIS-Elements (Nikon) or ZEN (Zeiss) software packages were used for image analysis.

### **Results and Discussion**

### EPS purification

A schematic of the protocol we developed to purify EPS exopolysaccharides from biofilms is shown in **Figure 2-1**. This methodology incorporates into one protocol many extraction and purification steps successfully demonstrated by others (Azeredo et al. 1999; Liu and Fang 2002; Oliveira et al.

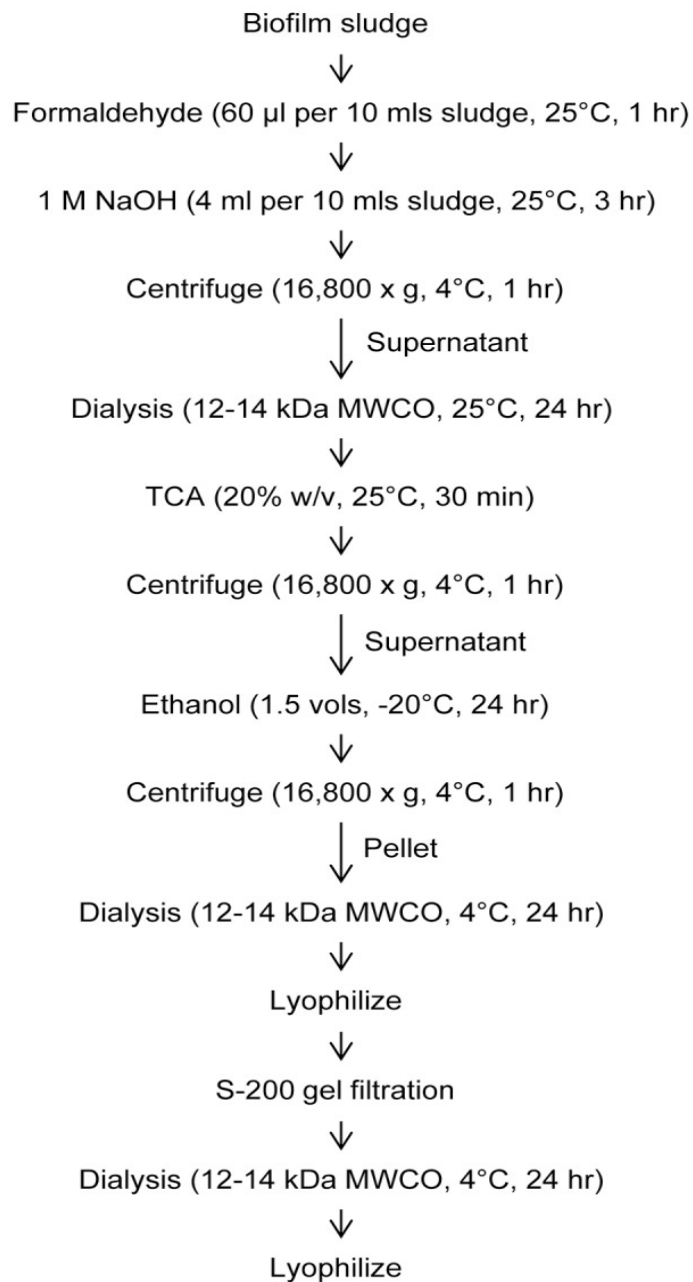


**Figure 2-1: Diagram of exopolysaccharide purification.** Depending on strain, yields range from 2– 15 mg of purified polysaccharide per starting 1.2 L of sludge. Work done by Patrick Bales and Emilija Renke.

1999; Sutherland and Wilkinson 1965; Anderson 2009; Comte 2007; Pan et al. 2010), along with selection steps for high molecular weight for exopolysaccharides (i.e.>15 kDa) through use of large pore dialysis and gel filtration. As detailed by specific examples in the sections below, our protocol did not result in isolation of surface-associated or capsular polysaccharides, indicating that the methods were specific for secreted exopolysaccharides. Additionally, the protocol was robust, allowing us to successfully extract EPS exopolysaccharide from all eight bacterial strains representing five species. Our yields ranged from 2–15 mg of purified EPS exopolysaccharide for each strain from 1.2 L of biofilm culture (three Fernbach flasks, each containing 400 ml of bacteria). This is lower than yields reported by other methods, but is most likely due to our selection of only the high molecular weight exopolysaccharide that forms the EPS backbone, which excludes lower molecular weight exopolysaccharides and oligosaccharides that would co-purify with more crude purification methods.

#### Composition and linkage analysis

The glycosyl composition results are summarized in **Table 2-1**. Across all samples, a total of 11 sugars and aminosugars were detected. Notably, mannose was found in exopolysaccharides of all strains and was the predominant carbohydrate in every strain except *E. coli*. Indeed, mannose accounted for ~80–90% of the total carbohydrate content in *P. aeruginosa* and *A. baumannii* species and ~40–50% of the total carbohydrate in *K. pneumoniae* and *S. epidermidis* species. Galactose and glucose were also found in all eight strains

tested and were often ranked as the second or third most abundant carbohydrate. Other carbohydrates were also found to be well represented in biofilm EPS exopolysaccharides. *N*-acetyl-glucosamine (GlcNAc) and galacturonic acid (GalA) were found in 6 of 8 strains while arabinose, fucose, rhamnose, and xylose were found in 5 of 8 strains. In contrast, *N*-acetyl-galactosamine (GalNAc) was only present in the *E. coli* and *S. epidermidis* strains and glucuronic acid (GlcA) was only found in a single *K. pneumoniae* strain.

The glycosyl linkage analysis for EPS exopolysaccharides of all strains is summarized in **Table 2-2**. Across all samples, 33 distinct residue-linkage combinations were detected. Consistent with the glycosyl composition results, a substantial proportion of the total linkages involved mannose. 2-linked mannose (2-Man) and terminally-linked mannose (t-Man) residues were detected in all samples, whereas 3-linked mannose (3-Man), 6-linked mannose (6-Man), and 4-linked glucose (4-Glc) were present in the EPS exopolysaccharide of 7 of the 8 strains tested. Mannose is also a common branch point for these complex structures as 2,6-linked mannose (2,6-Man) was present in 6 strains, 2,3-linked mannose (2,3-Man) was present in five strains, 3,6-linked mannose (3,6-Man) was present in three strains, and 2,3,4-linked mannose (2,3,4-Man) was present in one strain.

**Table 1.** Glycosyl Composition Analysis.

Glycosyl Residue	Abbreviation	<i>P. aeruginosa</i>					<i>K. pneumoniae</i>					<i>A. baumannii</i>					5. <i>epidermidis</i>		<i>E. coli</i>		Frequency
		700829	700888	700603	700831	BAA-1605	BAA-1878	NRS 101	43894												
Arabinose	Ara	1.6	2.4	–	–	1.5	1.1	0.5	–	–	–	–	–	–	–	–	–	–	–	5	
Fucose	Fuc	0.2	0.2	–	–	0.3	0.1	–	–	–	–	–	–	–	–	–	–	–	–	22.6	5
Galactose	Gal	3.0	3.7	14.0	7.8	4.0	13.2	1.7	2.1	–	–	–	–	–	–	–	–	–	–	8	
Galacturonic Acid	GalA	0.7	0.8	2.5	9.8	2.0	1.0	–	–	–	–	–	–	–	–	–	–	–	–	6	
Glucose	Glc	3.6	6.8	1.3	31.1	7.9	4.5	35.7	36.8	–	–	–	–	–	–	–	–	–	–	8	
Glucuronic Acid	GlCA	–	–	5.0	–	–	–	–	–	–	–	–	–	–	–	–	–	–	–	1	
Mannose	Man	89.5	84.3	49.4	38.3	84.0	79.3	52.8	9.8	–	–	–	–	–	–	–	–	–	–	8	
<i>N</i> -Acetyl-Galactosamine	GalNAc	–	–	–	–	–	–	–	–	–	–	–	–	–	–	–	–	–	–	26.8	2
<i>N</i> -Acetyl-Glucosamine	GlcNAc	–	–	0.8	0.7	0.4	1.3	3.5	1.9	–	–	–	–	–	–	–	–	–	–	6	
Rhamnose	Rha	1.0	1.3	27.0	10.0	0.1	–	–	–	–	–	–	–	–	–	–	–	–	–	5	
Xylose	Xyl	0.4	0.5	–	0.5	0.4	0.2	–	–	–	–	–	–	–	–	–	–	–	–	5	
Total:		100.0	100.0	100.0	100.0	100.0	100.0	100.0	100.0	100.0	100.0	100.0	100.0	100.0	100.0	100.0	100.0	100.0	100.0	100.0	

Values expressed as mole percent of total carbohydrate.

–, not detected.

doi:10.1371/journal.pone.0067950.t001

**Table 2-1: Glycosyl composition analysis.** Purified exopolysaccharides were analyzed by gas chromatography mass spectrometry. Work done by the Complex Carbohydrate Research Center (Athens, GA).

Glycosyl Linkage	Abbreviation	<i>P. aeruginosa</i>		<i>K. pneumoniae</i>		<i>A. baumannii</i>		5. <i>S. epidermidis</i>		<i>E. coli</i>	Frequency
		700829	700888	700603	700831	BAA-1605	BAA-1878	NRS 101	43894		
4-linked arabinopyranosyl residue	4-Ara	0.2	0.2	-	0.2	-	-	-	-	-	4
3-linked fucopyranosyl residue	3-Fuc	-	-	-	-	-	-	-	-	3.6	1
terminally-linked fucopyranosyl residue	t-Fuc	-	-	-	-	-	-	-	-	0.9	1
3-linked galactopyranosyl residue	3-Gal	-	0.3	18.2	-	0.3	-	-	-	-	3
3,6-linked galactopyranosyl residue	3,6 Gal	0.3	0.2	-	-	0.8	0.2	-	-	-	4
4-linked galactopyranosyl residue	4-Gal	1.2	1.6	-	0.2	1.1	1.6	-	1.1	1.1	6
terminally-linked galactopyranosyl residue	t-Gal	0.1	0.2	0.3	-	-	0.2	1.5	0.2	0.2	6
4-linked N-acetyl-galactosamine	4-GalNAc	-	-	-	-	-	-	-	-	0.1	1
6-linked N-acetyl-galactosamine	6-GalNAc	-	-	-	-	-	-	-	-	2.8	1
terminally-linked N-acetyl-galactosamine	t-GalNAc	-	-	-	-	-	-	-	-	0.4	1
2-linked glucopyranosyl residue	2-Glc	-	-	-	-	-	-	6.5	-	-	1
2-linked 6-deoxy-4-glucosamine	2-(6-deoxy)-4-GlcN	-	-	-	-	-	-	-	-	13.0	1
3-linked glucopyranosyl residue	3-Glc	1.2	1.3	-	14.4	-	1.3	4.0	-	-	5
3,6-linked glucopyranosyl residue	3,6-Glc	-	-	-	-	-	0.7	1.3	-	-	2
4-linked glucopyranosyl residue	4-Glc	0.2	0.4	0.4	0.4	-	0.4	1.2	39.2	-	7
4,6-linked glucopyranosyl residue	4,6-Glc	-	-	-	11.4	-	-	-	-	-	1
6-linked glucopyranosyl residue	6-Glc	0.6	0.7	-	0.4	1.3	0.8	1.3	-	-	6
terminally-linked glucopyranosyl residue	t-Glc	-	-	0.0	1.2	-	-	3.7	6.3	-	3
4-linked N-acetyl-glucosamine	4-GlcNAc	-	-	-	-	-	-	-	0.2	-	1
6-linked N-acetyl-glucosamine	6-GlcNAc	-	-	-	-	-	-	-	-	3.3	1
terminally-linked N-acetyl-glucosamine	t-GlcNAc	-	-	-	-	-	-	-	-	0.9	1
2-linked hexafuranosyl residue	2-HexF	-	-	-	12.2	-	-	-	-	-	1
2-linked mannopyranosyl	2-Man	20.6	19.3	40.1	13.8	20.2	19.2	6.0	2.0	-	8
2,3-linked mannopyranosyl residue	2,3-Man	1.3	1.2	15.4	0.5	1.2	-	-	-	-	5
2,3,4-linked mannopyranosyl residue	2,3,4-Man	-	-	-	11.6	-	-	-	-	-	1
2,6-linked mannopyranosyl residue	2,6-Man	32.3	28.5	-	16.1	32.5	28.5	32.3	-	-	6
3-linked mannopyranosyl residue	3-Man	16.7	16.0	15.4	5.2	16.5	15.9	7.5	-	-	7
3,6-linked mannopyranosyl residue	3,6-Man	0.6	0.7	-	0.4	-	-	-	-	-	3
4-linked mannopyranosyl residue	4-Man	-	0.4	-	-	-	0.4	1.2	-	-	3
6-linked mannopyranosyl residue	6-Man	1.4	1.5	-	1.2	2.2	1.6	5.7	0.7	-	7
terminally-linked mannopyranosyl residue	t-Man	23.3	27.4	1.3	10.5	25.4	27.4	27.8	25.3	-	8
2-linked rhamnopyranosyl residue	2-Rha	-	-	7.3	-	-	-	-	-	-	1
terminally-linked rhamnopyranosyl residues	t-Rha	-	-	1.6	0.3	-	-	-	-	-	2
2-linked xylopyranosyl residue	2-Xyl	-	0.1	-	-	-	0.1	-	-	-	2
<b>Total:</b>		<b>100.0</b>	<b>100.0</b>	<b>100.0</b>	<b>100.0</b>	<b>100.0</b>	<b>100.0</b>	<b>100.0</b>	<b>100.0</b>	<b>100.0</b>	

Values expressed as mole percent of total carbohydrate.  
 - , not detected.  
 doi:10.1371/journal.pone.0067950.t002

**Table 2-2: Glycosyl linkage analysis.** Purified exopolysaccharides were analyzed by gas chromatography mass spectrometry. Work done by the Complex Carbohydrate Research Center (Athens, GA).

### Strain variability within a species

For each of the three ESKAPE pathogens tested, we analyzed two independent strains, which provide a means to assess strain-to-strain variability by our methods. In the two *P. aeruginosa* strains, 700829 and 700888, both were found to be >85% mannose by composition, followed by minor constituents of glucose, galactose, arabinose, and rhamnose (**Table 2-1**). Likewise, the major linkages of EPS exopolysaccharides from both strains in order were 2,6-Man, t-Man, 2-Man, and 3-Man (**Table 2-2**). Similar to the *P. aeruginosa* results, both *A. baumannii* strains, BAA-1605 and BAA-1878, had a nearly identical composition and linkage profile not only to each other, but also to the *P. aeruginosa* strains. In sharp contrast, the two *K. pneumoniae* strains differed considerably from each other. While both strains had high mannose content, the next most abundant carbohydrates for strain 700603 were rhamnose, galactose and GlcA. For strain 700831, those residues were replaced by glucose, rhamnose, and GalA in order of importance. 700603 contained 5% GlcA, which was not found in 700831 and the latter contained trace amounts of arabinose, fucose, and xylose, which were all absent in the former. Thus, in instances where our data differ from historical results as described below, we cannot conclude whether these variations are attributable to differences in extraction/purification methods, or simply represent natural strain to strain heterogeneity within a species as displayed by the two *K. pneumoniae* strains we tested.

### Species-specific findings

Of the bacteria studied in this report, biofilms of *P. aeruginosa* are perhaps the best studied. *P. aeruginosa* produces alginate, a high molecular weight, acetylated polysaccharide that is well known for its association with the mucoid phenotype common in cystic fibrosis patients. It is composed of  $\beta$ -1,4 linked L-guluronic and mannuronic acids. In addition, some *P. aeruginosa* species are known to produce Psl, which consists of a repeating pentasaccharide of 3 mannose, 1 rhamnose, and 1 glucose (Byrd et al. 2009), and Pel, whose exact structure is not completely known, but is reported to have a high glucose content (Friedman and Kolter 2004; Friedman and Kolter 2004). Very little data are available on the specific strains we tested, 700829 and 700888, although 700888 has been sequenced. Its genome possesses all of the genes for production of alginate (*alg44*, *alg8*, *algA*-*algZ*, *mucA*-*mucC*) and Psl (*pslA*-*pslM*), but does not contain the genes for Pel. Since we found the EPS exopolysaccharide from both *P. aeruginosa* strains to be predominantly mannose (~85–90%) and the linkages were chiefly 2-Man, 3-Man, 2,6-Man, and t-Man, we conclude that the majority of the EPS exopolysaccharide we observed is consistent with Psl, although we cannot rule out additional structures.

Much is also known about exopolysaccharides of *S. epidermidis*, in particular the NRS-101 strain (a.k.a., RP62A; ATCC 35984) we employed for this study. This strain and similar *S. epidermidis* strains are known to have linear  $\beta$ -1,6-linked GlcNAc polysaccharides, termed the polysaccharide intercellular adhesion (PIA), encoded by the *icaADBC* operon that mediates intercellular

interactions during the biofilm mode of growth (Cramton et al. 1999; Mack et al. 1994). A separate, galactose-rich capsular polysaccharide adhesion (CPA) is also reported to be associated with this strain (Tojo et al. 1988). Christensen and colleagues used a mutant of RP62A that lacked the ability to make CPA and isolated a high molecular weight exopolysaccharide, called the slime associated antigen (SAA), which was found to be primarily glucose (~59%) (Christensen et al. 1990). In contrast, Peters *et al.* isolated a mannose-rich exopolysaccharide from a slime layer of *S. epidermidis* strain KH11 and called it the extracellular slime substance (ESS) (Peters et al. 1987). We did not observe any evidence of PIA, which would be expected given the methods we used and the surface localization of this polysaccharide. However, our results indicate the high molecular weight EPS exopolysaccharide is 52.8% mannose and 35.7% glucose, suggesting both SAA and ESS may be present in our sample. Further experimentation is required to define the structures of these polysaccharides.

The polysaccharides of *E. coli* associated with the capsular O serogroups and K-antigens have been studied extensively, but comparatively little is known about the non-capsule high molecular weight exopolysaccharides of the EPS (Whitfield and Roberts 1999). However, most *E. coli* strains are known to secrete colanic acid, which consists of glucose, galactose, fucose, GlcA, acetate, and pyruvate in molar proportions roughly 1:2:2:1:1:1, respectively (Stevenson et al. 1996; Sutherland 1969). Moreover, the O157:H7 strain we tested, ATCC 43894 (a.k.a. CDC EDL 932), has been shown to specifically generate colanic acid as its exopolysaccharide (Junkins and Doyle 1992). While our data show this

same strain produces glucose (36.8% of total carbohydrate), fucose, (22.6%), and galactose (2.1%) as would be expected for colanic acid, the proportions are not consistent with colanic acid and most noticeably, there is a complete absence of detectable GlcA. In addition, the presence of GalNAc (26.8%), mannose (9.8%), and GlcNAc (1.9%) were unexpected findings, suggesting we isolated a previously uncharacterized exopolysaccharide.

Similar to *E. coli*, the surface exopolysaccharides (K-antigens) of *K. pneumoniae*, numbering over 80 serovars, have been studied in detail. However, there have only been a few attempts to isolate the exopolysaccharide associated with biofilm EPS. Rättö and colleagues used an ethanol extraction protocol to isolate EPS exopolysaccharide from two similar *K. pneumoniae* strains and found each contained ~60% mannose, 20% galactose, and 17% GalA (Ratto et al. 2001). While both of our *K. pneumoniae* strains contained a high percentage of mannose as well as significant amounts of galactose and GalA, they also possessed considerable rhamnose as well as minor fractions of arabinose, fucose, GlcA, GlcNAc, and xylose, depending on strain. This indicates both strains may possess EPS exopolysaccharide structures that have not been previously characterized. Despite the remarkable heterogeneity in EPS exopolysaccharide composition between the two *K. pneumoniae* strains, it is interesting to note that the isolated exopolysaccharides bear no resemblance to the known K-antigens. For example, strain 700603 has a K6-type capsule composed of a repeating linear polysaccharide of fucose, glucose, mannose and GlcA in equal proportions (Elsässer-Beile 1978). In our analysis, the composition of these

moieties was 0% fucose, 1.3% glucose, 49.4% mannose, and 5.0% GlcA. Thus, we can conclude that our extraction/purification methods are effective at separating the high molecular weight EPS exopolysaccharide from capsular polysaccharides.

The EPS exopolysaccharide of *A. baumannii* is the least studied of all the pathogens we tested. Cell-associated poly- $\beta$ -1,6-linked GlcNAc has previously been linked to biofilm development in *A. baumannii* (Choi 2009), but our protocol should not have isolated this surface polysaccharide, which is confirmed by the composition results for the two *A. baumannii* strains we tested, each of which showed only  $\sim$ 1.0% GlcNAc. Crude extraction of EPS exopolysaccharide has been performed on other species of *Acinetobacter*, including *A. junii* (3 mannose: 1 galactose: 1 arabinose) (Yaday et al. 2012) and *A. calcoaceticus* (4 rhamnose: 1 glucose: 1 glucuronic acid: 1 mannose) (Kaplan et al. 1985) but neither of these composition ratios matches the results of our two *A. baumannii* strains (BAA-1605; BAA-1878), indicating our exopolysaccharide may be a new finding.

#### Mannose contribution to EPS

The most salient finding of our study was the high mannose content of the EPS exopolysaccharide across all species and strains (**Table 2-1**). As such, we investigated the binding of the Amaryllis HHA lectin to pathogen biofilms. HHA specifically binds  $\alpha$ 1,3 and  $\alpha$ 1,6-linked mannose units (Kaku 1990), linkages that are common to all 8 pathogens tested (**Table 2-2**). When designing lectin binding experiments, we focused on biofilms of *E. coli* strain 43894, since the EPS

exopolysaccharide of this strain had the lowest mannose content (9.8%) of all strains tested. As can be seen in **Figure 2-2A**, HHA binding results in an extracellular cloud around *E. coli* cells in 1 day biofilms. When 3 day biofilms are viewed by confocal microscopy (**Figure 2-2B**) HHA only binds to the outer surface of the ~40  $\mu\text{m}$  biofilm, presumably limited in diffusion by the density of the biofilm matrix. In the future, specificity of HHA lectin for mannose can be verified by immobilizing polymeric mannose on a nitrocellulose membrane and then testing for HHA binding by dot blotting. In contrast to the HHA lectin, which is a globular protein composed of 4 subunits, the small molecular weight nucleic acid stain penetrates the full thickness of the biofilm matrix, staining all *E. coli* cells within the matrix. Given the frequent use of mannose by microorganisms as a component of surface antigens or capsule, detection of mannose alone cannot be considered diagnostic for the presence of a biofilm. Nonetheless, mannose was ubiquitous in the biofilm exopolysaccharides of the five species we tested and even the EPS with the lowest mannose content was easily visualized by staining with the HHA lectin. Additional lectins or a lectin-based array (Angeloni et al. 2005) may be useful in future characterization of EPS composition from a broad range of organisms.

Previous studies of extracellular polysaccharide composition have detected high levels of mannose as the result of contamination of growth media components, specifically mannan from the yeast extract portion of tryptic soy broth (Pier et al 1983). While we cannot rule out the possibility of the presence of some contaminant mannose in our samples, the large differences between the

molar percentage of mannose present in the tested strains suggests that contaminants do not play an overwhelming role in this study. The lowest percent mannose makeup is less than 10% whereas the highest is almost 90%. In the future, removing mannose with a mannan-binding column prior to composition and/or linkage analysis, as suggested by Pier, et al (1983), may be done to rule out the influence of yeast extract contaminants. In addition, biofilms could be grown with chemically defined media lacking mannose.

#### EPS staining of *E. coli* strain 43894 biofilms.

It has long been known that the exopolysaccharide portion of the EPS plays a substantial role in bacterial adherence and resistance (Sutherland 2001; Hall-Stoodley et al. 2004; Parsek and Singh 2003) and the mannose results above suggests there may be commonalities between biofilm EPS that can be exploited for diagnostic and/or therapeutic purposes. For example, breaking the most common bonds that connect polysaccharide residues in the EPS could be an

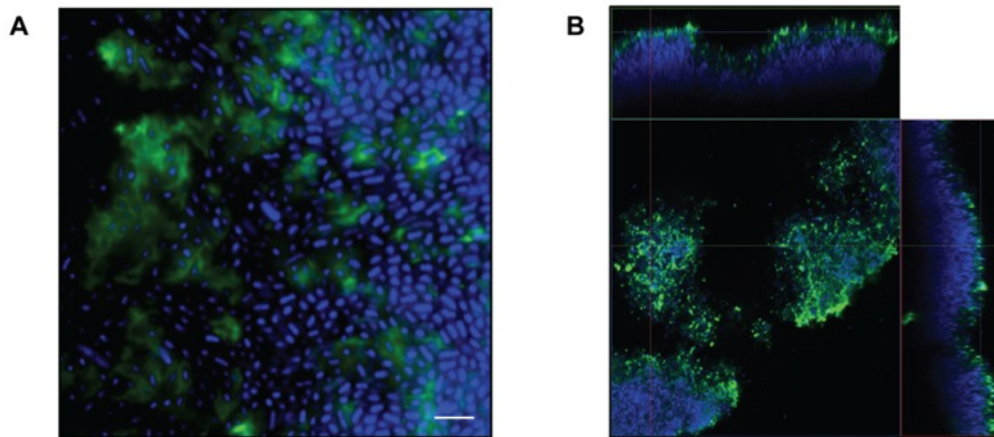


**Figure 2-2: EPS staining of *E. coli* strain 43894 biofilms.** The FITC-labeled mannose-specific HHA lectin was used to stain exopolysaccharides (green) and Hoechst 33342 was used to stain the bacterial nucleic acids (blue). (A.) Extracellular green staining of the EPS by FITC-HHA can be seen on 1 day old biofilms of *E. coli* at 200X. Scale bar =5 mm. (B.) Confocal image of 3 day old *E. coli* biofilms at 63X. The large square panel is a plan view looking down on the biofilm. The top and right-side rectangular panels are vertical sections representing the XZ plane and YZ plane, respectively, at the positions indicated by the colored lines. The biofilm is 40 mm thick (i.e. Z-axis). Work done by Patrick Bales and Yang Shen.

effective means of dispersing biofilms and making the subjacent bacteria more susceptible to treatment by antibiotics. Notably, bacteriophage have co-evolved with natural biofilms of host organisms for billions of years and have developed enzymatic domains on tail fiber and tailspike proteins that degrade polysaccharides of the EPS and capsule, allowing the phage access to surface receptors for infection (Casjens and Thuman-Commike 2011; Sutherland et al. 2004; Yurewicz et al. 1971). These enzymes, generically termed depolymerases, have been shown to degrade exopolysaccharides even in the absence of phage (Hughes et al. 1998), although extensive analysis of their specificity and utility as anti-biofilm agents has yet to be elucidated.

Another example of a potential anti-biofilm enzyme is dispersin B (DspB), a  $\beta$ -1,6-*N*-acetyl-glucosaminidase from the bacterium *Actinobacillus actinomycetemcomitans*. First described in 2003 (Kaplan 2003), this enzyme has the ability to degrade EPS from *Actinobacillus* (Kaplan 2004) and *S. epidermidis* (Chaignon 2007; Kaplan 2004) biofilms. While enzymatic digestion of the EPS exopolysaccharide is not expected to directly kill bacterial cells, the dissolution of biofilms or prevention of future biofilm formation should allow bacteria to become re-sensitized to antibiotics and immune system mechanisms (i.e., complement, antibodies, phagocytes, etc.) Alternatively, these agents could be used to prevent biofilm formation. For example, DspB has been successfully incorporated into a polyurethane material, showing that materials, such as medical implants, could be engineered with anti-biofilm enzymes to prevent colonization (Donelli et al. 2007).

Obtaining detailed structural characteristics by NMR for the current set of EPS exopolysaccharides in relationship to the composition and linkage data generated here will help validate our extraction and purification methods. Further characterization of ESKAPE biofilm EPS by the methods we employed here may also enable the identification and design of more effective anti-biofilm therapeutic agents.

### **Acknowledgments**

The authors acknowledge Parastoo Azadi and the Complex Carbohydrate Research Center at the University of Georgia, Athens for assistance with sample processing. We also thank Sara Linden and Debra Weinstein for technical assistance.

## CHAPTER 3

### **HexNW is a Highly Thermostabile Glucosaminidase that Disperses *S. epidermidis* Biofilms**

**Patrick M. Bales**<sup>1</sup>, Ryan D. Heselpoth<sup>1</sup>, & Daniel C. Nelson<sup>1,2</sup>

<sup>1</sup>Institute for Bioscience and Biotechnology Research, University of Maryland, Rockville, Maryland, United States of America, <sup>2</sup>Department of Veterinary Medicine, University of Maryland, College Park, Maryland, United States of America

This chapter has been submitted for publication.

## Abstract

*Staphylococcus epidermidis* is a bacterium that is found on the skin of almost all humans but is capable of opportunistic infection (often by colonizing medical implant devices). When it does so, it normally survives by growing as a biofilm. Biofilm-forming bacteria are notoriously difficult to eradicate due to the resistance to antimicrobials and other stressors provided by the extracellular polymeric substance (EPS). Polysaccharide intercellular adhesin (PIA) is a major constituent of *Staphylococcus epidermidis* EPS and is made up of partially deacetylated  $\beta$ -1,6-*N*-acetylglucosamine.

A bioinformatics search of putative hexosaminidases and glucosaminidases that may be able to break up *S. epidermidis* biofilms revealed an uncharacterized enzyme produced by *Neisseria wadsworthii*, henceforth referred to as HexNW. It was found to be active against a synthetic substrate containing *N*-acetylglucosamine and had a  $K_m$  of  $1.1 \pm 0.4$  mM and a  $V_{max}$  of  $4.0 \pm 0.5$  pmols/sec, but it did not display activity against chitin-like substrates. In addition, HexNW was found to be highly thermostable by measuring enzymatic activity after incubation at various temperatures and by performing circular dichroism and differential scanning calorimetry. Finally, HexNW was shown to be antagonistic to *S. epidermidis* biofilms by monitoring the release of amino sugars and colony-forming units from the surface of the biofilm. In addition, a 2-fold decrease in the minimum biofilm elimination concentration (MBEC) was observed when HexNW was used to supplement vancomycin treatment of a methicillin-resistant *S. epidermidis* strain.

The only other enzyme that has been studied that is effective against this species is dispersin B (DspB), which is homologous to HexNW (63%). The significant differences in amino acid sequence between these proteins as well as the thermostability of HexNW makes it promising tool to combat biofilm-related infections of *S. epidermidis*.

Identification of HexNW was done by Daniel Nelson. Synthesis was done by Life Technologies. Expression, purification, and all enzyme activity assays were done by Patrick Bales. Circular dichroism and differential scanning calorimetry experiments were done by Ryan Heselpoth.

## **Background**

While bacterial pathogenesis mechanisms, virulence factors, and antimicrobial resistance vary greatly between species, the ability and preference to grow as biofilms are common to the vast majority (Hall-Stoodley et al. 2004). Biofilms are formed when planktonic bacteria (i.e., free, individual cells) adsorb onto a wound surface and form colonies (Hall-Stoodley et al. 2004; Stewart et al. 2008; Stoodley et al. 2002). Once the colonies become established, genetic regulation causes them to secrete high molecular weight carbohydrates (i.e., polysaccharides) that serve as the structural backbone for the biofilm. Non-cellular components and debris, including additional carbohydrates, proteins, lipids, and nucleic acids, become entangled in the polysaccharide backbone and constitute the “slime” layer of a biofilm which is technically known as the extrapolymeric substance, or EPS (Flemming and Wingender 2010). The EPS is

thought to protect the bacteria from antimicrobials, antibodies, and circulating immune cells.

The natural resilience of biofilms along with the rise of antibiotic-resistant pathogens illustrates the urgent need for new and innovative ways to treat biofilm-related infections. Biofilms are responsible for complications such as secondary wound infections, chronic *P. aeruginosa* infection in the lungs of cystic fibrosis patients, and the colonization of medical implant devices. As an example, coagulase-negative staphylococci such as *Staphylococcus epidermidis*, which are typically viewed as less virulent than their coagulase-positive counterparts, including *S. aureus*, are responsible for about 250,000 cases of intravascular catheter infections per year with a cost of about \$25,000 per case and hospital stays exceeding 7 days (Otto 2012).

Research focused on ways of treating bacterial infections specific to biofilm-formers is lacking. Methods include the use of metal chelators, phages, or modifications to surfaces with silver nanoparticles (Bookstaver et al. 2009, Bartell et al. 1969, Kalishwaralal et al. 2010). In addition, proteins that digest components of the EPS (EPS depolymerases) can be effective (Hughes et al. 1998). As the matrix that encapsulates bacterial cells is degraded, the bacteria in the biofilm revert to a planktonic lifestyle and are resensitized to the action of the immune system and antibiotics.

Dispersin B (DspB) is a glycoside hydrolase produced by *Actinobacillus actinomycetemcomitans* that is the only well-studied EPS depolymerase to date. It is effective in breaking up biofilms of *S. epidermidis* which are formed on

polystyrene rods, polyurethane catheters, and Teflon catheters (Kaplan et al. 2004). In addition, DspB has been found to be effective against other  $\beta$ -1,6-*N*-acetylglucosaminine-containing biofilms. Izano, et al (2008) found that DspB prevented biofilm growth in both *S. epidermidis* and *S. aureus* when used to supplement growth media, while Darouiche and colleagues (2009) observed that DspB is effective at breaking up and dispersing *E. coli* biofilms. Dispersin B has also been used in unique applications to prevent and treat biofilms. It has been bound in conjunction with an antibiotic to polyurethane (a common material used in intravenous catheters) and is capable of preventing biofilm formation in that state. (Donelli et al. 2007). A T7 phage has even been engineered to express DspB, which greatly increases the killing ability of the phage towards *E. coli* biofilms (Lu 2007). A bioinformatics search for additional glucosaminidases revealed HexNW, which is the focus of this manuscript. It is homologous to DspB and is equally effective in breaking up *S. epidermidis* biofilms but has the great advantage of being highly thermostable.

## **Materials and methods**

### Bacterial strains, growth conditions, and biofilm formation

*E. coli* DH5 $\alpha$  was used for cloning and BL21 (DE3) was used for expression. While BL21 (DE3) was used as the expression strain, the expression vector (pBAD24) provides an arabinose-activated promoter that is not dependent on BL21 (DE3) expression of T7 RNA polymerase. Biofilms of *Staphylococcus*

*epidermidis* strain NRS 101, also known as RP62A and ATCC 35984, came from the Network on Antimicrobial Resistance in *Staphylococcus aureus* (NARSA). It is a *mecA* positive, slime positive strain sequenced by TIGR. For cloning, the growth media used was Luria Broth supplemented with ampicillin. NRS 101 biofilms were grown for 24 hours at 37°C without shaking. Plates used for biofilm formation included MBEC™ biofilm inoculator, physiology and genetics panel (Innovotech), CoStar® Corning® CellBIND® Surface 24 well polystyrene plates with lids, and NEST 96-well, polystyrene cell culture plates.

#### Gene synthesis, expression, and purification

Dispersin B- and HexNW-encoding plasmids (see GeneBank accession numbers AAP31025.1 and WP\_009115775.1 for corresponding proteins) were synthesized using the GeneArt® Gene Synthesis service provided by Life Technologies ([www.lifetechnologies.com](http://www.lifetechnologies.com)) after codon optimization for *E. coli* expression of BLAST-derived gene sequences. Depolymerase genes were cloned into the pBAD24 vector using restriction sites that were included in the gene synthesis. Also included were sequences encoding N-terminal 6xHis tags. Plasmids were transformed into BL21 cells, which were then grown until mid-log phase (OD<sub>600</sub> 1.3-1.7). Protein expression was induced with 0.25% arabinose and cultures were grown at 18°C for 4 hours or overnight. Depolymerases were harvested by centrifugation at 7,000 rpm for 15 minutes, resuspension in phosphate-buffered saline (PBS, 50 ml per liter of culture) plus 1 mM PMSF, and sonication for 10 min using a sonicator set to 30% duty cycle and level 6 output.

The resulting solution was centrifuged at 13,000 rpm for 1 hr. The supernatant was saved. Depolymerases were then purified from cell lysate by nickel affinity purification using Bio-Scale Mini Profinity IMAC cartridges (Biorad). After loading onto a charged column, the column was washed with 20 mM imidazole, 20 mM MES pH 6.5, and 1 M NaCl before eluting with 250 mM imidazole.

#### Enzyme activity assays

HexNW and DspB were combined with PBS and 4-nitrophenyl *N*-acetyl-D-glucosaminide (pNP-GlcNAc, Sigma) to directly measure enzymatic activity. This substrate consists of one N-acetylglucosamine unit and a nitrophenyl group (extinction coefficient of  $18,600 \text{ M}^{-1}\text{cm}^{-1}$ , Shibata et al. 1997). When cleaved, the emitted nitrophenyl group can be monitored colorimetrically by measuring absorbance at 405 nm. All reactions were done in NEST polystyrene 96-well plates and absorbance read at 405 nm using a Molecular Devices SpectraMax M5 spectrophotometer. The predicted molecular weights of HexNW (57.9 kDa) and DspB (42.0 kDa) and the reported molecular weight on pNP-GlcNAc (342.3 g/mol) were used to adjust enzymes to concentrations of 10  $\mu\text{M}$  and to adjust pNP-GlcNAc to final concentrations varying from 10  $\mu\text{M}$  to 5 mM. Unless otherwise described, reactions were done in 40 mM boric acid 40 mM phosphoric acid buffer (BP buffer) at pH 6.5. Kinetic assays were done at 20 second intervals and with 5 seconds of shaking before readings were taken. Kinetic assays were normally done for 30 minutes total. Enzyme kinetic readings were done using the Softmax Pro software version 5.4.1. Initial velocities were calculated by taking

data during time points in which  $R^2$  values for all replicas were at least 0.95 and were done by observing the change in milli-absorbance units (mAU) at 405 nm per minute.

The velocity at each substrate concentration was calculated by first converting from mAU/min to AU/sec. Using the assumptions of Beer's law, AU/sec was converted to M/sec. The reaction volume of 200  $\mu$ l was used to convert from M/sec to mol/sec. The velocity (mol/sec) was therefore calculated as follows:  $V$  (mol/sec) = (milliAU/min  $\times$  min/60 sec  $\times$  AU/1000 milliAU  $\times$  1 cm)/(18,600  $M^{-1}cm^{-1}$ )  $\times$  ( $2 \times 10^{-4}$  liters). The 18,600  $M^{-1}cm^{-1}$  value is the extinction coefficient of the 4-nitrophenoxide released from the substrate at 405 nm (Shibata, 1996). Maximal velocity  $V_{max}$  and the Michaelis-Menten constant  $K_m$  were calculated by hyperbolic regression analysis using the program Hyper32. Error (standard deviation) was estimated using the average values of triplicate reactions and was also calculated by the Hyper32 fitting program. The turnover number,  $k_{cat}$ , was calculated as follows:  $k_{cat}$  ( $s^{-1}$ ) = average  $V_{max}/E$ , where E is the mols of DspB or HexNW in the assay. E was determined by multiplying the molar concentration of each enzyme in mol/L times the reaction volume in liters. Therefore, at final enzyme concentrations of 10  $\mu$ M, both DspB and HexNW had 2 nmols per each 200  $\mu$ l reaction well in the 96 well plate.

### Chitinase experiments

HexNW and a chitinase (both at 1 mg/ml) from *Streptomyces griseus* (Sigma) were incubated with a chromogenic chitin substrate, 4-nitrophenyl  $\beta$ -D-

N, N', N''-triacetylchitotriose (Sigma, 1 mg/ml) or buffer for one hour at 37°C. Optical density at 405 nm was read as a measure of chitinase activity.

#### pH profile assays

Enzyme activity assays were done as described above, except that the concentration of pNP-GlcNAc substrate was always 1 mM while the pH was varied. This substrate concentration was chosen because it is close to the  $K_m$  values of DspB and HexNW and produced a robust increase in  $OD_{405}$  at 10  $\mu M$  DspB and HexNW. The buffer used was 40 mM boric acid 40 mM phosphoric acid buffer, which was adjusted to a range of pH values between 3 and 11.

#### Thermostability assays

Thermostability assays were done by incubating enzymes at various temperatures for 30 min, putting them on ice for 5 minutes followed by 10 minutes at room temperature, and then assaying enzymatic activity of the enzymes at 10  $\mu M$  as described above.

CD experiments were performed on a Chirascan CD Spectrometer (Applied Photophysics) equipped with a thermoelectrically controlled cell holder. For secondary structure far-UV analysis, the protein was at a 0.1 mg/ml concentration in 20 mM sodium phosphate buffer pH 7.0. CD spectra were obtained in the far-UV range (190-260 nm) in a 1 mm path length quartz cuvette at 1 nm steps with 5 second signal averaging per data point. Spectra were collected in triplicate, followed by averaging, baseline subtraction, smoothing and

conversion to mean residue ellipticity (MRE) by the Pro-Data software (Applied Photophysics). Secondary structure prediction was performed using the Provencher and Glockner method provided by DICHROWEB (Provencher and Glockner 1981; Whitmore and Wallace 2004). Melting experiments were performed by heating the protein at a 1 mg/ml concentration in 20 mM sodium phosphate buffer pH 7.0 from 20°C to 95°C at 1°C/min. MRE was monitored at 222 nm in a 1 mm path length quartz cuvette at 0.5°C steps with 5 second signal averaging per data point. The melting data was smoothed, normalized and fit with a Boltzmann sigmoidal curve when applicable. The first derivative of the melting curve was then calculated to determine the temperature ( $T_{1/2}$ ) for each sample at which the folded and unfolded state of the particular protein species was at equilibrium (Falass and Hartgerink 2012).

DSC experiments were performed on a Nano DSC Differential Scanning Calorimeter (TA Instruments) at a constant pressure of 3 atm. All samples were degassed for at least 20 minutes prior to the experiment. The sample and reference cells consist of an optimal operational volume of 0.3 ml and were calibrated with equal volumes of 20 mM sodium phosphate buffer pH 7.0 by means of three consecutive heating/cooling cycles from 5°C to 105°C and 105°C to 5°C. DspB and DspNW were then heated from 5°C to 105°C at a 1°C/min heating rate in 20 mM sodium phosphate buffer pH 7.0 using a final protein concentration of 1 mg/ml followed by immediate cooling from 105° to 5°C at 1°C/min. Data analysis by means of baseline subtraction and curve fitting was performed by the NanoAnalyze software (TA Instruments).

### Amino sugar assays

NRS 101 biofilms were grown for 26 hours, washed twice with water, aspirated, and then incubated with 0.25 mg/ml HexNW or boric acid phosphoric acid buffer, pH 6.5, for 1 hour at 37°C. The treatment fluid was then removed and spun at 12,000 rpm for 10 minutes. Supernatant containing released sugars (50 µL) was added to 100 µL pentadione solution, boiled for 1 hour, and then added to 100 µL of Ehrlich I solution according to the Morgan-Elson method (Strominger et al. 1959). Optical density at 530 nm was then measured to assay the presence of amino sugars. Each sample was performed in triplicate.

### CFU release

Biofilms were grown as described above. After treatment with enzyme (0.25 mg/ml) or PBS buffer for 1 hour at 37°C, the solution was spun at 12,000 rpm for 10 minutes and the pellet washed once with sterile TSB. After resuspension in TSB, the cell suspension was serially diluted and plated using spread plate technique to estimate the colony forming units released from the biofilms as a result of HexNW treatment. Each sample was performed in triplicate. Percent increase in CFU after biofilm treatment with HexNW was calculated by subtracting the CFU value of each replica from the average CFU value of mock-treated biofilms, dividing by the mock-treated CFU value, and then multiplying by 100. The standard deviation of all three replicas' CFU values was treated the same as HexNW CFU values (it was subtracted from mock-treated

CFU value, divided by the mock-treated CFU value, and then multiplied by 100) to give the error shown in the results figure.

### Minimum Inhibitory Concentration (MIC) and Minimum Biofilm Elimination Concentration (MBEC) Assays

For MIC determination, overnight cultures of *S. epidermidis* NRS 101 were grown in NEST 96-well plates at 37°C with shaking. The following day, two-fold dilutions of filtered vancomycin were done in another 96-well plate, from 64 µg/ml down to 0.125 µg/ml. Dilutions were done using sterile water. Control wells without any vancomycin were also made. Overnight culture was then added to the antibiotic or water-containing wells by pipetting 2 µl of culture into each well. The inoculated plate was then secured in a 37°C shaking incubator and allowed to grow overnight. The MIC is defined as the lowest concentration of vancomycin that prevents NRS 101 growth (Sepandj et al. 2004).

For MBEC determination, biofilms of NRS 101 were grown as described above, except in this instance, Innovotech MBEC™ biofilm inoculators (physiology and genetics panel) were used. These growth plates are in 96-well format and have polystyrene pegs attached to the plate lids such that when placed on the tray, the pegs are inserted into each well. After biofilm growth for 24 hrs at 37°C, growth media and planktonic cells were removed by shaking into a pan filled with bleach water. Biofilms on the pegs and tray were washed by dunking twice in a separate pan filled with water. Vancomycin was added to concentrations indicated and enzymes were added to a final concentration of 0.05

mg/ml. The lid was replaced onto the tray and allowed to incubate at 37°C for 3 hours without shaking. Following incubation, sterile TSB was added to a new 96-well plate (NEST) and used to wash the pegs by dunking. TSB (200 µL) was added to another new 96-well plate and the lid was placed onto this tray and secured with tape. The plate was then incubated overnight at 37°C. The next morning, growth was observed visually and by measuring optical density of the wells at 600 nm using a Molecular Devices SpectraMax M5 spectrophotometer. The MBEC is the lowest concentration that results in no growth when treated biofilms are exposed to sterile media (Sepandj et al. 2004).

## **Results**

### Identification, expression, and purification

HexNW (NCBI accession number ZP\_08938922.1) was identified as a possible  $\beta$ -1,6-*N*-glucosaminidase by performing protein BLAST conserved domain searches. It is produced by the mesophilic skin bacteria *Neisseria wadsworthii* (Wolfgang et al 2011). This domain is found in glycosyl hydrolase family 20 and has a TIM barrel fold (Marchler-Bauer et al. 2013). It is also homologous (63% identity) to the  $\beta$ -*N*-acetylglucosaminidase domain found in DspB (**Figure 3-1**). This domain encompasses amino acid residues 12 to 360 of this 508 amino acid protein. The C-terminal end of HexNW lacks homology to any particular protein domain, but can be speculated to help confer thermostability to the protein (see Future Directions). In addition, the 8 dispersin

B active site residues exactly match the corresponding amino acids on HexNW in terms of identity and spacing (**Figure 3-1**).

The gene encoding HexNW was synthesized as a plasmid with codon usage optimized for *E. coli* expression by Life Technologies. It was expressed in BL21 (DE3) cells after cloning into the pBAD24 expression vector, which uses arabinose induction. While it was synthesized with an N-terminal 6xHis tag and expressed well, it was necessary to switch the His tag to the C-terminal end of the protein to allow for purification using nickel column affinity chromatography (most likely due to the His tag being unexposed when at the N-terminus of the protein).

```

DspB 19  QKTSTKQTGLMLDIAHRFYSPEVIKSFIDTISLSGGNFLHLHPSDHENYAIESHLLNQRA 78
          Q + KQ GLMLD ARHFY VIK FIDTI+ SGGNFLHLHPSDHENYA+ESH+LNQRA
HexNW 46  QSVAPKQGGLMLDTARHFYPTNVIKDFIDTIAKSGGNFLHLHPSDHENYAIESHILNQRA 105

DspB 79  ENAVQGKDGIIYNPVTGKPFLSYRQLDDIKAYAKAKGIELIPELDSPNHMTAIFKLVQKD 138
          +A + DG+YINP TGKPFLS+ QL++IKAYAK+K IELIPE+DSPNHMT IF L++
HexNW 106 ADATRNADGVYINPVTGKPFLSPEQLEEIKAYAKSKNIELIPEVDSPNHMTTIFTLLEAH 165

DspB 139  RGVKYLQGLKSRQVDDEIDITNADSITFMQSLMSEVIDIFGDTSQHFHIGGDEFGYSVES 198
          RG ++ +KS+ D+EI+ITN +SI FM+SL+ EV D FGD+S+HFHIGGDEFGYSV+S
HexNW 166  RGKDFVNKIKSKYSDEEINITNPESIAFMKSLIGEVADAFGDSSRHFHIGGDEFGYSVDS 225

DspB 199  NHEFITYANKLSYFLEKKGLKTRMHNDGLIKNTPEQINPNIEITYHSYDGDTQDKNEAAE 258
          NHEFI YAN LS FL++KGL TR+HNDG+IK T +++NP I++TYHSYDGD Q+K + E
HexNW 226  NHEPIAYANDLSAFLKQKGLTTRIHNDGIIKATVDKLNPEIQVTTYHSYDGDVQNKQASQE 285

DspB 259  RRDMRVSLPELLAKGPTVLNYSYYLYIVPKASPTFSQDAAFAAKDVIKNWDLGVWDGRN 318
          RR +R S+P+L+ KGP+VLNYSYYLY+ PK S ++ FA +D+I W+LGVWDG N
HexNW 286  RRRIRTSMPDLIEKGFSVLNYSYYLVNPKQEWGTSYNSDFATRDIINRWNLGVWDGEN 345

DspB 319  TKNRVQNTHEIAGAALSIHGEDAKALKDETIQKNTKSLLEAVIHKTNGD 367
          +N V+NT +I GAAL+IHGED+A ++ +TIQK T LLE++I KT+ +
HexNW 346  QQNAVKNTDKIMGAALAIHGENAGSMSSKTIQKYTAGLLESIIRKTHAE 394

```

**Figure 3-1: HexNW alignment with dispersin B.** Numbers written represent the amino acid residue number of the protein that is named on the same line. The lines between DspB and HexNW lines represent the consensus sequence, with plus symbols (+) indicating residues that are not identical but have similar properties. Residue numbers begin at the N-terminus and continue towards the C-terminus. HexNW is 63% identical to DspB and most alignment is within the  $\beta$ -N-acetylglucosaminidase domain (DspB amino acids 12-360). Since HexNW has 508 amino acids, there is a significant portion of the C-terminus that does not align with DspB. Highlighted residues signify active site residues, all 8 of which are identical when comparing the two proteins.

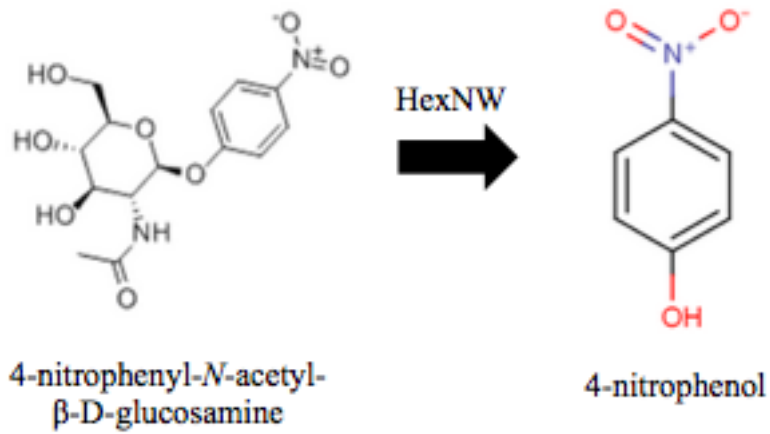
### Enzyme kinetics

Due to homology with DspB, a known  $\beta$ -1,6-*N*-acetylglucosaminidase, HexNW was tested for activity against a synthetic substrate: *para*-nitrophenylated *N*-acetylglucosamine (pNP-GlcNAc). HexNW was found to have activity against pNP-GlcNAc, cleaving the *para*-nitrophenol group off of the *N*-acetylglucosamine unit to allow for absorbance at 405 nm (see **Figure 3-2A**). This substrate was used as an approximation of the predicted real-world substrate of HexNW: poly-*N*-acetylglucosamine (**Figure 3-2B**)

Incubation of HexNW or DspB with pNP-GlcNAc at varying concentrations allowed the determination of  $K_m$  and  $V_{max}$  values, as shown in **Table 3-1**. Both enzymes had millimolar affinity for pNP-GlcNAc, although comparison of the  $K_m$  values suggests that DspB binds this substrate more tightly ( $K_m$  of 0.59 mM vs. 1.13 mM for DspB and HexNW, respectively). Dividing the average  $V_{max}$  values for each enzyme by the amount of enzyme present in each well (2 nmoles), yields the  $k_{cat}$ , which can be used to calculate the catalytic efficiency ( $k_{cat}/K_m$ ) of the enzymes. The DspB  $k_{cat}/K_m$  value of  $6.78 \text{ M}^{-1} \text{ s}^{-1}$  is consistent with value(s) in published literature. Fazekas et al. (2012) reported values increasing from 2.1 to  $8.6 \text{ M}^{-1} \text{ s}^{-1}$  depending on whether the substrate was a dimer, trimer, tetramer, or pentamer. Likewise, Manuel et al., (2007) reveals that HexNW binds to pNP-GlcNAc about half as tightly as DspB. HexNW maximum velocity ( $V_{max}$ ) is also about half that of DspB, suggesting that HexNW cleaves pNP-GlcNAc about half as fast as DspB. In comparison, HexNW has a  $k_{cat}/K_m$

value of  $1.77 \text{ M}^{-1} \text{ s}^{-1}$ , indicating similar efficiencies on the synthetic pNP-GlcNAc substrate. Additional studies on oligosaccharides of *N*-acetylglucosamine are required to see if HexNW also increases in efficiency with longer chain lengths.

A



B

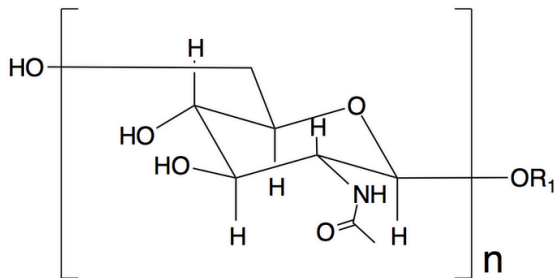


**Figure 3-2: Reaction of HexNW with pNP-GlcNAc.** HexNW reacts with pNP-GlcNAc (reactant) to produce 4-nitrophenol (product), which absorbs light at 405 nm (A). Also released is one unit of *N*-acetyl- $\beta$ -D-glucosamine (not shown). pNP-GlcNAc is similar to PNAG, except instead of one GlcNAc unit linked to *para*-nitrophenol, multiple GlcNAc units are linked at the 1,6 positions (B).

<b>Enzyme</b>	<b><math>V_{\max}</math> (pmols/sec)</b>	<b><math>K_m</math> (mM)</b>	<b><math>k_{\text{cat}}</math> (<math>\text{s}^{-1}</math>)</b>	<b><math>k_{\text{cat}}/K_m</math> (<math>\text{M}^{-1} \text{s}^{-1}</math>)</b>
<b>DspB</b>	$8.3 \pm 0.8$	$0.59 \pm 0.1$	$4.1 \times 10^{-3}$	6.78
<b>HexNW</b>	$4.0 \pm 0.5$	$1.1 \pm 0.4$	$2.0 \times 10^{-3}$	1.77

**Table 3-1: DspB and HexNW enzyme kinetics.** Kinetic parameters determined by analysis of steady state turnover of pNP-GlcNAc by DspB and HexNW via Michaelis-Menton kinetics.

Work done by Patrick Bales.

### Substrate specificity

Since the substrate used so far consisted of only one GlcNAc unit linked to a chromophore, any activity on this substrate can be seen as glucosaminidase activity without being able to specify if it is 1,4- or 1,6-glucosaminidase activity. Additional experiments were conducted to determine if HexNW acts on 1,4-linked GlcNAc or 1,6-linked GlcNAc. A substrate was purchased from Sigma and used to treat HexNW and a chitinase control (Sigma). Chitin consists of 1,4-linked *N*-acetylglucosamine, the only other linkage possibility for GlcNAc that is  $\beta$ -linked besides 1,6-linked GlcNAc. The purchased substrate, 4-nitrophenyl  $\beta$ -D-N, N', N''-triacetylchitotriose, consists of three 1,4-linked *N*-acetylglucosamine units and is commonly used to test for chitinase activity. The results, in **Figure 3-3**, show that HexNW does not react with chitin (1,4-linked GlcNAc). HexNW, therefore, is likely a 1,6-*N*-acetylglucosaminidase, similar to DspB. The relatively high OD<sub>405</sub> value of chitinase alone is likely due to the inherent absorbance of proteins at this wavelength.

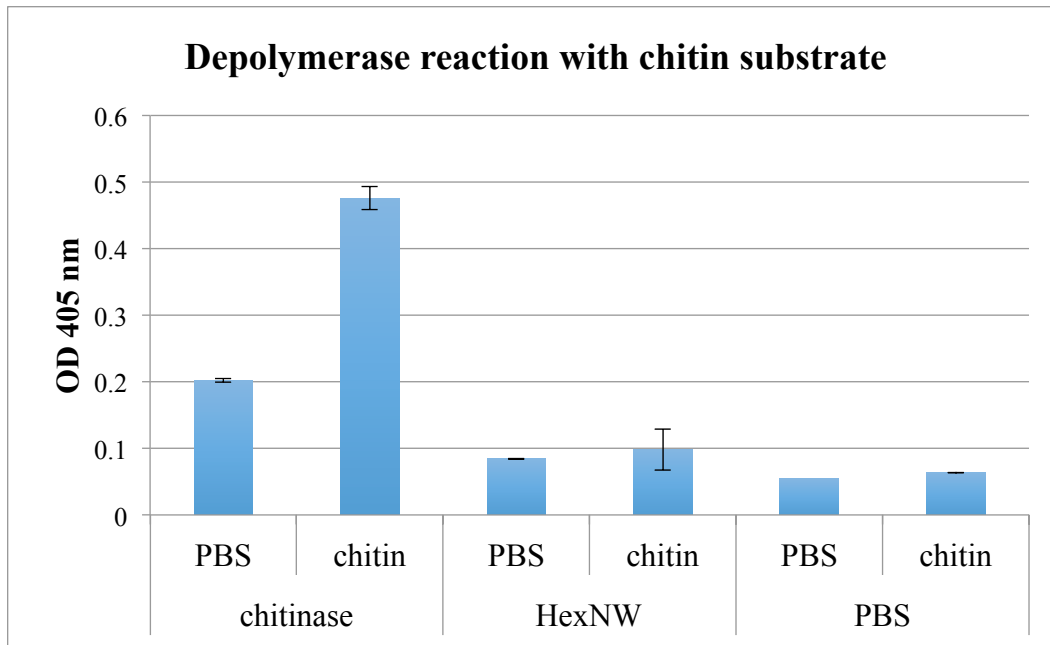


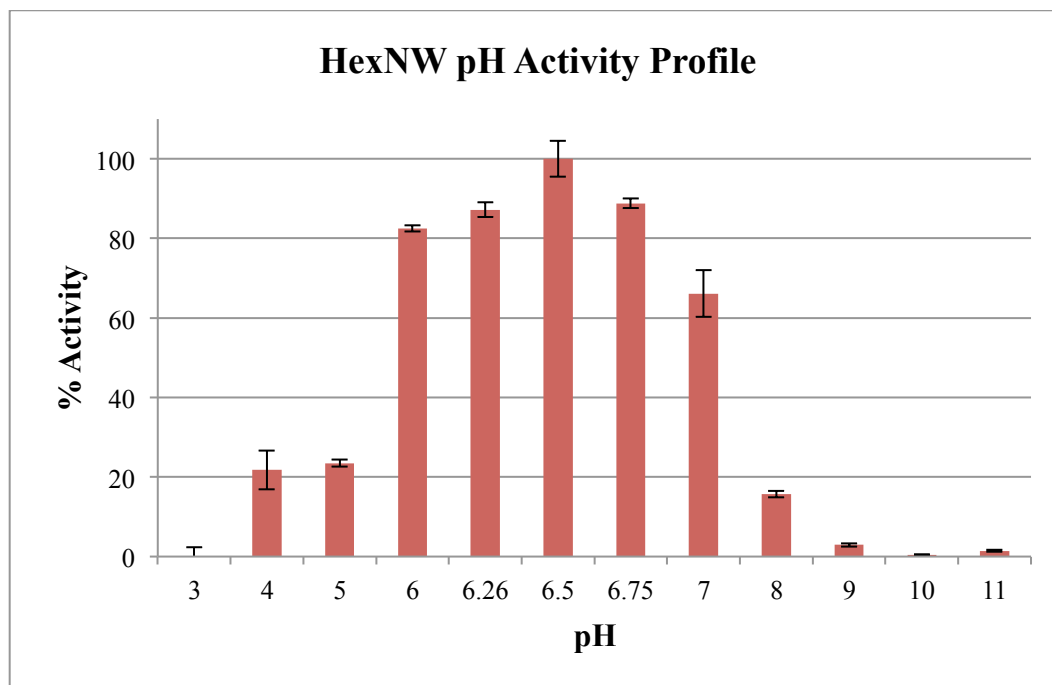
**Figure 3-3: Chitinase activity.** A *Streptomyces griseus* chitinase and HexNW were incubated with a chromogenic chitin substrate, 4-nitrophenyl  $\beta$ -D-N, N', N''-triacetylchitotriose to measure chitinase activity. The chitin substrate by itself was used as a control. Work done by Patrick Bales.

### pH activity profile

Having established HexNW as a glucosaminidase, it was subsequently tested using the same assay except at a set substrate concentration and varying pH values. This was done because pH is a useful parameter in assessing the ability of an enzyme to function in a variety of environmental conditions, which is important for protein therapeutics that may be applied in a number of ways (topical, ingestion, etc). **Figure 3-4A** shows that HexNW activity has a pH optimum of 6.5, with decreasing enzymatic activity at both higher and lower pH values. It is shown to have near-optimal activity between pH 6 and pH 7. Activity sharply drops off below pH 6 and above pH 7.

The relatively narrow pH range of HexNW may be related to possible pH effects on the substrate and active site residues. HexNW is likely a glycosyl hydrolase family 20  $\beta$ -hexosaminidase (determined by protein BLAST conserved domain searches). The hydrolysis of this group of enzymes is proposed to involve a glutamic acid residue as the proton donor and acceptor and a *N*-acetyl group on the substrate as the nucleophile (see **Figure 3-4B**). The transition state is stabilized by the carboxyl carbon of an active site aspartate. The pH profile of HexNW is likely dependent on the  $pK_a$  values of these important functional groups. The pH optimum of HexNW is 6.5 while the optimum pH of wild-type DspB is 5.8 (Suba et al 2007). In addition, the effect of pH changes on the *para*-nitrophenol group of pNP-GlcNAc ( $pK_a$  7.2) likely has some effect on the extinction coefficient of pNP-GlcNAc, which may account for some of the differences in activity between the different pH values tested.

**A**



**B**

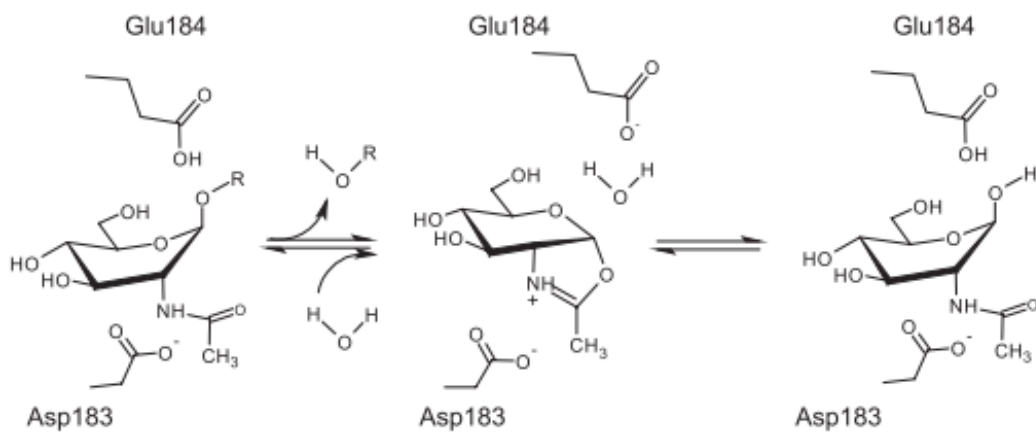


**Figure 3-4: HexNW pH effects.** HexNW (10  $\mu$ M) was added to pNP-GlcNAc (1 mM) in BP buffer of various pH values in order to measure the dependence of activity on pH (A). The proposed hydrolysis mechanism of glycosyl hydrolase family 20 is given in (B), in which Glu184 and Asp183 are active site residues and the substrate (middle) is pNP-GlcNAc (Manuel et al 2007). Work done by Patrick Bales.

### Thermostability

Prior to incubation with pNP-GlcNAc, HexNW was subjected to various temperatures for 10 min in order to assess its ability to withstand the unfolding effect of heat. The results, described in **Figure 3-5**, show that HexNW maintains near 100% activity at tested temperatures up to 45°C. It then shows a reduction in activity at temperatures above 50°C with no activity detected at any tested temperature which is 60°C or higher. DspB, on the other hand, starts showing a reduction in activity between 30 and 37°C and no activity is observed at tested temperatures that are 45°C or higher. Based on this assay, therefore, HexNW unfolds at least 15°C above the melting point of DspB and is substantially more thermostable than DspB.

To further explore the thermostable nature of HexNW, circular dichroism (CD) and differential scanning calorimetry (DSC) were performed to estimate the melting temperature of HexNW and DspB. Since the unique CD spectrum of a protein is based on secondary structure, measuring a molecule's CD spectrum along a temperature gradient can be used to detect the temperature at which a protein unfolds. Using this method, DspB was found to have a melting temperature of 44.4°C whereas HexNW had a melting temperature of 60.3°C (see **Figure 3-6A**). DSC, on the other hand, measures the molar heat capacity of solutions by detecting the amount of heat required to raise the solution by a given temperature. Because organized protein structures have higher heat capacities than unorganized structures, DSC is well-suited to detect thermal transitions as a protein solution is heated up (thermal transitions representing the unfolding of

protein structures). Using DSC, DspB was found to have a melting point of 44.25°C and HexNW was found to have a melting point of 58.00°C (**Figure 3-6B**). The melting points were found by observing the first thermal transition, which in proteins general corresponds to secondary rather than primary structure degradation. Thus, by multiple methods, the  $T_m$  of HexNW is ~15°C greater than DspB. The melting points of all thermal transitions for DspNW and DspB by DSC are recorded in **Table 3-2**. A summary of the melting point information from both CD and DSC experiments in **Figure 3-6** is given in **Table 3-3**.

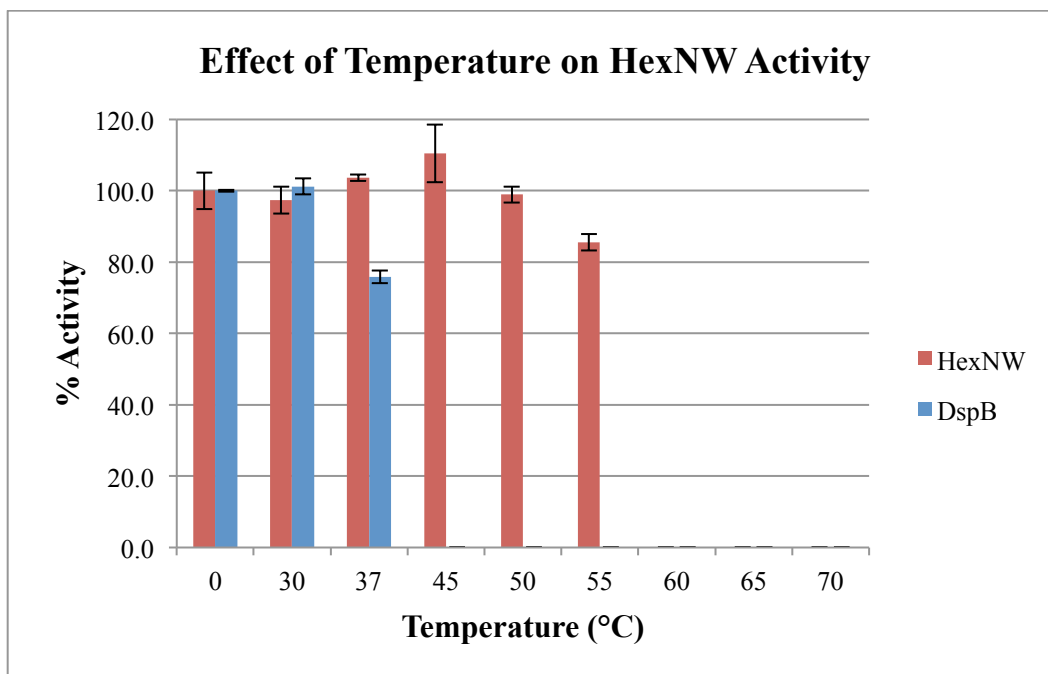
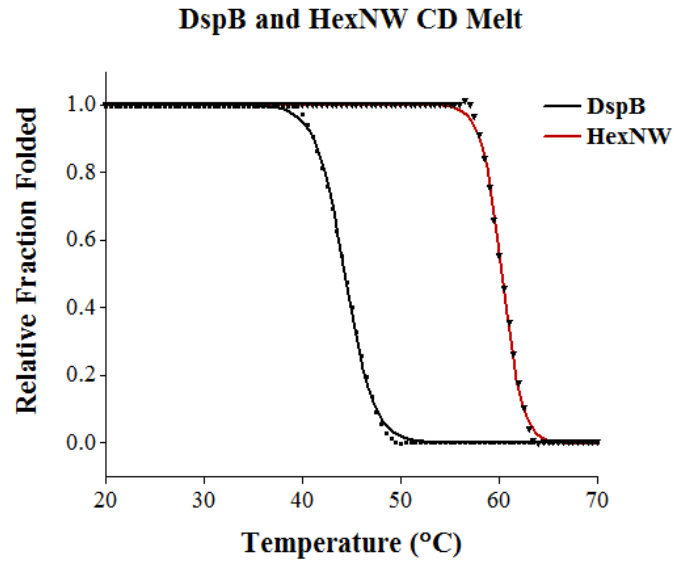


**Figure 3-5: Temperature stability.** HexNW and DspB (10  $\mu$ M) were incubated for 10 min at the given temperature before being placed on ice and then allowed to come to room temperature. Enzymatic activity was then assayed with 1 mM pNP-GlcNAc. Activity measurements were done for both enzymes at all listed temperatures (activities for both enzymes at 60°C, 65°C, and 70°C were zero). Work done by Patrick Bales.

A



B

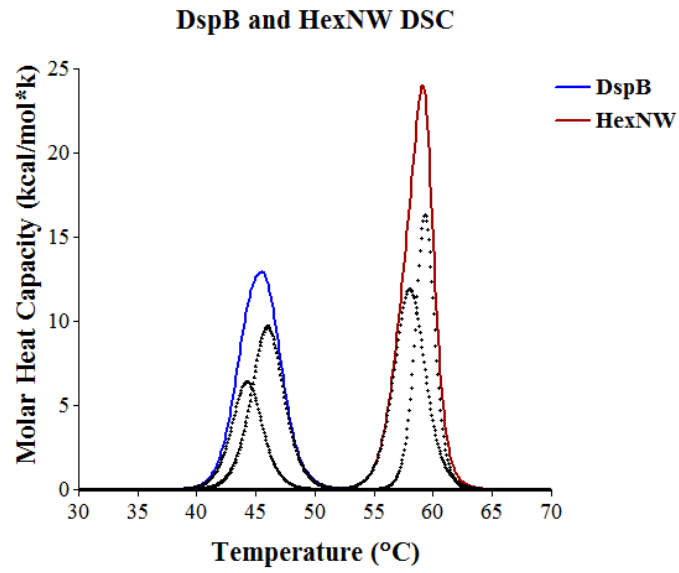


**Figure 3-6. CD and DSC melting point analysis.** For CD analysis (A), spectra of DspB and HexNW were obtained in the far-UV range and melting was done by heating the proteins 1°C/minute. The melting temperature for DspB was 44.4°C and 60.3°C for HexNW. For DSC analysis (B), samples were degassed for 20 min and heated at a rate of 1°C/minute. The melting temperature for DspB was 44.25°C while it was 58.00°C for HexNW. Colored curves represent the overall changes in heat capacity for each sample while the black, dotted curves underneath the colored curves represent changes in heat capacity associated with each of 2 thermal transitions that were observed for each protein. PBS buffer was used as a negative control. Work done by Ryan Heselpoth.

Enzyme	$T_{G1}$ (°C)	$T_{G2}$ (°C)	$\Delta H_{VH1}$ (kcal/mol)	$\Delta H_{VH2}$ (kcal/mol)
DspB	44.25	46.00	234.88	222.51
HexNW	58.00	59.29	251.54	406.77

**Table 3-2: DSC thermostability data.** DspB, HexNW, and buffer samples were gradually heated to measure heat capacity.  $T_{G1}$  and  $T_{G2}$  represent the temperatures at each of 2 thermal transitions of the samples, whereas  $\Delta H_{VH1}$  and  $\Delta H_{VH2}$  represent change in enthalpy. Work done by Ryan Heselpoth.

<b>DspB</b>		<b>HexNW</b>	
Melting point by CD (°C)	Melting point by DSC (°C)	Melting point by CD (°C)	Melting point by DSC (°C)
44.4	44.25	60.3	58.0

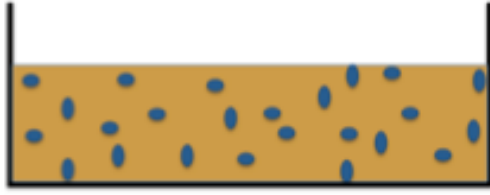
**Table 3-3: Melting point summary.** Melting point was precisely estimated using 2 methods (DSC and CD).

### Antibiofilm properties

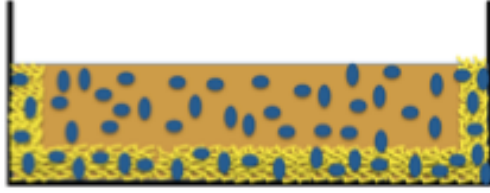
To assess the ability of HexNW to degrade bacterial biofilms, it was incubated with 24 hour biofilms of *S. epidermidis* strain NRS 101. See **Figure 3-7** for a schematic that illustrates how biofilms were grown and treated. NRS 101 was chosen because DspB, a homologue of HexNW, is most effective against biofilms of *S. epidermidis*. In addition, NRS 101 is a known biofilm producer and is also methicillin-resistant, making any antibiofilm activity against the strain particularly important due to the growing number of infections caused by antibiotic-resistant bacteria.

In **Figure 3-8**, the results of an assay comparing the release of amino sugars, as measured by the Morgan-Elson assay, between HexNW- and buffer-treated biofilms is shown. Since HexNW is predicted to degrade biofilms by digesting the polysaccharide portion of the EPS, HexNW treatment should result in an increase of soluble amino sugars in the medium surrounding the biofilm. **Figure 3-8** illustrates a 20% increase in amino sugars released as a result of HexNW treatment, supporting this hypothesis.

A



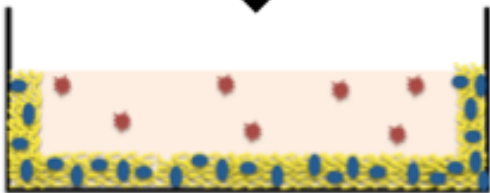
B



C



D



E



**Figure 3-7: Biofilm treatment schematic.** In (A), inoculation of a well with biofilm-forming bacteria is depicted. After incubation at 37°C without shaking, bacterial cells have multiplied and formed a biofilm on the sides and bottom of the well (B). In (C), the well has been washed and buffer has been added. In (D), the addition of EPS depolymerase is shown and (E) depicts the depolymerase-mediated breakdown of the EPS and subsequent release of adherent cells, which can be measured by serial dilution and spread plating. Depolymerase activity on EPS polysaccharides can also be measured by performing a sugar-detecting assay such as the Morgan-Elson assay.

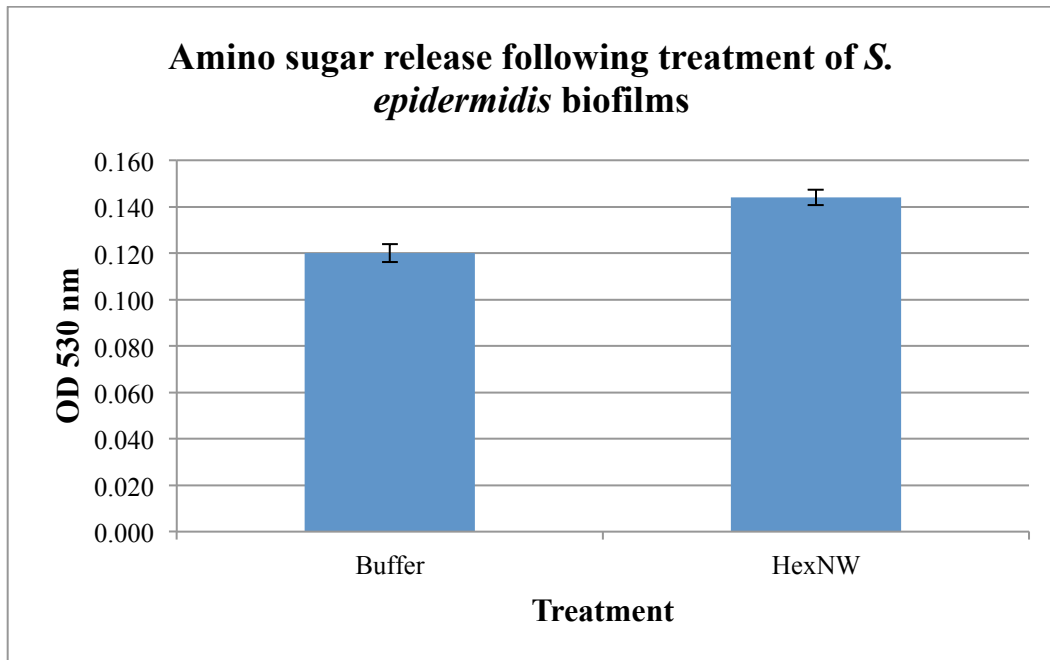


**Figure 3-8: Morgan-Elson assay.** The number of amino sugars released from *S. epidermidis* biofilms was estimated following HexNW or buffer treatment. Sugars were detected colorimetrically at an optical density of 530 nm. Work done by Patrick Bales.

Next, the effect of HexNW treatment on the dispersal of bacterial cells from the biofilm was estimated by measuring the colony-forming units released into the treatment medium. The results, shown in **Figure 3-9**, demonstrate that HexNW treatment released 165% more viable cells than treatment with buffer. Release of biofilm cells into the surrounding medium mirrors biofilm cells' dispersal in nature (see Chapter 1), which is specifically mediated by enzymes such as DspB that are produced by the biofilm-forming cells. Being able to measure cell dispersal, therefore, is a worthwhile means of detecting the activity of EPS depolymerases.

Finally, the effect of HexNW treatment on the Minimum Biofilm Elimination Concentration (MBEC) of vancomycin on *S. epidermidis* NRS 101 biofilms was assessed. The MBEC is defined as the lowest antimicrobial concentration tested which results in complete killing of biofilm cells. This is measured by first treating biofilms with various concentrations of an antimicrobial and then assessing biofilm cell viability by the addition of growth media. The MBEC is then the lowest antimicrobial concentration that results in no visible growth following overnight incubation of treated biofilms in media. The Minimum Inhibitory Concentration (MIC), on the other hand, is the lowest concentration of an antibiotic required to prevent planktonic (rather than biofilm) cell growth. **Table 3-4** shows the results of testing the effect of HexNW and DspB on the MBEC of vancomycin. It was predicted that the enzymes would cause the release of cells from the biofilm and thus reduce the MBEC. The MBEC when vancomycin was supplemented with either 0.05 mg/ml DspB or

HexNW was 1,024  $\mu\text{g/ml}$ , whereas the MBEC when only PBS was added was 2,048  $\mu\text{g/ml}$ , indicating that HexNW and DspB are capable of reducing the amount of vancomycin needed to eliminate NRS 101 biofilms by half. Also shown in **Table 3-3** is the MIC of vancomycin for NRS 101, which was found to be 4  $\mu\text{g/ml}$ . Neither DspB nor HexNW treatment had any effect on the MIC of vancomycin for NRS 101 (**Table 3-4**). The stark contrast between MIC and MBEC in the case of vancomycin treating NRS 101 illustrates the protective abilities of the biofilm EPS.

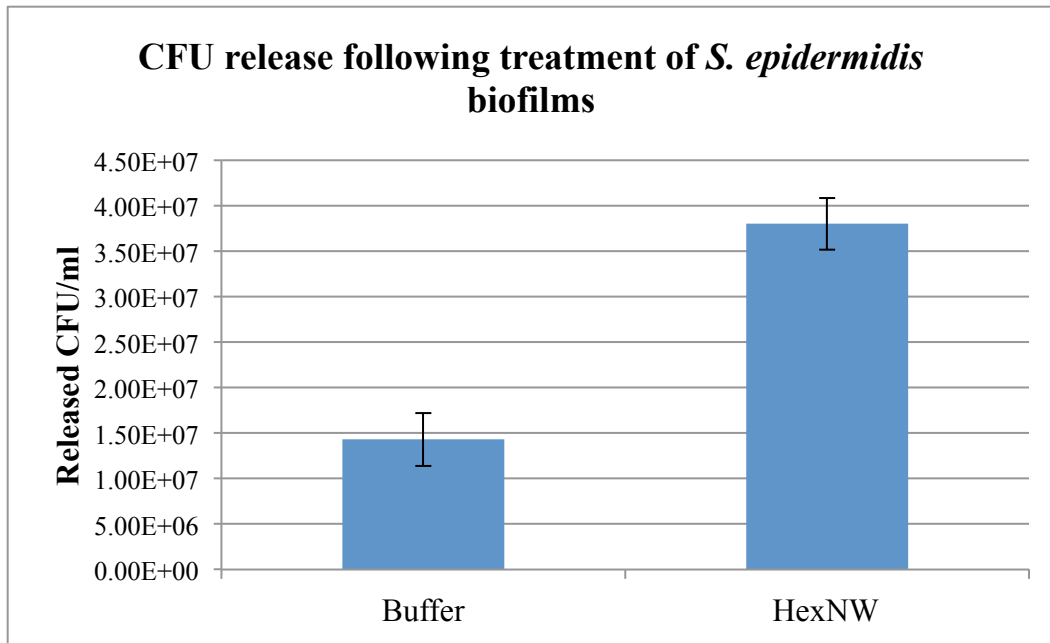


**Figure 3-9: CFU release.** Biofilms (grown for 24 hr) were treated with 0.25 mg/ml HexNW or PBS buffer. After 1 hr incubation at 37°C, cells were enumerated by spread plating. Work done by Patrick Bales.

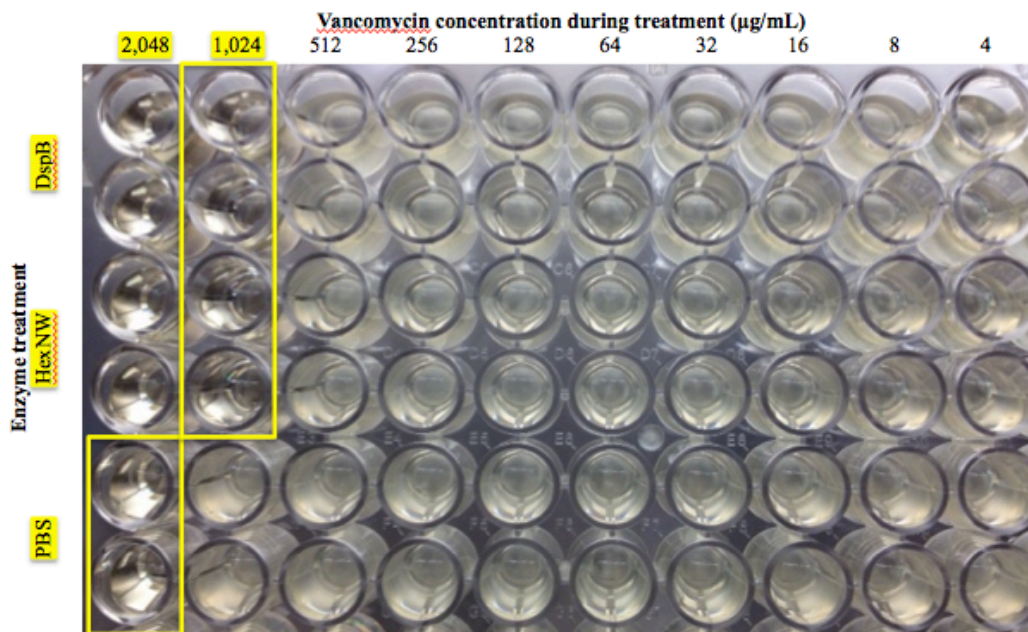


**Figure 3-10: Depolymerase-mediated reduction in MBEC.** Vancomycin of varying concentrations and HexNW, DspB, or buffer were added to washed *S. epidermidis* biofilms. After incubation, washing, addition of sterile media, and overnight incubation, sterilized wells result in lack of visual growth. Addition of HexNW or DspB reduces the necessary concentration of vancomycin for biofilm sterilization (MBEC) from 2,048 µg/ml to 1,024 µg/ml. Work done by Patrick Bales.

	<b>DspB</b>	<b>HexNW</b>	<b>Control</b>
<b>MIC (µg/ml)</b>	4	4	4
<b>MBEC (µg/ml)</b>	1,024	1,024	2,048

**Table 3-4: MBEC and MIC values.** The MBEC values of vancomycin when DspB, HexNW, or buffer were added to *S. epidermidis* biofilms were measured. Also measured were MIC values. Work done by Patrick Bales.

## Discussion

HexNW has been shown to be a thermostable enzyme that has potential as a therapeutic against *S. epidermidis* biofilms. Because it is active against a synthetic *N*-acetylglucosamine substrate, homologous to DspB (a known  $\beta$ -1,6-*N*-acetylglucosaminidase), and not active when used to treat a trimeric chitin substrate (which contains *N*-acetylglucosamine residues linked in  $\beta$ -1,4 linkages), it is likely that HexNW is a  $\beta$ -1,6-*N*-acetylglucosaminidase similar to DspB. When used with 4-nitrophenyl *N*-acetyl-D-glucosaminide as a substrate, HexNW was shown to be about half as active as DspB. It is notable, however, that when comparing the MBEC-reducing effects of DspB and HexNW, they perform equally well. Therefore, while HexNW may have less activity than DspB, this disparity does not seem to have an effect when HexNW is being used to treat actual biofilms.

By measuring the activity of HexNW at various pH values, it was determined that it is active at physiological pH. When the resistance of HexNW to high-temperatures was tested by incubating at different temperatures and then testing activity with 4-nitrophenyl *N*-acetyl-D-glucosaminide, it was found to be highly thermostable. This was then confirmed by CD and DSC analysis. Thermostability is a desirable trait in a therapeutic because it directly correlates with shelf life (Anderson and Scott 1991). One can imagine that a product that is capable of long-term storage at room temperature would be much more valuable than one that requires constant refrigeration. In addition, the ability of an antimicrobial to function at human body temperature (37°C) is essential. As

shown in **Figure 3-6**, DspB has a melting temperature (temperature at which point about 50% of DspB molecules are unfolded) of about 44°C and begins activity loss at about 37°C. HexNW, on the other hand, has a melting point of between 58 and 60°C and is fully active at 37°C. Future experiments may focus on the long-term thermostability of HexNW by assessing activity after extended incubation at various temperatures.

HexNW has proven to be a promising biofilm depolymerase based on the results of multiple experiments. The increased number of amino sugars in the biofilm treatment medium indicates that HexNW treatment is acting to break up the polysaccharide portion of the biofilm EPS (Izano et al. 2008). In addition, HexNW treatment resulted in the release of colony-forming units from the biofilm. Finally, HexNW increased the effectiveness of vancomycin treatment of *S. epidermidis* biofilms by lowering the minimum biofilm elimination concentration (MBEC) by half. This experiment is particularly noteworthy because these types of therapeutics—those that don't actually kill bacterial cells but simply disperse the biofilm matrix—will likely be used in combination with other treatments (such as antibiotics) when applied in clinical situations (Rogers et al. 2010). As HexNW causes the release of cells from the biofilm, the accessibility of the bacteria to vancomycin increased and thus lowered the concentration of vancomycin required for full sterilization of the peg biofilms. In the future, the ability of HexNW to disrupt biofilms will be further questioned. Biofilm flow cells can be used in conjunction with live-dead staining to visualize the effect of HexNW on biofilm structure with a confocal microscope. Catheter

models or animal models of infection are other possible experiments. In addition, it will be useful to test HexNW on other strains of *S. epidermidis* than NRS 101. Since DspB has been shown to prevent biofilm formation in *S. aureus* (Izano et al. 2008), similar experiments can be done for HexNW. HexNW might also be used to treat *E. coli* biofilms since *E. coli* is known to have an appreciable amount of *N*-acetylglucosamine in its EPS (Wang et al. 2004; Bales et al 2013).

### **Acknowledgments**

The authors acknowledge Parastoo Azadi and the Complex Carbohydrate Research Center at the University of Georgia, Athens for assistance with sample processing. We also thank Sarah May and Sara Linden for technical assistance.

## **CHAPTER 4**

### **Other Putative EPS Depolymerases**

This chapter contains unpublished preliminary data I collected and partial characterization of several enzymes not discussed elsewhere in this thesis. It is anticipated that full characterization for some of these enzymes will be continued in the laboratory by future graduate students.

Identification of depolymerases was done by Daniel Nelson and Patrick Bales. Initial characterization of depolymerases was done by Emilija Renke, Sarah May, and Patrick Bales. Additional characterization of all alginate lyases, including purification and enzyme activity analysis, was done by Steve Swift. Characterization of Tsp1 and other depolymerases was done by Patrick Bales. The crystal structure of Tsp1 was determined by Chen Chen, Julia Greenfield, and Osnat Herzberg.

#### **Selection of depolymerases**

Efforts to discover biofilm-dispersing agents were focused on enzymes that are capable of degrading the polysaccharide portion of the biofilm EPS matrix (EPS depolymerases) due to our lab's experience working with antibacterial enzymes, their proven ability to inhibit biofilm formation, and their capacity to degrade already-formed, mature biofilms. The wide structural diversity among biofilm organisms' EPS along with the occurrence of multi-species biofilms necessitates investigation of methods to treat biofilms based on a

broad range of polysaccharase activities. A summary of EPS depolymerases synthesized, expressed, purified, and initially characterized is given in **Table 4-1**.

Depolymerase candidates were selected based on thorough literature and bioinformatics searches for enzymes that degrade particular polysaccharides known to be a main constituent of bacterial biofilms of certain relevant pathogens. Alginate, for example, is known to be a significant constituent of *P. aeruginosa* biofilms (Mann and Wosniak 2012; Wosniak et al. 2003), conferring considerable

Protein	GenBank accession number	Origin	Target pathogen	Mechanism of action	Predicted MW (kDa)	Expression	N-term tag purifiable	C-term tag purifiable
DspB	AAP31025.1	Actinobacillus actinomycetemcomitans dispersin	Staph	$\beta$ (1,6)-N-acetyl glucosaminidase	42	Y	Y	-
Sf6	AAQ12204.1	Tail-spike of Sf6, a P22-like phage of <i>Shigella flexneri</i>	Possibly <i>E. coli</i>	Endorhamnosidase	157.6	Y	Y	-
Tsp1	AEM91896.1	CPA_120 myophage tail-spike	<i>E. coli</i> O157:H7	?	81.96	Y	N	Y
HexNW	WP_009115775.1	Related to DspB, from <i>Neisseria wadsworthii</i>	Staph spp., <i>E. coli</i>	Putative 1,6-glucosaminidase	57.9	Y	N	Y
DspAA	EGY31409.1	Related to DspB, from <i>Aggregatibacter</i> sp.	Staph spp., <i>E. coli</i>	Putative 1,6-glucosaminidase	46.7	Y	N	N
LyaeU	AEO50363.1	Related to <i>Klebsiella alginata</i> lyase, from uncultured	<i>P. aeruginosa</i>	Putative alginata lyase	36.2	Y	N	Y
LyaseSD	YP_527950.1	Related to <i>Klebsiella alginata</i> lyase, from <i>S. degradans</i>	<i>P. aeruginosa</i>	Putative alginata lyase	57.1	Y	N	N
AlgMsp	BAJ62034.1	Microbulbifer protein related to <i>Klebsiella alginata</i> lyase	<i>P. aeruginosa</i>	Putative alginata lyase	39	Y	N	Y
LyasePA	YP_001346982.1	Related to <i>Klebsiella alginata</i> lyase, from <i>P. aeruginosa</i>	<i>P. aeruginosa</i>	Putative alginata lyase	41.6	Y	N	Y
LyaseSM	YP_004791784.1	Related to <i>Pseudomonas alginata</i> lyase, from <i>S. maltophilia</i>	<i>P. aeruginosa</i>	Putative alginata lyase	37.7	Y	N	Y
GlucEg	YP_002746062.1	Related to <i>E. coli</i> glucuronidase, from <i>S. equi</i>	<i>K. pneumonia</i>	Putative $\beta$ -glucuronidase	69.2	Y	Y	-
GlucNH	XP_003046865.1	Related to <i>E. coli</i> glucuronidase, from <i>N. haematococca</i>	<i>K. pneumonia</i>	Putative $\beta$ -glucuronidase	68.9	Y	Y	-
GlucFO	EGU88110.1	Related to <i>E. coli</i> glucuronidase, from <i>F. oxysporum</i>	<i>K. pneumonia</i>	Putative $\beta$ -glucuronidase	69.1	Y	Y	-
NagZ	ADX02168.1	Related to <i>E. coli</i> NagZ, sequenced from <i>Acinetobacter</i>	<i>Acinetobacter baumannii</i>	N-acetyl glucosaminidase	39	Y	Y	-
Bdm	YP_001902664.1	Related to biofilm dispersing $\beta$ -mannosidase from <i>Xanthomonas</i>	<i>PA, KP, and AB</i>	Putative $\beta$ -mannosidase	85.61	Y	Y	-

**Table 4-1: Summary of synthesized depolymerases.** Fifteen putative EPS depolymerases were identified, synthesized, and expressed. Attempts were made to purify the depolymerases (most were successful). Work done by Patrick Bales and Daniel Nelson.

structural stability. It is associated highly with the “mucoid” phenotype, which is usually the phenotype of *P. aeruginosa* causing pneumonia in the lungs of cystic fibrosis patients. Toward this end, we searched for and discovered several potential alginate lyases (LyaseU, LyaseSD, AlgMsp, LyasePA, and LyaseSM) in GenBank and other databases. All genes were codon-optimized for expression in *E. coli*, chemically synthesized, and cloned into the pBAD24 arabinose-inducible expression system. For the lyases, N-terminal 6-His tags engineered into the gene construct for purification caused misfolding and/or the inability to purify the recombinant enzyme. However, when the His tags were moved to the C-terminus, we were able to purify four of the five enzymes. Lyase SD continues to produce inclusion bodies whether it possesses a tag or not. Of the four soluble, purified alginate lyases, we focused our characterization studies on AlgMsp because it has not been previously characterized and it was expressed with the highest yields. Dr. Steve Swift, a postdoctoral associate in our laboratory, took over the project during the expression and purification stages. He has shown that AlgMsp is highly active against purified alginate and the full characterization of this enzyme has been submitted for publication (see Appendix C).

Biofilms of *K. pneumoniae*, despite a high incidence of antibiotic resistance (Anderl et al. 2000; Boucher et al. 2009), have not been well studied and represent a medically important target for development of anti-biofilm enzymes. Literature searches suggested a role for glucuronic acid in *K. pneumoniae* biofilms (Bessler et al. 1973; Niemann et al. 1977), so glucuronidases were considered as possible depolymerases of *K. pneumoniae*

biofilms. GlucEQ, GlucNH, and GlucFO listed and described in **Table 4-1**, were synthesized due to putative glucuronidase activity. Although characterization is still preliminary, all three glucuronidases are extremely soluble and can be purified in large quantities.

Similar to *K. pneumoniae*, *Acinetobacter baumannii* is also not well studied despite its high clinical relevance. Literature searches suggested a role of  $\beta$ -1,4-*N*-acetylglucosamine in the EPS of *A. baumannii* (Fregolino et al. 2011; Vötsch and Templin 2000). NagZ, which is produced by *A. baumannii* and is a putative *N*-acetylglucosaminidase, was therefore synthesized. This protein is related to a protein of the same name which is found in *E. coli* and is best known for its role in the induction of *E. coli*  $\beta$ -lactamase activity (Asgarali et al. 2009).

Tailspike proteins of bacteriophages were also considered as possible EPS depolymerases because of their recognized role in degrading bacterial EPS so as to allow access of the phage to the host cell surface (Ghalambor et al. 1971; Müller et al. 2008). Sf6 is a well-described endorhamnosidase produced by the Sf6 phage, which is a P22-like phage of *Shigella flexneri* (Müller et al. 2008), although its role in degradation of biofilms has not been studied in the literature. Tsp1 is one of four putative tail spikes of CBA120, a myophage of *E. coli* O157:H7 (Chen et al. 2014). It is SDS- and protease-resistant, thermostable, and exhibits a trimeric,  $\beta$ -sheet-heavy structure that is typical of phage tailspike proteins. While we were evaluating Tsp1 and the other putative depolymerases, we were approached by Dr. Osnat Herzberg who was interested in crystallizing

Tsp1. This collaboration yielded two publications on the structural details on this enzyme (see Appendix 1 and 2).

Dispersin B (DspB), a well-studied  $\beta$ -1,6-*N*-acetylglucosaminidase that degrades *S. epidermidis* biofilms, was synthesized as a control depolymerase with a known activity. In addition, two DspB homologs, NexNW and DspAA, were also synthesized. DspAA was not soluble under any expression conditions. In contrast, DspB and HexNW were abundantly soluble and have been described in detail in Chapter 3. By investigating enzymes that degrade 1,6-linked *N*-acetylglucosamine, new methods of treating infections caused by bacteria that produce this polysaccharide (including *S. epidermidis*, *S. aureus*, and *E. coli*) will be uncovered (Wang et al. 2004; Bales et al. 2013).

Finally, Chapter 2 details an investigation into the structure of the high molecular weight polysaccharide portion of the EPS of several pathogens (*K. pneumoniae*, *A. baumannii*, *S. epidermidis*, *E. coli* O157:H7, and *P. aeruginosa*). A salient finding of that study was the high prevalence of mannose detected. The possible preponderance of mannose residues in the EPS of multiple pathogens makes mannosidases attractive possibilities as anti-biofilm agents. For this reason, Bdm, a putative mannosidase produced by *Xanthomonas campestris* pv. *campestris*, was synthesized as a putative depolymerase that may have activity against EPS from a wide range of pathogenic organisms.

### **Preliminary anti-biofilm experiments**

Preliminary experiments were aimed at demonstrating the potential of these enzymes as biofilm-targeting therapeutics. Briefly, wells of 96-well plates were seeded with 1:100 diluted overnight solutions (diluted in T-soy broth) of the listed pathogens and EPS depolymerases (0.1 mg/ml final concentration) in a final volume of 200  $\mu$ l. Plates were incubated at 37°C without shaking to allow formation of static biofilms. The wells were then aspirated, washed twice with 200  $\mu$ L water, and the biofilm biomass was stained with 0.1% crystal violet for 10 minutes. Following dye incubation, the dye was aspirated and the wells washed twice with water. SDS detergent was added (1%) and allowed to sit at room temperature for 10 minutes, after which the solution in each well was transferred to fresh plates and the OD at 600 nm was read using a Molecular Devices SpectraMax M5 spectrophotometer to quantify formation of biofilms in enzyme treated vs. PBS control wells. Depolymerase effectiveness was estimated by subtracting the average OD of PBS-treated wells by that of depolymerase treated wells, dividing by the OD of PBS-treated wells, multiplying by 100, and then subtracting the resulting percentage value from 100.

According to **Figure 4-1**, synthesized depolymerases exhibit activity on a wide-range of pathogenic bacteria. Strains that were less affected by depolymerase action were *P. aeruginosa* strains 700888 and 27853. This may be due to the fact that these strains formed biofilms that were less thick than the others and thus exhibit decreased sensitivity to this assay. Interestingly, all depolymerases appeared to be active against the same bacterial strains, perhaps

owing to the exceptional heterogeneity of bacterial biofilm structure. Future members of the Nelson lab will have the opportunity to investigate the enzymatic activities and biofilm-degrading properties of these proteins further.

## Depolymerase Prevention of Biofilms

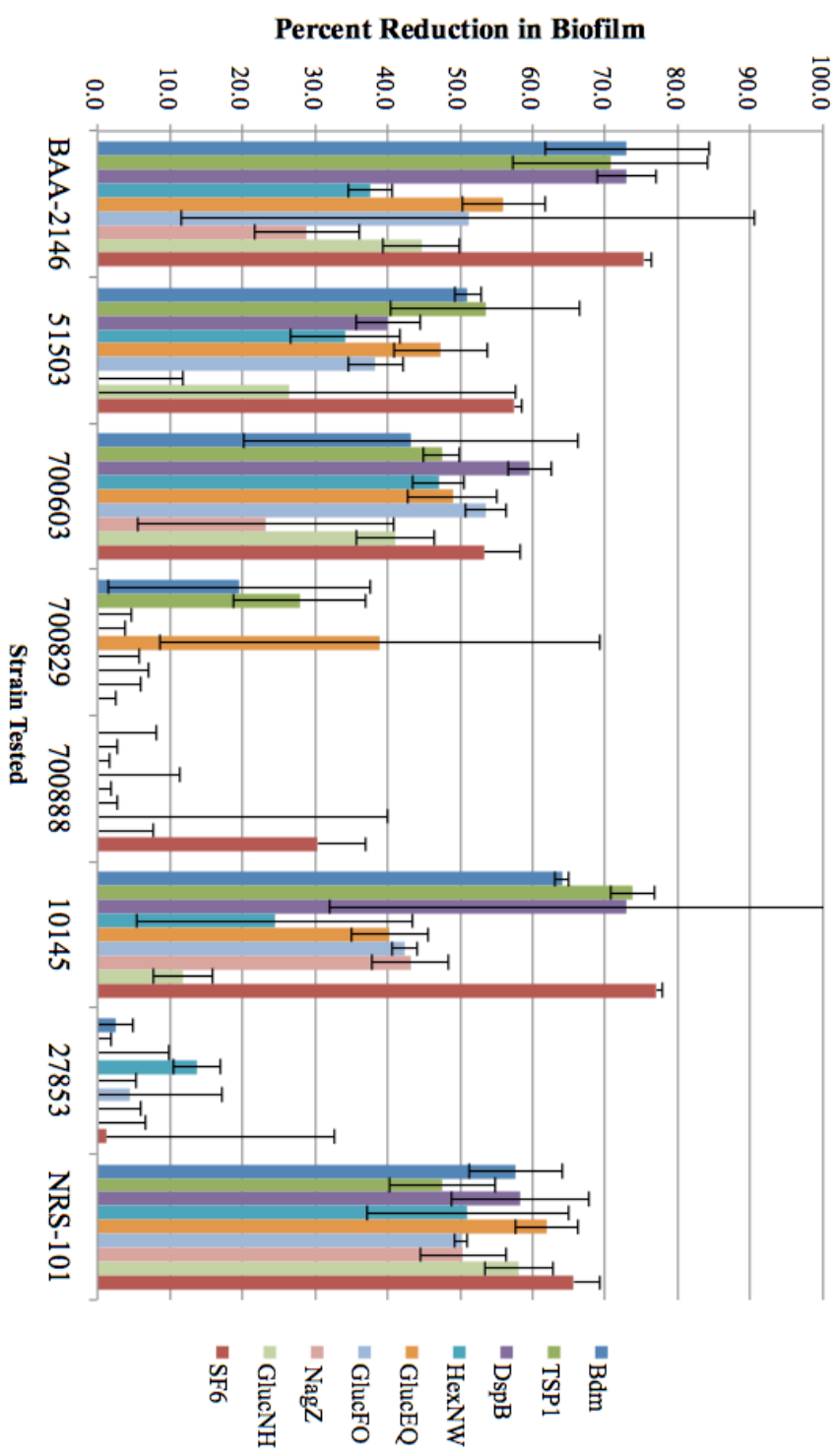


**Figure 4-1: Depolymerase-mediated prevention of biofilm formation.** Biofilms of strains BAA-2146, 51505, 700603 (*K. pneumoniae*), 700829, 700888, 10145, 27853, (*P. aeruginosa*), and NRS 101 (*S. epidermidis*), were grown in the presence of the indicated depolymerases. Work done by Patrick Bales.

## CHAPTER 5

### Discussion and Future Directions

A *S. epidermidis* biofilm-degrading enzyme, HexNW, has been described. It exhibits anti-biofilm activity in a way that is very applicable to possible future therapeutic applications (synergy with vancomycin reducing its MBEC by one-half). For a protein originating from a mesophilic bacterium, it is very thermostable with a  $T_m$  of about 58-60°C. Since a large proportion of medical implant device-related infections are linked to biofilm-forming strains of *S. epidermidis* (Otto 2012), HexNW has the potential to be clinically useful. The high melting point of HexNW will make it even more useful because it is less subject to heat-inactivation when stored in sub-optimal conditions.

In addition to HexNW, 14 depolymerases were synthesized and are in various stages of analysis. Taken together, we have synthesized and purified enzymes that can potentially degrade the biofilms of many clinically important human pathogens, including *S. epidermidis*, *E. coli* strain 0157:H7, *Pseudomonas aeruginosa*, *Klebsiella pneumoniae*, and *Acinetobacter baumannii*. Previous literature and also our findings regarding the EPS exopolysaccharide structure of these pathogens indicate that the structure of bacterial biofilms is variable and complex. For this reason, it is likely that in order to effectively disperse the biofilms of multiple pathogens, or even a single species, a cocktail of multiple enzymes will be needed so as to degrade all of the important structural components of those pathogens' biofilms (Jassim et al. 2012).

## Future directions

Future experiments regarding the structural analysis of biofilm exopolysaccharides may include utilizing lectin staining to rapidly screen bacterial biofilms for certain components (Angeloni et al. 2005). In addition, nuclear magnetic resonance (NMR) may be used to validate data obtained by our lab with the help of the Complex Carbohydrate Research Center (Athens, GA). Since we have purified several putative biofilm EPS depolymerases (see **Table 4-1**) besides HexNW, which has already been investigated in detail, there is a great deal of additional investigation left to be done.

Regarding HexNW, future experiments may focus on the long-term thermostability of HexNW by assessing activity after extended incubation at various temperatures. In addition, the regions of HexNW that are responsible for catalytic activity and thermostability may be investigated. Also, the ability of HexNW to disrupt biofilms can be questioned further. Biofilm flow cells can be used in conjunction with live-dead staining to visualize the effect of HexNW on biofilm structure with a confocal microscope. Catheter models or animal models of infection represent additional lines of investigation. In addition, it will be useful to test HexNW on other strains of *S. epidermidis* besides NRS 101. Since DspB has been shown to prevent biofilm formation in *S. aureus*, similar experiments can be done for HexNW (Izano et al. 2008). HexNW might also be used to treat *E. coli* biofilms since *E. coli* is known to have an appreciable amount of *N*-acetylglucosamine in its EPS (Wang et al. 2004; Bales et al. 2013).

## CONCLUDING REMARKS

Ample evidence has been provided for the urgent need to develop new ways of treating biofilm-related infections. Due to the large contribution of the polysaccharide portion of the EPS to the resilience and adherence properties of biofilms, increasing our understanding of the structure of these exopolysaccharides and also investing in the discovery of methods to degrade them are worthwhile goals. This thesis has detailed the composition of these exopolysaccharides in the biofilms of several important human pathogens. The identification and characterization of HexNW, a novel  $\beta$ -1,6-*N*-acetylglucosaminidase, has also been described. It represents a possible means of combating the numerous medical device-related infections caused by *S. epidermidis*. In addition, many other possible EPS depolymerases have been purified and may develop into therapeutics for other bacterial species. This thesis presents a variety of possible solutions to a major problem that is plaguing human health.

## APPENDIX A

### **Challenging the State of the Art in Protein Structure Prediction: Highlights of Experimental Target Structures for the 10<sup>th</sup> Critical Assessment of Techniques for Protein Structure Prediction Experiment CASP10**

This appendix contains the abstract for the following co-authored publication:

Kryshtafovych, A., Moult, J., **Bales, P.M.**, Bazan, J.F., Biasini, M., Burgin, A., Chen, C., Cochran, F.V., Craig, T.K., Das, R., Fass, D., Garcia-Doval, C., Herzberg, O., Lorimer, D., Luecke, H., Ma, X., Nelson, D.C., van Raaij, M.J., Rohwer, F., Segall, A., Seguritan, V., Zeth, K., & Schwede, T. (2014). Challenging the State of the Art in Protein Structure Prediction: Highlights of Experimental Target Structures for the 10<sup>th</sup> Critical Assessment of Techniques for Protein Structure Prediction Experiment CASP10. *Proteins*, 82 Suppl 2, 26–42. doi:10.1002/prot.24489

#### **Abstract**

For the last two decades, CASP has assessed the state of the art in techniques for protein structure prediction and identified areas which required further development. CASP would not have been possible without the prediction targets provided by the experimental structural biology community. In the latest

experiment, CASP10, more than 100 structures were suggested as prediction targets, some of which appeared to be extraordinarily difficult for modeling. In this article, authors of some of the most challenging targets discuss which specific scientific question motivated the experimental structure determination of the target protein, which structural features were especially interesting from a structural or functional perspective, and to what extent these features were correctly reproduced in the predictions submitted to CASP10. Specifically, the following targets will be presented: the acid-gated urea channel, a difficult to predict transmembrane protein from the important human pathogen *Helicobacter pylori*; the structure of human interleukin (IL)-34, a recently discovered helical cytokine; the structure of a functionally uncharacterized enzyme OrfY from *Thermoproteus tenax* formed by a gene duplication and a novel fold; an ORFan domain of mimivirus sulfhydryl oxidase R596; the fiber protein gene product 17 from bacteriophage T7; the bacteriophage CBA-120 tailspike protein; a virus coat protein from metagenomic samples of the marine environment; and finally, an unprecedented class of structure prediction targets based on engineered disulfide-rich small proteins.

## APPENDIX B

### Crystal Structure of ORF210 from *E. coli* O157:H7 Phage

#### CBA120 (TSP1), a Putative Tailspike Protein

This appendix contains the abstract for the following co-authored publication:

Chen, C., **Bales, P.M.**, Greenfield, J., Heselpoth, R. D., Nelson, D. C., & Herzberg, O. (2014). Crystal Structure of ORF210 from *E. coli* O157:H7 Phage CBA120 (TSP1), a Putative Tailspike Protein. *PLoS One*, 9(3), e93156. doi:10.1371/journal.pone.0093156

#### **Abstract**

Bacteriophage tailspike proteins act as primary receptors, often possessing endoglycosidase activity toward bacterial lipopolysaccharides or other exopolysaccharides, which enable phage absorption and subsequent DNA injection into the host. Phage CBA120, a contractile long-tailed *Viunlikevirus* phage infects the virulent *Escherichia coli* O157:H7. This phage encodes four putative tailspike proteins exhibiting little amino acid sequence identity, whose biological roles and substrate specificities are unknown. Here we focus on the first tailspike, TSP1, encoded by the *orf210* gene. We have discovered that TSP1 is resistant to protease degradation, exhibits high thermal stability, but does not cleave the O157 antigen. An immune-dot blot has shown that TSP1 binds strongly to non-O157:H7 *E. coli* cells and more weakly to *K. pneumoniae* cells,

but exhibits little binding to *E. coli* O157:H7 strains. To facilitate structure-function studies, we have determined the crystal structure of TSP1 to a resolution limit of 1.8 Å. Similar to other tailspike proteins, TSP1 assembles into elongated homotrimers. The receptor binding region of each subunit adopts a right-handed parallel β helix, reminiscent yet not identical to several known tailspike structures. The structure of the N-terminal domain that binds to the virion particle has not been seen previously. Potential endoglycosidase catalytic sites at the three subunit interfaces contain two adjacent glutamic acids, unlike any catalytic machinery observed in other tailspikes. To identify potential sugar binding sites, the crystal structures of TSP1 in complexes with glucose, α-maltose, or α-lactose were determined. These structures revealed that each sugar binds in a different location and none of the environments appears consistent with an endoglycosidase catalytic site. Such sites may serve to bind sugar units of a yet to be identified bacterial exopolysaccharide.

## APPENDIX C

### Characterization of AlgMsp, an Alginate Lyase from *Microbulbifer* sp. 6532A

This appendix contains the abstract for the following co-authored manuscript that has been submitted for publication:

Swift, S.M., Hudgens, J.W., Heselpoth, R.D., **Bales, P.M.**, & Nelson, D.C.  
Characterization of AlgMsp, an Alginate Lyase from *Microbulbifer* sp. 6532A.  
(Submitted)

#### **Abstract**

Alginate is a polysaccharide consisting of mannuronic acid and guluronic acid residues. It is produced by certain seaweeds and bacteria. Seaweed alginate is used in food and industrial chemical processes. Bacterial alginate is characteristic to pathogenic *Pseudomonas aeruginosa*. Alginate lyases cleave this polysaccharide into short oligo-uronates, and have potential applications in industry and medicine. An alginate lyase gene, *algMsp*, from *Microbulbifer* sp. 6532A, was synthesized as an *E.coli* codon-optimized clone. The resulting protein, AlgMsp, was expressed and purified from *E. coli*, and then the recombinant 37 kDa protein was characterized. The alginate lyase displayed highest activity at pH 8 and 0.2 M NaCl. Activity of the alginate lyase was greatest at 50°C, but was not stable over time at 50°C. The alginate lyase was still

highly active at 25°C, and had little or no loss of activity after 24 hours at 25°C. AlgMsp did not require divalent cations for activity. Comparing activity of the lyase against polymannuronic acid and polyguluronic acid substrates showed higher specific activity with polymannuronic acid, but greater affinity to polyguluronic acid. Prolonged AlgMsp-mediated degradation of alginate produced dimer, trimer, tetramer, and pentamer oligo-uronates.

## BIBLIOGRAPHY

- Ander JN, Franklin MJ, Stewart PS. Role of antibiotic penetration limitation in *Klebsiella pneumoniae* biofilm resistance to ampicillin and ciprofloxacin. *Antimicrobial agents chemother.* 2000; 44(7):1818-1824.
- Anderson G, Scott M. Determination of product shelf life and activation energy for five drugs of abuse. *Clinical chemistry.* 1991; 37:398–402.
- Anderson S. Characterization of bacterial biofilms for wastewater treatment. Stockholm: Royal Institute of Technology, Thesis (2009).
- Angeloni S, Ridet JL, Kusy N, Gao H, Crevoisier F, Guinchart S, Kochhar S, Sigrist H, Sprenger N. Glycoprofiling with micro-arrays of glycoconjugates and lectins. *Glycobiology.* 2005; 15:31–41.
- Asgarali A, Stubbs K, Oliver A, Vocadlo DJ, Mark BL. Inactivation of the glycoside hydrolase NagZ attenuates antipseudomonal beta-lactam resistance in *Pseudomonas aeruginosa*. *Antimicrobial agents and chemotherapy.* 2009; 53(6):2274–82.
- Bales PM, Renke EM, May SL, Shen Y, Nelson DC. Purification and characterization of biofilm-associated EPS exopolysaccharides from ESKAPE organisms and other pathogens. *PLoS One.* 2013; 8(6):e67950.
- Banerjee I, Pangule RC, Kane RS. Antifouling coatings: recent developments in the design of surfaces that prevent fouling by proteins, bacteria, and marine organisms. *Advanced materials.* 2011; 23(6):690–718.
- Bartell PF, Orr TE. Origin of polysaccharide depolymerase associated with bacteriophage infection. *Journal of virology.* 1969; 3(3):290–6.
- Bessler W, Freund-Molbert E, Knufermann H, Rudolph C, Thurow H, Stirm S. A bacteriophage-induced depolymerase active on *Klebsiella* K11 capsular polysaccharide. *Virology.* 1973; 56(1):134–151.
- Biscola FT, Abe CM, Guth BEC. Determination of adhesin gene sequences in, and biofilm formation by, O157 and non-O157 Shiga toxin-producing *Escherichia coli* strains isolated from different sources. *Applied and environmental microbiology.* 2011 April;77(7):2201–8.

Böckelmann U, Janke A, Kuhn R, Neu TR, Wecke J, Lawrence JR, Szewzyk U. Bacterial extracellular DNA forming a defined network-like structure. *FEMS microbiology letters*. 2006; 262(1):31–8.

Bookstaver PB, Williamson JC, Tucker BK, Raad II, Sherertz RJ. Activity of novel antibiotic lock solutions in a model against isolates of catheter-related bloodstream infections. *The Annals of pharmacotherapy*. 2009; 43:210–219.

Boucher HW, Talbot GH, Bradley JS, Edwards JE, Gilbert D, Rice LB, Scheld M, Spellberg B, Bartlett J. Bad bugs, no drugs: no ESCAPE! An update from the Infectious Diseases Society of America. *Clinical infectious diseases : an official publication of the Infectious Diseases Society of America*. 2009; 48:1–12.

Byrd MS, Sadovskaya I, Vinogradov E, Lu H, Sprinkle AB, Richardson SH, Ma L, Ralston B, Parsek MR, Anderson EM, et al. Genetic and biochemical analyses of the *Pseudomonas aeruginosa* Psl exopolysaccharide reveal overlapping roles for polysaccharide synthesis enzymes in Psl and LPS production. *Molecular microbiology*. 2009; 73:622–638.

Calhoun JH, Murray CK, Manring MM. Multidrug-resistant organisms in military wounds from Iraq and Afghanistan. *Clinical orthopaedics and related research*. 2008; 466(6):1356–62.

Campoccia D, Montanaro L, Arciola CR. A review of the clinical implications of anti-infective biomaterials and infection-resistant surfaces. *Biomaterials*. 2013; 34(33):8018–29.

Carlson G, Dragoo JL, Samimi B, Bruckner D a, Bernard GW, Hedrick M, Benhaim P. Bacteriostatic properties of biomatrices against common orthopaedic pathogens. *Biochemical and biophysical research communications*. 2004; 321(2):472–8.

Casjens SR, Thuman-Commike PA. Evolution of mosaically related tailed bacteriophage genomes seen through the lens of phage P22 virion assembly. *Virology*. 2011; 411:393–415.

Chaignon P, Sadovskaya I, Ragunah C, Ramasubbu N, Kaplan JB, Jabbouri S. Susceptibility of staphylococcal biofilms to enzymatic treatments depends on their chemical composition. *Applied microbiology and biotechnology*. 2007; 75:125–132.

Chen X, Schluesener HJ. Nanosilver: a nanoproduct in medical application. *Toxicology letters*. 2008; 176(1):1–12.

Choi AHK, Slamti L, Avci FY, Pier GB, Maira-Litrán T. The pgaABCD locus of *Acinetobacter baumannii* encodes the production of poly-beta-1-6-N-acetylglucosamine, which is critical for biofilm formation. *Journal of bacteriology*. 2009; 191(19):5953–63.

- Ciucanu I, Kerek F. A simple and rapid method for the permethylation of carbohydrates. *Carbohydrate research*. 1984; 131:209–217.
- Comte S, Guibaud G, Baudu M. Effect of extraction method on EPS from activated sludge: An HPSEC investigation. *Journal of hazardous materials*. 2007; 140:129–137.
- Cramton SE, Gerke C, Schnell NF, Nichols WW, Götz F. The intercellular adhesion (ica) locus is present in *Staphylococcus aureus* and is required for biofilm formation. *Infection and immunity*. 1999; 67:5427–5433.
- Crawford RW, Gibson DL, Kay WW, Gunn JS. Identification of a bile-induced exopolysaccharide required for *Salmonella* biofilm formation on gallstone surfaces. *Infection and immunity*. 2008; 76:5341–5349.
- Cristensen GD, Barker LP, Mawhinney TP, Baddour LM, Simpson WA. Identification of an antigenic marker of slime production for *Staphylococcus epidermidis*. *Infection and immunity*. 1990; 58:2906–2911.
- Cusumano CK, Pinkner JS, Han Z, Greene SE, Ford B a, Crowley JR, Henderson JP, Janetka JW, Hultgren SJ. Treatment and prevention of urinary tract infection with orally active FimH inhibitors. *Science translational medicine*. 2011; 3(109):109-115.
- Danese PN, Pratt LA, Kolter R. Exopolysaccharide production is required for development of *Escherichia coli* K-12 biofilm architecture. *Journal of bacteriology*. 2000; 182:3593–3596.
- Darouiche RO, Mansouri MD, Gawande P V, Madhyastha S. Antimicrobial and antibiofilm efficacy of triclosan and DispersinB combination. *The Journal of antimicrobial chemotherapy*. 2009; 64(1):88–93.
- Davies DG. The involvement of cell-to-cell signals in the development of a bacterial biofilm. *Science*. 1998; 280(5361):295–298.
- Desrousseaux C, Sautou V, Descamps S, Traoré O. Modification of the surfaces of medical devices to prevent microbial adhesion and biofilm formation. *The Journal of hospital infection*. 2013; 85(2):87–93.
- Dibdin GH, Assinder SJ, Nichols WW, Lambert P. Mathematical model of beta-lactam penetration into a biofilm of *Pseudomonas aeruginosa* while undergoing simultaneous inactivation by released beta-lactamases. *The Journal of antimicrobial chemotherapy*. 1996; 38(5):757–69.
- Donelli G, Francolini I, Romoli D, Guaglianone E, Piozzi a, Rangunath C, Kaplan JB. Synergistic activity of dispersin B and cefamandole nafate in inhibition of staphylococcal biofilm growth on polyurethanes. *Antimicrobial agents and chemotherapy*. 2007; 51(8):2733–40.

- Donlan RM. Preventing biofilms of clinically relevant organisms using bacteriophage. *Trends in microbiology*. 2009; 17(2):66–72.
- DuBois M, Gilles KA, Hamilton JK, Rebers PA, Smith F. Colorimetric method for determination of sugars and related substances. *Analytical chemistry*. 1956; 28:350–356.
- Elsässer-Beile U, Friebolin H, Stirm S. Primary structure of *Klebsiella* serotype 6 capsular polyssacharide. *Carbohydr research*. 1978; 65: 245–249.
- Fallas JA, Hartgerink JD. Computational design of self-assembling register-specific collagen heterotrimers. *Nature communications*. 2012; 3:1087.
- Fazekas E, Kandra L, Gyemant G. Model for  $\beta$ -1,6-*N*-acetylglucosamine oligomer hydrolysis catalyzed by dispersinB, a biofilm degrading enzyme. *Carbohydrate research*. 2012; 363:7-13.
- Flemming H-C, Wingender J. The biofilm matrix. *Nature reviews microbiology*. 2010; 8:623–633.
- Flemming, H-C JW. Relevance of microbial extracellular polymeric substances (EPSs) - Part I: Structural and ecological aspects. *Water science and technology*. 1999; 43:1–8.
- Fregolino E, Gargiulo V, Lanzetta R, Parrilli M, Holst O, Castro C De. Identification and structural determination of the capsular polysaccharides from two *Acinetobacter baumannii* clinical isolates, MG1 and SMAL. *Carbohydrate research*. 2011; 346(7):973–7.
- Friedman L, Kolter R. Genes involved in matrix formation in *Pseudomonas aeruginosa* PA14 biofilms. *Molecular microbiology*. 2004; 51:675–690.
- Friedman L, Kolter R. Two genetic loci produce distinct carbohydrate-rich structural components of the *Pseudomonas aeruginosa* biofilm matrix. *Journal of bacteriology*. 2004; 186:4457–4465.
- Gerke C, Kraft A, Schweitzer O, Chem JB, Su R. Characterization of the *N*-acetylglucosaminyltransferase activity involved in the biosynthesis of the *Staphylococcus epidermidis* polysaccharide intercellular adhesin. *Journal biological chemistry*. 1998; 273(29):18586-93.
- Ghalambor ALI, Duckworth DH, Edward C. Catalytic capsular and molecular polysaccharide properties of a phage induced depolymerase. *Journal biological chemistry*. 1971; 246:5607-5616.
- Götz F. *Staphylococcus* and biofilms. *Molecular microbiology*. 2002; 43:1367–1378.

Guiton PS, Hung CS, Kline K a, Roth R, Kau AL, Hayes E, Heuser J, Dodson KW, Caparon MG, Hultgren SJ. Contribution of autolysin and sortase a during *Enterococcus faecalis* DNA-dependent biofilm development. *Infection and immunity*. 2009; 77(9):3626–38.

Hall-Stoodley L, Costerton JW, Stoodley P. Bacterial biofilms: from the natural environment to infectious diseases. *Nature reviews microbiology*. 2004; 2:95–108.

Harjai K, Kumar R, Singh S. Garlic blocks quorum sensing and attenuates the virulence of *Pseudomonas aeruginosa*. *FEMS immunology and medical microbiology*. 2010; 58(2):161–8.

Hughes KA, Sutherland IW, Jones M V. Biofilm susceptibility to bacteriophage attack: the role of phage-borne polysaccharide depolymerase. *Microbiology*. 1998; 144:3039–3047.

Izano E a, Amarante M a, Kher WB, Kaplan JB. Differential roles of poly-N-acetylglucosamine surface polysaccharide and extracellular DNA in *Staphylococcus aureus* and *Staphylococcus epidermidis* biofilms. *Applied and environmental microbiology*. 2008; 74(2):470–6.

Junkins AD, Doyle MP. Demonstration of exopolysaccharide production by enterohemorrhagic *Escherichia coli*. *Current microbiology*. 1992; 25:9–17.

Kaku H, Van Damme EJ, Peumans WJ, Goldstein IJ. Carbohydrate-binding specificity of the daffodil (*Narcissus pseudonarcissus*) and amaryllis (*Hippeastrum hybr.*) bulb lectins. *Archives of biochemistry and biophysics*. 1990 June;279(2):298–304.

Kalishwaralal K, BarathManiKanth S, Pandian SRK, Deepak V, Gurunathan S. Silver nanoparticles impede the biofilm formation by *Pseudomonas aeruginosa* and *Staphylococcus epidermidis*. *Colloids and surfaces. B, biointerfaces*. 2010; 79(2):340–4.

Kaplan JB, Ragunath C, Ramasubbu N, Fine DH. Detachment of *Actinobacillus actinomycetemcomitans* biofilm cells by an endogenous beta-hexosaminidase activity. *Journal of bacteriology*. 2003; 185:4693–4698.

Kaplan JB, Ragunath C, Velliyagounder K, Fine DH, Ramasubbu N. Enzymatic detachment of *Staphylococcus epidermidis* biofilms. *Antimicrobial agents and chemotherapy*. 2004; 48:2633–2636.

Kaplan JB, Velliyagounder K, Ragunath C, Rohde H, Mack D, Knobloch JK-M, Ramasubbu N. Genes involved in the synthesis and degradation of matrix polysaccharide in *Actinobacillus actinomycetemcomitans* and *Actinobacillus pleuropneumoniae* biofilms. *Journal of bacteriology*. 2004; 186:8213–8220.

- Kaplan N, Rosenberg E, Jann B, Jann K. Structural studies of the capsular polysaccharide of *Acinetobacter calcoaceticus* BD4. *European journal of biochemistry/FEBS*. 1985; 152:453–458.
- Kassa T, Chhibber S. Thermal treatment of the bacteriophage lysate of *Klebsiella pneumoniae* B5055 as a step for the purification of capsular depolymerase enzyme. *Journal of virological methods*. 2012; 179(1):135–41.
- Kharidia R, Liang JF. The activity of a small lytic peptide PTP-7 on *Staphylococcus aureus* biofilms. *Journal of microbiology*. 2011; 49(4):663–8.
- Kives J, Orgaz B, SanJos C. Polysaccharide differences between planktonic and biofilm-associated EPS from *Pseudomonas fluorescens* B52. *Colloids and surfaces B: biointerfaces*. 2006; 52:123–127.
- Kolodkin-Gal I, Cao S, Chai L, Böttcher T, Kolter R, Clardy J, Losick R. A self-produced trigger for biofilm disassembly that targets exopolysaccharide. *Cell*. 2012; 149(3):684–92.
- Kolodkin-Gal I, Romero D, Cao S, Clardy J, Kolter R, Losick R. D-amino acids trigger biofilm disassembly. *Science*. 2010; 328(5978):627–9.
- Körstgens V, Flemming HC, Wingender J, Borchard W. Influence of calcium ions on the mechanical properties of a model biofilm of mucoid *Pseudomonas aeruginosa*. *Water science and technology*. 2001; 43:49–57.
- Kostakioti, M.K., Hadjifrangiskou, M. H. Bacterial biofilms: development, dispersal, and therapeutic strategies in the dawn of the postantibiotic era. *Cold spring harb perspect med*. 2013; 3(4):a010306.
- Lawrence JR, Korber DR, Hoyle BD, Costerton JW, Caldwell DE. Optical sectioning of microbial biofilms. *Journal of bacteriology*. 1991; 173(20):6558–67.
- Lawrence JR, Swerhone GDW, Kuhlicke U, Neu TR. In situ evidence for microdomains in the polymer matrix of bacterial microcolonies. *Canadian journal of microbiology*. 2007; 3(3):450–8.
- Lery LM, Frangeul L, Tomas A, Passet V, Almeida AS, Bialek-Davenet S, Barbe V, Bengoechea J a, Sansonetti P, Brisse S, et al. Comparative analysis of *Klebsiella pneumoniae* genomes identifies a phospholipase D family protein as a novel virulence factor. *BMC biology*. 2014 May 29;12(1):41.
- Lewis K. Riddle of biofilm resistance. *Antimicrobial agents and chemotherapy*. 2001; 45:999–1007.
- Liu H, Fang HHP. Extraction of extracellular polymeric substances (EPS) of sludges. *Journal of biotechnology*. 2002; 95:249–256.

- Lu TK, Collins JJ. Dispersing biofilms with engineered enzymatic bacteriophage. *Proceedings of the National Academy of Sciences of the United States of America*. 2007; 104(27):11197–202.
- Mack D, Nedelmann M, Krokotsch A, Schwarzkopf A, Heesemann J, Laufs R. Characterization of transposon mutants of biofilm-producing *Staphylococcus epidermidis* impaired in the accumulative phase of biofilm production: genetic identification of a hexosamine-containing polysaccharide intercellular adhesin. *Infection and immunity*. 1994; 62:3244–3253.
- Mann EE, Wozniak DJ. *Pseudomonas* biofilm matrix composition and niche biology. *FEMS microbiology reviews*. 2012; 36(4):893-916.
- Manuel SGA, Rangunath C, Sait HBR, Izano EA, Kaplan JB. Role of active-site residues of dispersinB, a biofilm-releasing  $\beta$ -hexosaminidase from a periodontal pathogen, in substrate hydrolysis. *FEBS journal*. 2007; 274:5987-5999.
- Marchler-Bauer A et al. CDD: conserved domains and protein three-dimensional structure. *Nucleic Acids Res*. 2013;41(D1):D384-52.
- Mathee K, Ciofu O, Sternberg C, Lindum PW, Campbell JI, Jensen P, Johnsen AH, Givskov M, Ohman DE, Molin S, et al. Mucoid conversion of *Pseudomonas aeruginosa* by hydrogen peroxide: a mechanism for virulence activation in the cystic fibrosis lung. *Microbiology*. 1999; 145:1349–1357.
- Matsukawa M, Greenberg EP. Putative exopolysaccharide synthesis genes influence *Pseudomonas aeruginosa* biofilm development. *Journal of bacteriology*. 2004; 186:4449–4456.
- Merkle RK, Poppe I. Methanolysis Solvolysis. *Methods in enzymology*. 1994; 230:3–15.
- Molin S, Tolker-Nielsen T. Gene transfer occurs with enhanced efficiency in biofilms and induces enhanced stabilisation of the biofilm structure. *Current opinion in biotechnology*. 2003; 14(3):255–261.
- Monds RD, O’Toole G. The developmental model of microbial biofilms: ten years of a paradigm up for review. *Trends in microbiology*. 2009; 17(2):73–87.
- Müller JJ, Barbirz S, Heinle K, Freiberg A, Seckler R, Heinemann U. An intersubunit active site between supercoiled parallel beta helices in the trimeric tailspike endorhamnosidase of *Shigella flexneri* Phage Sf6. *Structure*. 2008; 16(5):766–75.
- National Institutes of Health. Research on Microbial Biofilms (PA-03-047). National Institutes of Health. 2002

- Niemann H, Kwiatkowski B, Westphal U, Stirm S. *Klebsiella* serotype 25 capsular polysaccharide: primary structure and depolymerization by a bacteriophage-borne glycanase. *Journal of bacteriology*. 1977; 130(1):366–74.
- Njoroge J, Sperandio V. Jamming bacterial communication: new approaches for the treatment of infectious diseases. *EMBO molecular medicine*. 2009; 1(4):201–10.
- O’Toole G, Kolter R. Flagellar and twitching motility are necessary for *Pseudomonas aeruginosa* biofilm development. *Molecular microbiology*. 1998; 30(2):295–304.
- Oliveira R, Marques F, Azeredo J. Purification of polysaccharides from a biofilm matrix by selective precipitation of proteins. *Biotechnology techniques*. 1999; 13(6):391–393.
- Otto M. Molecular basis of *Staphylococcus epidermidis* infections. *Seminars in immunopathology*. 2012; 34(2):201–14.
- Otzen D, Nielsen PH. We find them here, we find them there: functional bacterial amyloid. *Cellular and molecular life sciences*. 2008; 65(6):910–27.
- Pan X, Liu J, Zhang D, Chen X, Li L, Song W, Yang J. A comparison of five extraction methods for extracellular polymeric substances (EPS) from biofilm by using three dimensional excitation-emission matrix (3DEEM) fluorescence spectroscopy. *Water SA*. 2010; 36:111-116.
- Parsek MR, Singh PK. Bacterial biofilms: an emerging link to disease pathogenesis. *Annual review of microbiology*. 2003; 57:677–701.
- Peters GF, Schumacher-Perdreau B, Jansen M, Bay M, Pulverer G. Biology of *S. epidermidis* extracellular slime. *Zentrabl bakteriol suppl*. 1987; 16:15–32.
- Pier GB, Cohen M, Jennings H. Further purification and characterization of high-molecular-weight polysaccharide from *Pseudomonas aeruginosa*. *Infection and immunity*. 1983 December;42(3):936–41.
- Pompilio a, Scocchi M, Pomponio S, Guida F, Di Primio a, Fiscarelli E, Gennaro R, Di Bonaventura G. Antibacterial and anti-biofilm effects of cathelicidin peptides against pathogens isolated from cystic fibrosis patients. *Peptides*. 2011; 32(9):1807–14.
- Provencher SW, Glöckner J. Estimation of globular protein secondary structure from circular dichroism. *Biochemistry*. 1981; 20(1):33–7.
- Puckett SD, Taylor E, Raimondo T, Webster TJ. The relationship between the nanostructure of titanium surfaces and bacterial attachment. *Biomaterials*. 2010; 31(4):706–13.

- Qin Z, Yang L, Qu D, Molin S, Tolker-Nielsen T. *Pseudomonas aeruginosa* extracellular products inhibit staphylococcal growth, and disrupt established biofilms produced by *Staphylococcus epidermidis*. *Microbiology*. 2009; 155:2148–56.
- Rättö M, Mustranta A, Siika-aho M. Strains degrading polysaccharides produced by bacteria from paper machines. *Applied microbiology and biotechnology*. 2001; 57:182–185.
- Revdiwala S, Rajdev BM, Mulla S. Characterization of bacterial etiologic agents of biofilm formation in medical devices in critical care setup. *Critical care research and practice*. 2012; 2012:945805.
- Rogers S, Huigens RW, Cavanagh J, Melander C. Synergistic effects between conventional antibiotics and 2-aminoimidazole-derived antibiofilm agents. *Antimicrobial agents and chemotherapy*. 201; 54(5):2112–8.
- Ryder C, Byrd M, Wozniak DJ. Role of polysaccharides in *Pseudomonas aeruginosa* biofilm development. *Current opinion in microbiology*. 2007; 10(6):644–8.
- Sandal I, Inzana TJ, Molinaro A, Castro C De, Shao JQ, Apicella MA, Cox AD, Michael FS, Berg G. Identification, structure, and characterization of an exopolysaccharide produced by *Histophilus somni* during biofilm formation. *BMC Microbiology*. 2011; 11:186 doi: 10.1186/1471-2180-11-186.
- Sauer K, Camper AK. Characterization of phenotypic changes in *Pseudomonas putida* in response to surface-associated growth. *Journal bacterial*. 2001; 183(22): 6579-89.
- Secinti KD, Özalp H, Attar A, Sargon MF. Nanoparticle silver ion coatings inhibit biofilm formation on titanium implants. *Journal of clinical neuroscience*. 2011; 18(3):391–5.
- Seo MJ. Biochemical characterization of the exopolysaccharide purified from *Laetiporus sulphureus* mycelia. *Journal of microbiology and biotechnology*. 2011; 21:1287–1293.
- Sepandj F, Ceri H, Gibb A, Read R, Olson M. Minimum inhibitory concentration (MIC) versus minimum biofilm eliminating concentration (MBEC) in evaluation of antibiotic sensitivity of gram-negative bacilli causing peritonitis. *Peritoneal dialysis international*. 2004; 24(1):65–7.
- Shaw T, Winston M, Rupp CJ, Klapper I, Stoodley P. Commonality of elastic relaxation times in biofilms. *Physical review letters*. 2004; 93(9):098102.

- Shemesh M, Tam A, Steinberg D. Expression of biofilm-associated genes of *Streptococcus mutans* in response to glucose and sucrose. *Journal of medical microbiology*. 2007; 56:1528–1535.
- Shibata H, Yagi T. Rate assay of *N*-acetyl- $\beta$ -D-hexosaminidase with 4-nitrophenyl *N*-acetyl- $\beta$ -D-glucosaminide as an artificial substrate. *Clinica chimica acta*. 1996; 251:53–64.
- Sreerama N, Woody RW. Estimation of protein secondary structure from circular dichroism spectra: comparison of CONTIN, SELCON, and CDSSTR methods with an expanded reference set. *Analytical biochemistry*. 2000; 287:252–260.
- Stevenson G, Andrianopoulos K, Hobbs M, Reeves PR. Organization of the *Escherichia coli* K-12 gene cluster responsible for production of the extracellular polysaccharide colanic acid. *Journal of bacteriology*. 1996; 178:4885–4893.
- Stewart PS, Franklin MJ. Physiological heterogeneity in biofilms. *Nature reviews microbiology*. 2008; 6(3):199–210.
- Stoodley P, Cargo R, Rupp CJ, Wilson S, Klapper I. Biofilm material properties as related to shear-induced deformation and detachment phenomena. *Journal of industrial microbiology & biotechnology*. 2002; 29:361–367.
- Stoodley P, Sauer K, Davies DG, Costerton JW. Biofilms as complex differentiated communities. *Annual review of microbiology*. 2002; 56:187–209.
- Strathmann M, Wingender J, Flemming HC. Application of fluorescently labelled lectins for the visualization and biochemical characterization of polysaccharides in biofilms of *Pseudomonas aeruginosa*. *Journal of microbiological methods*. 2002; 50:237–248.
- Strominger JL, Park JT, Thompson RE, Thompson E. Composition of the cell wall of *Staphylococcus aureus*: its relation to the mechanism of action of penicillin. *Journal of biological chemistry*. 1959; 234:3263–3268.
- Sutherland I. Biofilm exopolysaccharides: a strong and sticky framework. *Microbiology*. 2001; 147:3–9.
- Sutherland IW, Hughes KA, Skillman LC, Tait K. The interaction of phage and biofilms. *FEMS microbiology letters*. 2004; 232:1–6.
- Sutherland IW, Wilkinson JF. Depolymerases for bacterial exopolysaccharides obtained from phage-infected bacteria. *Journal of general microbiology*. 1965; 39(3):373–83.
- Sutherland IW. Structural studies on colanic acid, the common exopolysaccharide found in the enterobacteriaceae, by partial acid hydrolysis. *Biochemical journal*. 1969; 115:935–945.

Taraszkiewicz A, Fila G, Grinholc M, Nakonieczna J. Innovative strategies to overcome biofilm resistance. *Biomedical research international*. 2013; doi: 10.1155/2013/150653.

Thompson JE, Pourhossein M, Waterhouse A, Hudson T, Goldrick M, Derrick JP, Roberts IS. The K5 lyase KflA combines a viral tail spike structure with a bacterial polysaccharide lyase mechanism. *The Journal of biological chemistry*. 2010; 285(31):23963–9.

Tojo M, Yamashita N, Goldmann DA, Pier GB. Isolation and characterization of a capsular polysaccharide adhesin from *Staphylococcus epidermidis*. *The Journal of infectious diseases*. 1988; 157:713–722.

Tsuneda S, Aikawa H, Hayashi H, Yuasa A, Hirata A. Extracellular polymeric substances responsible for bacterial adhesion onto solid surface. *FEMS microbiology letters*. 2003; 223:287–292.

von Eiff C, Jansen B, Kohlen W, Becker K. Infections associated with medical devices: pathogenesis, management and prophylaxis. *Drugs*. 2005; 65:179–214.

Vötsch W, Templin MF. Characterization of a beta-N-acetylglucosaminidase of *Escherichia coli* and elucidation of its role in muropeptide recycling and beta - lactamase induction. *The Journal of biological chemistry*. 2000; 275(50):39032–8.

Walters, MC, Roe F, Bugnicourt A, Franklin MJ, Stewart PS. Contributions of antibiotic penetration, oxygen limitation, and low metabolic activity to tolerance of *Pseudomonas aeruginosa* biofilms to ciprofloxacin and tobramycin. *Antimicrob agents chemother*. 2003; 47(1):317-23.

Wang X, Iii JFP, Romeo T. The pgaABCD Locus of *Escherichia coli* promotes the synthesis of a polysaccharide adhesin required for biofilm formation. *Journal bacteriol*. 2004; 186(9):2724-34.

Whitchurch CB, Tolker-Nielsen T, Ragas PC, Mattick JS. Extracellular DNA required for bacterial biofilm formation. *Science*. 2002; 295(5559):1487.

Whitfield C. Biosynthesis and assembly of capsular polysaccharides in *Escherichia coli*. *Annual review of biochemistry*. 2006 January;75:39–68.

Whitfield C, Roberts IS. Structure, assembly and regulation of expression of capsules in *Escherichia coli*. *Molecular microbiology*. 1999; 31:1307–1319.

Whitmore L, Wallace BA. DICHROWEB, an online server for protein secondary structure analyses from circular dichroism spectroscopic data. *Nucleic acids research*. 2004; 32:W668–W673.

Worlitzsch D, Tarran R, Ulrich M, Schwab U, Cekici A, Meyer KC, Birrer P, Bellon G, Berger J, Weiss T, et al. Effects of reduced mucus oxygen

concentration in airway *Pseudomonas* infections of cystic fibrosis patients. *Journal clinical investigation*. 2002; 109(3):317–325.

Wozniak DJ, Wyckoff TJO, Starkey M, Keyser R, Azadi P, O'Toole G, Parsek MR. Alginate is not a significant component of the extracellular polysaccharide matrix of PA14 and PAO1 *Pseudomonas aeruginosa* biofilms. *Proceedings of the National Academy of Sciences of the United States of America*. 2003; 100(13):7907–12.

Yadav KK, Mandal AK, Sen IK, Chakraborti S, Islam SS, Chakraborty R. Flocculating property of extracellular polymeric substances produced by a biofilm-forming bacterium *Acinetobacter junii* BB1A. *Applied biochemistry and biotechnology*. 2012; 168(6):1621-34.

Yang D, Biragyn A, Kwak LW, Oppenheim JJ. Mammalian defensins in immunity: more than just microbicidal. *Trends in immunology*. 2002; 23(6):291–6.

York WS, Darvill AG, McNeil M, Stevenson TT, Albersheim P. Isolation and characterization of plant cell walls and cell wall components. *Methods Enzymol*. 1986; 118: 3–4.

Zogaj X, Nimtz M, Rohde M, Bokranz W, Römling U. The multicellular morphotypes of *Salmonella typhimurium* and *Escherichia coli* produce cellulose as the second component of the extracellular matrix. *Molecular microbiology*. 2001; 39(6):1452–63.